

# Triangulating Meet-in-the-Middle Attack (Full Version)

Boxin Zhao<sup>1</sup>, Qingliang Hou<sup>3</sup>, Lingyue Qin<sup>2,1,4</sup>, and Xiaoyang Dong<sup>2,1,4</sup>(✉)

<sup>1</sup> Zhongguancun Laboratory, Beijing, P.R.China  
zhaobx@mail.zgclab.edu.cn

<sup>2</sup> Tsinghua University, Beijing, P.R.China  
{qinly,xiaoyangdong}@tsinghua.edu.cn

<sup>3</sup> School of Cyber Science and Technology, Shandong University, Qingdao, P.R.China  
qinglianghou@mail.sdu.edu.cn

<sup>4</sup> State Key Laboratory of Cryptography and Digital Economy Security, Tsinghua University, Beijing, P.R.China

**Abstract.** To penetrate more rounds with Meet-in-the-Middle (MitM) attack, the neutral words are usually subject to some linear constraints, *e.g.*, Sasaki and Aoki’s *initial structure* technique. At CRYPTO 2021, Dong *et al.* found the neutral words can be nonlinearly constrained. They introduced a table-based method to precompute and store the solution space of the neutral words, which led to a huge memory complexity. In this paper, we find some nonlinearly constrained neutral words can be solved efficiently by Khovratovich *et al.*’s triangulation algorithm (TA). Furthermore, motivated by the structured Gaussian elimination paradigm developed by LaMacchia *et al.* [37] and Bender *et al.* [6], we improve the TA to deal with the case when there are still many unprocessed equations, but no variable exists in only one equation (the original TA will terminate). Then, we introduce the new MitM attack based on our improved TA, called *triangulating MitM attack*.

As applications, the memory complexities of the single-plaintext key-recovery attacks on 4-/5-round AES-128 are significantly reduced from  $2^{80}$  to the practical  $2^{24}$  or from  $2^{96}$  to  $2^{40}$ . Besides, a series of new one/two-plaintext attacks are proposed for reduced AES-192/-256 and Rijndael-EM (basic primitives of NIST PQC candidate FAEST). A partial key-recovery experiment is conducted on 4-round AES-128 to verify the correctness of our technique. For AES-256-DM, the memory complexity of the 10-round preimage attack is reduced from  $2^{56}$  to  $2^8$ , thus an experiment is also implemented. Without our technique, the impractical memories  $2^{80}$  or  $2^{56}$  of previous attacks in the precomputation phase will always prevent any kind of (partial) experimental simulations.

In the full version, we extend our techniques to Sponge functions. We figure out some memory efficient attacks, *e.g.*, reducing the memories of Qin *et al.*’s 4-round attack on Keccak[1024] and Dong *et al.*’s 3-round attack on Xoodyak-XOF from  $2^{108}$  to  $2^{52}$ , or from  $2^{118}$  to the current  $2^{37}$ . Besides, the first 3-round collision attack on Xoodyak-XOF with 128-bit target is given, while previous MitM approaches are always worse than the birthday bound due to the high memory. The memories of the MitM

attacks on 3-/4-round Ascon are reduced from  $2^{24}/2^{34}$  to  $2^{14}/2^{14}$ , which have been partially implemented to verify the attacks.

**Keywords:** AES · Triangulating MitM · Key-recovery · Hash Function · Triangulation Algorithm

## 1 Introduction

The Rijndael block cipher [17] was designed by Daemen and Rijmen in 1997 and accepted by NIST as the AES (Advanced Encryption Standard) standard in October 2000. Today, it is probably the most widely used block cipher. In 2024, NIST announced the 2nd round candidates for the contest of additional digital signature schemes for the NIST PQC, including FAEST [5]. In FAEST, the secret signing key is an AES key, while the public verification key is **one plaintext-ciphertext pair for FAEST based on AES-128, and two plaintext-ciphertext pairs for FAEST based on AES-192 and AES-256**. The plaintext-ciphertext pairs are obtained by encrypting some random messages with AES under the signing key. Therefore, the security of FAEST is reduced to the security of AES with **one or two known plaintext-ciphertext pairs**. Therefore, it is important to study the security of AES in this scenario. In fact, attacks on AES with data complexity restricted to only a few known or chosen plaintexts have been studied extensively [11, 10, 19, 54, 47, 4, 28]. Among these attacks, the single plaintext-ciphertext attacks are based on the Meet-in-the-Middle (MitM) approach or Guess-and-Determine [11].

The MitM attack proposed by Diffie and Hellman in 1977 is a time-memory trade-off cryptanalysis of symmetric-key primitives [21]. Currently, the MitM attack has been successfully applied to block ciphers and hash functions with more sophisticated techniques, such as the internal state guessing [29], splice-and-cut [1], initial structure [50], bicliques [8, 35], 3-subset MitM [9], (indirect) partial matching [1, 50], guess-and-determine [51, 33], sieve-in-the-middle [13], match-box [31], dissection [23], non-linear initial structure [32], MitM in differential view [36, 30], and differential MitM [12], etc. Automating MitM attack was first reported in CRYPTO 2011 and 2016 [11, 20], which present attacks on AES with low data complexity, or even a single plaintext-ciphertext pair. In 2018, Sasaki [48] first tried to automate MitM with Mixed Integer Linear Programming (MILP). At EUROCRYPT 2021, Bao *et al.* [2] built a fully automated MitM preimage attack using MILP on AES-like hashing. Later, the automated MitM models were improved with more techniques by Dong *et al.* [26], Bao *et al.* [3], and Chen *et al.* [14], or further developed for the sponge functions by Schrottenloher and Stevens [52, 53], Qin *et al.* [45], and Dong *et al.* [27].

In the MitM attacks, as shown in Figure 1, the iterative round-based computation of the compression function or block cipher is divided at a certain round (starting point) into two chunks. The two chunks are computed independently and end at a common matching point. In both chunks, the computation involves different message words, denoted by  $N^+$  and  $N^-$  respectively. So one chunk

86 computes all possible values of the involved message words  $N^+$  independently  
87 of the message words  $N^-$  involved in the other chunk. The different words  $N^+$   
88 and  $N^-$  are called the *neutral words*. At EUROCRYPT 2009, Sasaki and Aoki  
89 proposed the *initial structure* (IS) technique with the purpose of skipping sev-  
90 eral rounds at the beginning of two chunks to enhance the MitM attack [50].  
91 As shown in Figure 1, the two chunks are in the opposite direction, and only  
92 a few consecutive starting rounds are overlapped, which form the so-called IS.  
93 Although the two sets of neutral words  $N^+$  and  $N^-$  appear simultaneously at  
94 these rounds, they are only involved in the computation of one chunk each. This  
95 is achieved by assigning some linear constraints to the values of neutral words of  
96 one chunk, such that different values lead to constant impact on the computation  
97 of the opposite chunk. The constrained space of the values of the neutral words  
is derived by solving the linear systems via Gaussian elimination. At CRYPTO

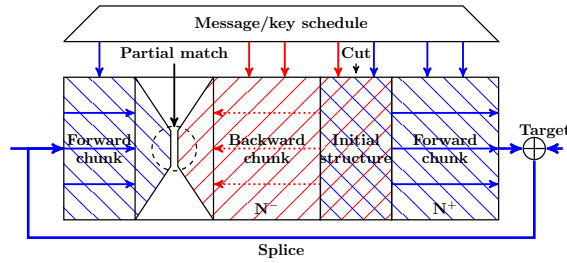


Fig. 1: The Splice-and-cut MitM Attack [1]

98  
99 2021, Dong *et al.* [26] noticed that in many potential MitM characteristics, the  
100 two sets of neutral words  $N^+$  and  $N^-$  are constrained by some nonlinear con-  
101 straints, such that different values lead to a constant impact on the computation  
102 of the opposite chunk only if the nonlinear system holds. Therefore, Dong *et al.*  
103 presented a table-based technique to obtain the constrained space of the values  
104 of the neutral words. The drawback of Dong *et al.*'s approach is that it requires  
105 a huge amount of memory to prepare two hash tables, and many attacks based  
106 on this method need huge memory, *e.g.*, [26,45].

107 **Our Contribution.** At CT-RSA 2009, Khovratovich, Biryukov, and Nikolic  
108 presented the triangulation algorithm (TA) [34] to solve the nonlinear system.  
109 Combining TA and rebound attack [43], Dong *et al.* proposed the triangulating  
110 rebound attack [25].

111 In this paper, motivated by the structured Gaussian elimination paradigm  
112 developed by LaMacchia *et al.* [37] and Bender *et al.* [6], we improve the tri-  
113 angulation algorithm to deal with the case where there are still many unpro-  
114 cessed equations but no variable exists in only one equation (the original TA  
115 will terminate immediately). Moreover, with the help of the improved triangula-  
116 tion algorithm, we find a memory-efficient approach to derive the value space of

the nonlinear constrained neutral words for MitM, thereby solving the memory problem of Dong *et al.*'s MitM attacks [26]. We name this new method as the *triangulating MitM attack*. With this advanced method in hand, we achieve the following results:

- **Improved key-recovery attacks on AES with single/two plaintext-ciphertext pairs:** This setting directly impacts the security of NIST PQC candidate FAEST [5], where only one plaintext-ciphertext pair acts as the public key in FAEST-128 (based on AES-128), and two plaintext-ciphertext pairs act as the public key in FAEST-192/-256 (based on AES-192/-256). The encryption key of AES acts as secret signing key in FAEST. Our goal is to recover the secret signing key with the public key, *i.e.*, single/two plaintext-ciphertext pairs. Once the secret signing key is recovered, a forgery attack on FAEST is found. The cryptanalysis records on up to 5-round AES in this setting are kept by Bouillaguet, Derbez, and Fouque from CRYPTO 2011 [11] and Derbez's PhD thesis [19]. We break their 10+ year record by significantly reducing the memory complexities of both the 4-round and 5-round attacks on AES-128 by a factor of  $2^{56}$ , *i.e.*, from  $2^{80}$  to the practical  $2^{24}$  and from  $2^{96}$  to  $2^{40}$ . Due to the practical memory, the new 4-round attack has been practically verified by a 4-byte partial key-recovery experiment in Sect. 4.2. With the help of Leurent and Pernot's new representation of AES's key schedule [39], we also improve both the time and memory complexities of the 4-round key-recovery attack on AES-128 and also propose the attacks on 6-round AES-192 and 7-round AES-256 with two plaintext-ciphertext pairs.
- **Key-recovery attacks on Rijndael-EM with one plaintext-ciphertext pair:** The high-performance versions of FAEST are based on Rijndael-EM [5]. We first convert the key-recovery attacks on Rijndael-EM into the preimage attacks on its hashing mode. By applying the triangulating MitM attack, we find the preimage attacks and then convert them back to key-recovery attacks with one plaintext-ciphertext pair on 7-/8-/9-round Rijndael-EM-128/192/256, respectively.
- **DM Hashing mode with AES-256:** The memory complexity of the preimage attack on 10-round AES-256-DM is reduced from the impractical  $2^{56}$  [26] to the practical  $2^8$ . Therefore, an experiment is performed to find a 40-bit partial target preimage to verify our technique in Sect. 4.6. Without our improvement, the impractical memory of size  $2^{56}$  in the precomputation will prevent any (partial) experiments.
- **Applications to the MitM attacks on Sponge functions:**
  - We improve the 4-round preimage attacks on Keccak[1024] and also give the first MitM preimage attack on 4-round Keccak[768]. Compared to Qin *et al.*'s 4-round attack on Keccak[1024] [46], the memory complexity is significantly reduced from  $2^{108}$  to  $2^{52}$  with the same time complexity.
  - For Xoodyak-XOF, we significantly reduce the memory of Dong *et al.*'s 3-round preimage attack [27] from  $2^{118}$  to the current  $2^{37}$ . Then, the first 3-round collision attack on Xoodyak-XOF with 128-bit target is introduced. Previously, Dong *et al.*'s MitM attack [27] needs to prepare a huge hash

- table of size  $2^{118}$  before the MitM phase, which is already worse than the birthday bound  $2^{64}$ , and cannot be converted into collision attack.
- We also improve the attacks on reduced Ascon-XOF with 128-bit target, Subterranean 2.0, and Gimli-XOF with 128-bit target. The experiments of the partial attacks on 3-/4-round Ascon-XOF are conducted in Supplementary Material H to verify the technique.

All our codes including the experiments on 4-round AES-128, 10-round AES-256-DM, and 3-/4-round Ascon-XOF are given at

<https://github.com/boxindev/Triangulation-MitM>

The summary of key recovery attacks on AES and Rijndael-EM is given in Table 1. The summary of the results on the hash functions is given in Table 2.

Table 1: Key-recovery attacks on AES and Rijndael-EM with low data. KP: known plaintext; CP: Chosen plaintext; ACC: Adaptive chosen plaintext and ciphertext.

Target	Methods	Rounds	Data	Time	Memory	Generic	Ref.
AES-128	MitM	$3^{\dagger}/10$	1KP	$2^{96}$	$2^{72}$	$2^{128}$	[11]
	MitM	$4^{\dagger}/10$	1KP	$2^{120}$	$2^{80}$	$2^{128}$	[11]
	MitM	$4^{\dagger}/10$	1KP	$2^{120}$	<b><math>2^{24}</math></b>	$2^{128}$	Sect. 4.2
	MitM	$4^{\dagger}/10$	1KP	<b><math>2^{112}</math></b>	<b><math>2^{56}</math></b>	$2^{128}$	Sect. 4.3
	MitM	$5/10$	1KP	$2^{120}$	$2^{96}$	$2^{128}$	[19]
	MitM	$5/10$	1KP	$2^{120}$	<b><math>2^{40}</math></b>	$2^{128}$	Sect. 4.1
	MitM	$4^{\dagger}/10$	2CP	$2^{80}$	$2^{80}$	$2^{128}$	[11]
	MitM	$5^{\dagger}/10$	8CP	$2^{64}$	$2^{56}$	$2^{128}$	[19]
	Partial Sum	$5/10$	$2^8$ CP	$2^{40}$	small	$2^{128}$	[55]
	R-Boomerang	$5/10$	$2^9$ ACC	$2^{23}$	$2^9$	$2^{128}$	[28]
	Yoyo	$5/10$	$2^{11}$ ACC	$2^{31}$	small	$2^{128}$	[47]
AES-192	MitM	$6/12$	<b><math>2</math>KP</b>	$2^{176}$	$2^{72}$	$2^{192}$	Sect. 4.4
	MitM	$6/12$	$2^8$ CP	$2^{109.6}$	$2^{109.6}$	$2^{192}$	[19]
	Multiple-of-8	$7/12$	$2^{26}$ CP	$2^{146.3}$	$2^{40}$	$2^{192}$	[4]
AES-256	MitM	$7/14$	<b><math>2</math>KP</b>	$2^{248}$	$2^{72}$	$2^{256}$	Sect. 4.5
	MitM	$6/14$	$2^8$ CP	$2^{122}$	$2^{113}$	$2^{256}$	[19]
	MitM	$7/14$	$2^8$ CP	$2^{170}$	$2^{186}$	$2^{256}$	[19]
	MitM	$7/14$	$2^{26}$ CP	$2^{146}$	$2^{40}$	$2^{256}$	[4]
Rijndael-EM-128	MitM	$7/10$	1KP	$2^{112}$	$2^{32}$	$2^{128}$	Sect. 5.1
Rijndael-EM-192	MitM	$8/12$	1KP	$2^{176}$	$2^{16}$	$2^{192}$	Sect. 5.2
Rijndael-EM-256	MitM	$9/14$	1KP	$2^{248}$	$2^8$	$2^{256}$	Sect. 5.3

$\dagger$ : The attacks cover  $x$  full rounds of AES.

## 2 Preliminaries

### 2.1 AES and Rijndael

AES-128/192/256 [17] is a 128-bit block cipher with a 128/192/256-bit key, respectively. In contrast, the block length of Rijndael [17] can be 128/192/256 bits. The state is treated as a  $4 \times N_{col}$  ( $N_{col} = 4, 6, 8$ ) two-dimensional array of bytes. The  $i$ -th ( $i \geq 0$ ,  $MC^{(-1)} = P$ ) round of Rijndael round function (Figure 2) typically consists of the following operations:

Table 2: A Summary of the attacks on Hash functions.

Target	Attacks	Methods	Rounds	Time	Memory	Generic	Ref.
Keccak[768]	Preimage	Rotational	4/24	$2^{378}$	-	$2^{384}$	[44]
		Linear Structure	4/24	$2^{375}$	-		[42]
		Algebraic	4/24	$2^{374}$	$2^{224}$		[22]
		MitM	4/24	$2^{367}$	<b><math>2^{157}</math></b>		Sect. I.3
Keccak[1024]	Preimage	Rotational	4/24	$2^{506}$	-	$2^{512}$	[44]
		MitM	4/24	$2^{504}$	$2^{108}$		[46]
		MitM	4/24	$2^{504}$	<b><math>2^{52}</math></b>		Sect. I.1
		Algebraic†	4/24	$2^{502}$	$2^{482}$		[22]
		MitM	4/24	$2^{500}$	<b><math>2^{118}</math></b>		Sect. I.2
Ascon-XOF	Preimage	MitM	3/12	$2^{120}$	$2^{39}$	$2^{128}$	[46]
		MitM	3/12	$2^{114}$	$2^{24}$		[18]
		MitM	3/12	$2^{114}$	<b><math>2^{14}</math></b>		Sect. H.1
		MitM	4/12	$2^{124}$	$2^{54}$		[46]
		MitM	4/12	$2^{124}$	$2^{34}$		[18]
		MitM	4/12	$2^{124}$	<b><math>2^{14}</math></b>		Sect. H.2
AES-256	Preimage	MitM	9/14	$2^{120}$	$2^8$	$2^{128}$	[2]
		MitM	10/14	$2^{120}$	$2^{56}$		[26]
		MitM	10/14	$2^{120}$	<b><math>2^8</math></b>		Sect. 4.6
Xoodoo-XOF 128-bit Tag	Preimage	MitM	3/12	$2^{125}$	$2^{97}$	$2^{128}$	[45]
		MitM	3/12	$2^{121}$	$2^{118}$		[27]
		MitM	3/12	$2^{121}$	<b><math>2^{37}</math></b>		Sect. G.1
	Collision	MitM	3/12	<b><math>2^{60.5}</math></b>	<b><math>2^{60.5}</math></b>	$2^{64}$	Sect. G.2
Gimli-XOF	Preimage	MitM	9/24	$2^{104}$	$2^{70}$	$2^{128}$	[41]
		MitM	10/24	$2^{125}$	$2^{64}$		Sect. J
Subterranean 2.0	Preimage	MitM	Full	$2^{160}$	$2^{100}$	$2^{224}$	[27]
		MitM	Full	$2^{152}$	$2^{91}$		Sect. K

- 180 – AddRoundKey (AK): XOR a round key  $RK^{(i)}$  into the state  $MC^{(i-1)}$  to pro-  
 181 duce  $A^{(i)}$ . The key schedule for AES is given in Figure 15, 16, 17 in Supple-  
 182 mentary Material B.
- 183 – SubBytes (SB): Substitute each cell of  $A^{(i)}$  according to an S-box to get  $SB^{(i)}$ .
- 184 – ShiftRows (SR): For  $N_{col} = 4, 6$ , rotate the  $i$ th row of  $SB^{(i)}$  to the left by  $i$   
 185 bytes ( $i = 0, 1, 2, 3$ ). For  $N_{col} = 8$ , rotate the 0, 1, 2, 3rd row to the left by  
 186 0, 1, 3, 4 bytes, respectively.
- 187 – MixColumns (MC): Update each column of  $SR^{(i)}$  by left-multiplying an MDS  
 188 matrix shown in Eq. (25) in Supplementary Material B to get  $MC^{(i)}$ .

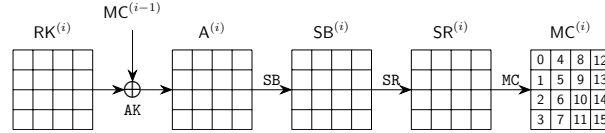


Fig. 2: One Round of AES

- 189 AES in FAEST [5]. FAEST is a 2nd-round candidate of NIST PQC - Additional  
 190 Digital Signature Schemes. FAEST's one-way function is defined using AES and

191 Rijndael. Taking the FAEST-128 as an example, which is based on AES-128, the  
 192 plaintext-ciphertext pair  $(P, C = \text{AES-128}(k, P))$  is used as the public key of the  
 193 signature scheme (verification key) and encryption key  $k$  is used as the secret  
 194 key (signing key). If an adversary can recover the encryption key  $k$  given only  
 195 a single plaintext-ciphertext pair  $(P, C)$  of AES-128, *i.e.*, the public key of the  
 196 signature scheme, then he can compute the secret signing key  $k$ . This allows  
 197 him to forge a signature by following exactly the honest prover protocol with  
 198 the recovered signing key  $k$ . This demonstrates that a key recovery attack with  
 199 one data complexity on AES-128 leads to a signature forgery on FAEST. In  
 200 FAEST-192/-256 based on AES-192/-256, the size of  $k$  is larger than the block  
 201 size, and FAEST-192/-256 uses two  $(P, C)$  pairs as the public key (verification  
 202 key). Because one  $(P, C)$  pair with only 128-bit information cannot prove a 192  
 203 or 256-bit knowledge of the secret signing key  $k$ . Therefore, the key-recovery  
 204 attack on AES-192/-256 with two plaintext-ciphertext pairs matters for FAEST-  
 205 192/-256. FAEST additionally uses Rijndael in Even-Mansour (EM) mode, *i.e.*,  
 206 FAEST-EM, where Rijndael block cipher is used as a permutation in EM mode.  
 207 The original key of Rijndael block cipher is published as part of the public key  
 208 (along with one plaintext-ciphertext), and the new block cipher Rijndael-EM's  
 209 key is the secret signing key. Therefore, the original key of Rijndael block cipher  
 210 is a known constant when performing the key-recovery attack on Rijndael-EM.

## 211 2.2 Preliminaries of Basic Meet-in-the-Middle Attack

212 The following notations will be used in the MitM framework.

Symbol	Description
$\mathcal{E}$	The encryption process.
$\mathcal{K}$	The key schedule process.
$I^{\mathcal{E}}/I^{\mathcal{K}}$	Starting state for encryption, key schedule, respectively.
$E^+/E^-$	Ending state for the forward/backward computation.
$\mathcal{B}^{\mathcal{E}}/\mathcal{B}^{\mathcal{K}}$	Blue cells ■ in starting state $I^{\mathcal{E}}/I^{\mathcal{K}}$ .
213 $\mathcal{R}^{\mathcal{E}}/\mathcal{R}^{\mathcal{K}}$	Red cells ■ in starting state $I^{\mathcal{E}}/I^{\mathcal{K}}$ .
$\mathcal{G}^{\mathcal{E}}/\mathcal{G}^{\mathcal{K}}$	Gray cells ■ in starting state $I^{\mathcal{E}}/I^{\mathcal{K}}$ .
$\mathcal{M}^+/\mathcal{M}^-$	Matching cells in the ending state $E^+/E^-$ .
$\lambda^+ =  \mathcal{B}^{\mathcal{E}}  +  \mathcal{B}^{\mathcal{K}} $	The initial degree of freedom for the forward computation.
$\lambda^- =  \mathcal{R}^{\mathcal{E}}  +  \mathcal{R}^{\mathcal{K}} $	The initial degree of freedom for the backward computation.
214 $\pi^+/\pi^-$	Certain constraints on the starting state.

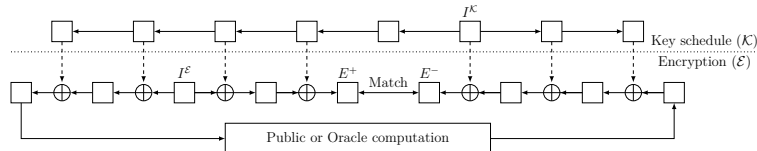


Fig. 3: A high-level overview of the MitM attacks [26]

At CRYPTO 2021, Dong *et al.* [26] gave a formal description of the MitM attack as shown in Figure 3. Assume that the states involved in the encryption ( $\mathcal{E}$ ) and key schedule ( $\mathcal{K}$ ) contain  $n$  and  $\bar{n}$   $w$ -bit cells, respectively. The public or oracle computation in Figure 3 can be a simple exclusive-or of a given target value for preimage attacks, or an oracle of block cipher for key-recovery attacks.

Dong *et al.* [26] specified several states for MitM in Figure 3, *i.e.*, two starting states  $I^\mathcal{E}, I^\mathcal{K}$ , the ending state  $E^+$  for the forward computation (the computation path starting from  $(I^\mathcal{E}, I^\mathcal{K})$  leading to  $E^+$ ), and similarly the ending state  $E^-$  for the backward computation. The cells of  $(I^\mathcal{E}, I^\mathcal{K})$  are partitioned into different subsets with different meanings. Let  $\mathcal{B}^\mathcal{E}, \mathcal{B}^\mathcal{K}, \mathcal{R}^\mathcal{E}, \mathcal{R}^\mathcal{K}, \mathcal{M}^+,$  and  $\mathcal{M}^-$  be some ordered subsets of  $\mathcal{N} = \{0, 1, \dots, n-1\}$  or  $\bar{\mathcal{N}} = \{0, 1, \dots, \bar{n}-1\}$  such that  $\mathcal{B}^\mathcal{E} \cap \mathcal{R}^\mathcal{E} = \emptyset, \mathcal{B}^\mathcal{K} \cap \mathcal{R}^\mathcal{K} = \emptyset, \mathcal{G}^\mathcal{E} = \mathcal{N} - \mathcal{B}^\mathcal{E} \cup \mathcal{R}^\mathcal{E}$  and  $\mathcal{G}^\mathcal{K} = \bar{\mathcal{N}} - \mathcal{B}^\mathcal{K} \cup \mathcal{R}^\mathcal{K}$ . The index sets are used to reference the cells of the states, *e.g.*, for a 16-cell state  $I$  and  $\mathcal{B}^\mathcal{E} = \{0, 1, 3\}$ , we have  $I[\mathcal{B}^\mathcal{E}] = I[0, 1, 3] = (I[0], I[1], I[3])$ .

The cells  $(I^\mathcal{E}[\mathcal{B}^\mathcal{E}], I^\mathcal{K}[\mathcal{B}^\mathcal{K}])$ , visualized as ■ cells, are called neutral words of the forward computation, and the cells  $(I^\mathcal{E}[\mathcal{R}^\mathcal{E}], I^\mathcal{K}[\mathcal{R}^\mathcal{K}])$ , visualized as ■ cells, are called neutral words of the backward computation. The initial degrees of freedom for the forward and backward computation are defined as  $\lambda^+ = |\mathcal{B}^\mathcal{E}| + |\mathcal{B}^\mathcal{K}|$  and  $\lambda^- = |\mathcal{R}^\mathcal{E}| + |\mathcal{R}^\mathcal{K}|$  respectively, that is, the numbers of ■ cells and ■ cells in the starting states.  $I^\mathcal{E}[\mathcal{G}^\mathcal{E}]$  and  $I^\mathcal{K}[\mathcal{G}^\mathcal{K}]$  are visualized as ■ cells. Define  $\ell^+$  functions  $\pi^+ = (\pi_1^+, \dots, \pi_{\ell^+}^+)$  whose values can be computed with the knowledge of the ■ cells  $(I^\mathcal{E}[\mathcal{G}^\mathcal{E}], I^\mathcal{K}[\mathcal{G}^\mathcal{K}])$  and ■ cells  $(I^\mathcal{E}[\mathcal{B}^\mathcal{E}], I^\mathcal{K}[\mathcal{B}^\mathcal{K}])$  in the starting states, where

$$\pi_i^+ : \mathbb{F}_2^{w \cdot (|\mathcal{G}^\mathcal{E}| + |\mathcal{G}^\mathcal{K}| + |\mathcal{B}^\mathcal{E}| + |\mathcal{B}^\mathcal{K}|)} \rightarrow \mathbb{F}_2^w$$

is a function mapping  $(I^\mathcal{E}[\mathcal{G}^\mathcal{E}], I^\mathcal{K}[\mathcal{G}^\mathcal{K}], I^\mathcal{E}[\mathcal{B}^\mathcal{E}], I^\mathcal{K}[\mathcal{B}^\mathcal{K}])$  to a  $w$ -bit word. Similarly, we define a sequence of  $\ell^-$  functions  $\pi^- = (\pi_1^-, \dots, \pi_{\ell^-}^-)$  whose values can be computed with the knowledge of the ■ cells  $(I^\mathcal{E}[\mathcal{G}^\mathcal{E}], I^\mathcal{K}[\mathcal{G}^\mathcal{K}])$  and ■ cells  $(I^\mathcal{E}[\mathcal{R}^\mathcal{E}], I^\mathcal{K}[\mathcal{R}^\mathcal{K}])$ .  $\pi^+$  and  $\pi^-$  will be used to represent certain constraints on the neutral words of the forward and backward computations, respectively, as given in Property 1.

*Property 1. For any fixed  $\mathbf{c}^+ = (a_1, \dots, a_{\ell^+}) \in \mathbb{F}_2^{w \cdot \ell^+}$  and  $\mathbf{c}^- = (b_1, \dots, b_{\ell^-}) \in \mathbb{F}_2^{w \cdot \ell^-}$ , when the cells  $(I^\mathcal{E}[\mathcal{G}^\mathcal{E}], I^\mathcal{K}[\mathcal{G}^\mathcal{K}])$  are fixed to an arbitrary constant, the neutral words fulfill the following systems:*

$$\begin{cases} \pi_1^+ (I^\mathcal{E}[\mathcal{G}^\mathcal{E}], I^\mathcal{K}[\mathcal{G}^\mathcal{K}], I^\mathcal{E}[\mathcal{B}^\mathcal{E}], I^\mathcal{K}[\mathcal{B}^\mathcal{K}]) = a_1 \\ \pi_2^+ (I^\mathcal{E}[\mathcal{G}^\mathcal{E}], I^\mathcal{K}[\mathcal{G}^\mathcal{K}], I^\mathcal{E}[\mathcal{B}^\mathcal{E}], I^\mathcal{K}[\mathcal{B}^\mathcal{K}]) = a_2 \\ \vdots \\ \pi_{\ell^+}^+ (I^\mathcal{E}[\mathcal{G}^\mathcal{E}], I^\mathcal{K}[\mathcal{G}^\mathcal{K}], I^\mathcal{E}[\mathcal{B}^\mathcal{E}], I^\mathcal{K}[\mathcal{B}^\mathcal{K}]) = a_{\ell^+} \end{cases} \quad \begin{cases} \pi_1^- (I^\mathcal{E}[\mathcal{G}^\mathcal{E}], I^\mathcal{K}[\mathcal{G}^\mathcal{K}], I^\mathcal{E}[\mathcal{R}^\mathcal{E}], I^\mathcal{K}[\mathcal{R}^\mathcal{K}]) = b_1 \\ \pi_2^- (I^\mathcal{E}[\mathcal{G}^\mathcal{E}], I^\mathcal{K}[\mathcal{G}^\mathcal{K}], I^\mathcal{E}[\mathcal{R}^\mathcal{E}], I^\mathcal{K}[\mathcal{R}^\mathcal{K}]) = b_2 \\ \vdots \\ \pi_{\ell^-}^- (I^\mathcal{E}[\mathcal{G}^\mathcal{E}], I^\mathcal{K}[\mathcal{G}^\mathcal{K}], I^\mathcal{E}[\mathcal{R}^\mathcal{E}], I^\mathcal{K}[\mathcal{R}^\mathcal{K}]) = b_{\ell^-} \end{cases} \quad (1) \quad (2)$$

Then  $E^+[\mathcal{M}^+]$  can be derived from neutral words  $(I^\mathcal{E}[\mathcal{B}^\mathcal{E}], I^\mathcal{K}[\mathcal{B}^\mathcal{K}])$  and  $E^-[\mathcal{M}^-]$  can be derived from neutral words  $(I^\mathcal{E}[\mathcal{R}^\mathcal{E}], I^\mathcal{K}[\mathcal{R}^\mathcal{K}])$ , independently.

For any given  $(I^\mathcal{E}[\mathcal{G}^\mathcal{E}], I^\mathcal{K}[\mathcal{G}^\mathcal{K}])$  and  $\mathbf{c}^+ = (a_1, \dots, a_{\ell^+})$ , the solution space of  $(I^\mathcal{E}[\mathcal{B}^\mathcal{E}], I^\mathcal{K}[\mathcal{B}^\mathcal{K}])$  induced by Eq. (1) is denoted by

$$\mathbb{B}(I^\mathcal{E}[\mathcal{G}^\mathcal{E}], I^\mathcal{K}[\mathcal{G}^\mathcal{K}], \mathbf{c}^+).$$

Since there are  $\lambda^+ = |\mathcal{B}^\mathcal{E}| + |\mathcal{B}^\mathcal{K}|$   $w$ -bit variables and  $\ell^+$  equations, we expect  $2^{w \cdot (\lambda^+ - \ell^+)}$  solutions, and we call  $\text{DoF}^+ = \lambda^+ - \ell^+$  the *degree of freedom (DoF)*



243 for the forward computation. Similarly, the solution space of  $(I^{\mathcal{E}}[\mathcal{R}^{\mathcal{E}}], I^{\mathcal{K}}[\mathcal{R}^{\mathcal{K}}])$   
 244 induced by Eq. (2) is denoted by  $\mathbb{R}(I^{\mathcal{E}}[\mathcal{G}^{\mathcal{E}}], I^{\mathcal{K}}[\mathcal{G}^{\mathcal{K}}], \mathbf{c}^-)$ , whose size is  $2^{w \cdot (\lambda^- - \ell^-)}$ .  
 245 We call  $\text{DoF}^- = \lambda^- - \ell^-$  the *DoF for the backward computation*. Assume the  
 246 computation connecting  $E^+[\mathcal{M}^+]$  and  $E^-[\mathcal{M}^-]$  forms an  $m$ -cell filter, which is  
 247 denoted as the degree of matching ( $\text{DoM} = m$ ). The MitM attack is Algorithm  
 248 1. To find a preimage of  $h$ -cell target, the complexity of Algorithm 1 is about

$$(2^w)^{h - \min\{\text{DoF}^+, \text{DoF}^-, \text{DoM}\}} + \mathcal{T}_{pre}, \quad (3)$$

249 where  $\mathcal{T}_{pre}$  is the time complexity to precompute  $\mathbb{B}(I^{\mathcal{E}}[\mathcal{G}^{\mathcal{E}}], I^{\mathcal{K}}[\mathcal{G}^{\mathcal{K}}], \mathbf{c}^+)$  and  
 250  $\mathbb{R}(I^{\mathcal{E}}[\mathcal{G}^{\mathcal{E}}], I^{\mathcal{K}}[\mathcal{G}^{\mathcal{K}}], \mathbf{c}^-)$  in Line 2.

---

**Algorithm 1: The MitM Attack**

---

- 1 Assign  $(I^{\mathcal{E}}[\mathcal{G}^{\mathcal{E}}], I^{\mathcal{K}}[\mathcal{G}^{\mathcal{K}}])$  and  $\mathbf{c}^+$ , and  $\mathbf{c}^-$  to some constants.
  - 2 Solve Eq. (1) and (2) to obtain  $\mathbb{B}(I^{\mathcal{E}}[\mathcal{G}^{\mathcal{E}}], I^{\mathcal{K}}[\mathcal{G}^{\mathcal{K}}], \mathbf{c}^+)$  and  
 $\mathbb{R}(I^{\mathcal{E}}[\mathcal{G}^{\mathcal{E}}], I^{\mathcal{K}}[\mathcal{G}^{\mathcal{K}}], \mathbf{c}^-)$ .
  - 3 For values in  $\mathbb{B}(I^{\mathcal{E}}[\mathcal{G}^{\mathcal{E}}], I^{\mathcal{K}}[\mathcal{G}^{\mathcal{K}}], \mathbf{c}^+)$ , compute  $E^+[\mathcal{M}^+]$  and insert it into  $L$
  - 4 For values in  $\mathbb{R}(I^{\mathcal{E}}[\mathcal{G}^{\mathcal{E}}], I^{\mathcal{K}}[\mathcal{G}^{\mathcal{K}}], \mathbf{c}^-)$ , compute  $E^-[\mathcal{M}^-]$  to match  $L$
  - 5 In case of partial-matching exists in the above step, for the surviving pairs,  
 check for a full-state match. In case none of them are fully matched, repeat  
 the procedure by changing the values of fixed bytes till finding a full match.
- 

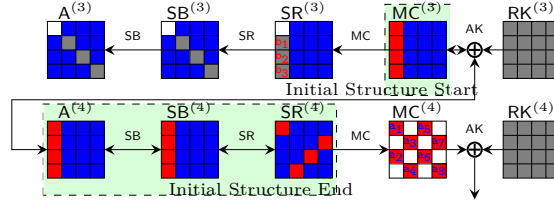


Fig. 4: Sasaki and Aoki's initial structure of MitM attack on AES

251 **Sasaki and Aoki's Initial Structure [50].** In Line 2 of Algorithm 1, we  
 252 have to solve Eq. (1) and (2). In most previous MitM attacks, the system of  
 253 equations is linear and easy to solve [49,2]. At EUROCRYPT 2009, Sasaki and  
 254 Aoki formalized this linear case as the *initial structure* technique [50]. Take the  
 255 *initial structure* of Sasaki's 7-round MitM attack [49] on AES as an example  
 256 (also given in Figure 14), which covers from state  $\text{MC}^{(3)}$  to  $\text{SR}^{(4)}$  in Figure 4,  
 257 where the red/blue neutral words satisfy some linear equation system, *i.e.*, the  
 258 cancellations are linear. For example, Eq. (4) are the linear computations for red

259 neutral words,

$$\begin{cases} b_1 = 9 \cdot \text{MC}^{(3)}[0] \oplus e \cdot \text{MC}^{(3)}[1] \oplus b \cdot \text{MC}^{(3)}[2] \oplus d \cdot \text{MC}^{(3)}[3] \\ b_2 = d \cdot \text{MC}^{(3)}[0] \oplus 9 \cdot \text{MC}^{(3)}[1] \oplus e \cdot \text{MC}^{(3)}[2] \oplus b \cdot \text{MC}^{(3)}[3] \\ b_3 = b \cdot \text{MC}^{(3)}[0] \oplus d \cdot \text{MC}^{(3)}[1] \oplus 9 \cdot \text{MC}^{(3)}[2] \oplus e \cdot \text{MC}^{(3)}[3] \end{cases}, \quad (4)$$

260 where  $\mathbf{c}^- = (b_1, b_2, b_3)$ ,  $\ell^- = 3$ . After satisfying the cancellations in Eq. (4), the  
 261 value space of the red neutral words  $\text{MC}^{(3)}[0-3]$  is reduced from  $2^{w \cdot \lambda^-} = 2^{8 \times 4}$   
 262 to  $2^{w \cdot (\lambda^- - \ell^-)} = 2^8$ , and the value of  $\text{MC}^{(3)}[0-3]$  from the space of size  $2^8$   
 263 has a constant impact on the backward computation. The value space of neutral  
 264 words is easily obtained by solving the linear system Eq. (4). Therefore, the time  
 265 complexity  $\mathcal{T}_{pre}$  in Eq. (3) is usually ignored [49, 2].

266 **Dong *et al.*'s Nonlinear Constrained Neutral Words [26].** As noticed by  
 267 Dong *et al.* [26], the Eq. (1) and (2) of many interesting MitM characteristics  
 268 are nonlinear systems in practice, and there is no efficient method to solve them.  
 269 Therefore, Dong *et al.* presented a table-based technique in Algorithm 2 which  
 270 can be applied in attacks relying on such MitM characteristics without solving  
 271 the equations. The major drawback of Dong *et al.*'s approach is that it would  
 272 require a huge amount of memory to prepare two hash tables  $V$  and  $U$ , and  
 273 many attacks based on this method need huge memory, *e.g.*, [26, 45].

---

**Algorithm 2:** Computing the solution spaces of the neutral words

---

**Input:**  $(I^\mathcal{E}[\mathcal{G}^\mathcal{E}], I^\mathcal{K}[\mathcal{G}^\mathcal{K}]) \in \mathbb{F}_2^{w \cdot (|\mathcal{G}^\mathcal{E}| + |\mathcal{G}^\mathcal{K}|)}$   
**Output:**  $V, U$

```

1  $V \leftarrow [], U \leftarrow []$ 
2 for  $(I^\mathcal{E}[\mathcal{B}^\mathcal{E}], I^\mathcal{K}[\mathcal{B}^\mathcal{K}]) \in \mathbb{F}_2^{w \cdot (|\mathcal{B}^\mathcal{E}| + |\mathcal{B}^\mathcal{K}|)}$  do
3    $\mathbf{v} \leftarrow \pi^+(I^\mathcal{E}[\mathcal{G}^\mathcal{E}], I^\mathcal{K}[\mathcal{G}^\mathcal{K}], I^\mathcal{E}[\mathcal{B}^\mathcal{E}], I^\mathcal{K}[\mathcal{B}^\mathcal{K}])$  by Eq. (1)
4   Insert  $(I^\mathcal{E}[\mathcal{B}^\mathcal{E}], I^\mathcal{K}[\mathcal{B}^\mathcal{K}])$  into  $V$  at index  $\mathbf{v}$ 
5 end
6 for  $(I^\mathcal{E}[\mathcal{R}^\mathcal{E}], I^\mathcal{K}[\mathcal{R}^\mathcal{K}]) \in \mathbb{F}_2^{w \cdot (|\mathcal{R}^\mathcal{E}| + |\mathcal{R}^\mathcal{K}|)}$  do
7    $\mathbf{u} \leftarrow \pi^-(I^\mathcal{E}[\mathcal{G}^\mathcal{E}], I^\mathcal{K}[\mathcal{G}^\mathcal{K}], I^\mathcal{E}[\mathcal{R}^\mathcal{E}], I^\mathcal{K}[\mathcal{R}^\mathcal{K}])$  by Eq. (2)
8   Insert  $(I^\mathcal{E}[\mathcal{R}^\mathcal{E}], I^\mathcal{K}[\mathcal{R}^\mathcal{K}])$  into  $U$  at index  $\mathbf{u}$ 
9 end
```

---

### 274 2.3 Triangulation Algorithm (TA)

275 The triangulation algorithm (TA) was introduced by Khovratovich, Biryukov,  
 276 and Nikolic [34] at CT-RSA 2009, which is a Gaussian-like elimination pro-  
 277 cess to solve the nonlinear system. The algorithm expresses all transformations

as equations that link the internal variables. Variables refer to bits or bytes/-words depending on the trail. In the triangulation algorithm, *free variables* form the basis of the nonlinear system, which are to be assigned with arbitrary values. The variables that can be determined by the free variables are called *dependent variables*. The idea is to build a set of *dependent variables* that includes many variables. The more such variables we have among the dependent variables, the more conditions are satisfied at no cost. The heart of the triangulation algorithm is to search for dependent variables. The formal process can be described as follows.

1. Given the system of equations with fixed predefined values as constants.
2. Label all variables and equations as unprocessed. Initially, all variables and equations are marked as unprocessed, meaning they have not yet been simplified or solved.
3. Identify a variable that appears in only one unprocessed equation. Label both the variable and the corresponding equation as processed. If there is no such variable, label all the unprocessed equations as processed, exit.
4. Repeat Step 3 if there are still unprocessed equations.
5. If all equations have been processed, mark all the remaining unprocessed variables as free variables.
6. Assign random values to free variables and compute the remaining variables.

For example, Eq. (5) is a nonlinear system of 7 byte-variables  $s, t, u, v, x, y, z \in \mathbb{F}_2^8$ , and  $F, G, H$ , and  $L$  are bijective functions. After applying TA, we get Eq. (6), where  $x$  and  $s$  are free variables and by varying them we deduce the values of the other 5 dependent variables.

$$\left\{ \begin{array}{l} F(x \oplus s) \oplus v = 0, \\ G(x \oplus u) \oplus s \oplus L(y \oplus z) = 0, \\ v \oplus G(u \oplus s) = 0, \\ H(z \oplus s \oplus v) \oplus t = 0, \\ u \oplus H(t \oplus x) = 0, \end{array} \right. \quad (5) \quad \left\{ \begin{array}{l} L(y \oplus z) \oplus G(u \oplus x) \oplus s = 0, \\ z \oplus H^{-1}(t \oplus v \oplus s) = 0, \\ t \oplus H^{-1}(u \oplus x) = 0, \\ u \oplus G^{-1}(v \oplus s) = 0, \\ v \oplus F(x \oplus s) = 0. \end{array} \right. \quad (6)$$

The TA algorithm is used by Khovratovich *et al.* to speed up the collision search on AES hashing mode [34]. They described the hash function as a system of equations with S-boxes, and added equations to force the message and chaining value to obey their differential characteristic inside the function. Solving these equations will produce a collision. At CRYPTO 2022, Dong *et al.* combined the TA and rebound attack [43] to propose the triangulating rebound attack [25], where the TA is used to solve certain nonlinear system to connect multiple inbound phases efficiently. Therefore, TA was mainly exploited in differential attacks previously, and in this paper we will exploit TA in MitM attacks.

### 3 Triangulating MitM Attack Framework

#### 3.1 Limitations of Khovratovich *et al.*'s TA.

The previous triangulation algorithm faces a significant limitation in Step 3 to Step 5 in Sect. 2.3 when there are still many unprocessed equations, but

no variable exists in only one equation. For example, if there is another byte-equation

$$P(s \oplus v \oplus t) \oplus z = 0, \quad (7)$$

then together with Eq. (5), only one dependent variable  $y$  can be obtained. Similar to [34], consider the equation system as a *matrix of dependencies*, where the rows correspond to equations, and the columns to variables. In Eq. (8), the matrix before TA represents the system combining Eq. (5) and the additional Eq. (7). When applying Khovratovich *et al.*'s TA given in Sect. 2.3, after determining one dependent variable  $y$ , the remaining six variables in the remaining 5 equations would be directly marked as free variables since there is no variable that appears in only one unprocessed equation, and the TA terminates. We move the 5 equations to the top of the right matrix of Eq. (8) and mark them in cyan. In this case, Khovratovich *et al.*'s TA can not reduce the system and eliminate potential free variables further. Then, we have to randomly assign values for the six free variables  $s, t, u, v, x, z \in \mathbb{F}_2^8$  and check if the 5 byte-equations (the first 5 rows in cyan) are satisfied, whose probability is  $2^{-40}$ . Once satisfied,  $y$  is deduced to satisfy the last equation. The time complexity is around  $2^{40}$ .

$$\text{Before TA: } \begin{pmatrix} s & t & u & v & x & y & z \\ 1 & 0 & 0 & 1 & 1 & 0 & 0 \\ 1 & 0 & 1 & 0 & 1 & 1 & 1 \\ 1 & 0 & 1 & 1 & 0 & 0 & 0 \\ 1 & 1 & 0 & 1 & 0 & 0 & 1 \\ 0 & 1 & 1 & 0 & 1 & 0 & 0 \\ 1 & 1 & 0 & 1 & 0 & 0 & 1 \end{pmatrix} \xrightarrow[\text{Khovratovich } et al.'s \text{ TA}]{\text{after extract } y} \begin{pmatrix} y & s & t & u & v & x & z \\ 0 & 1 & 0 & 1 & 1 & 0 & 0 \\ 0 & 1 & 0 & 1 & 1 & 0 & 0 \\ 0 & 1 & 1 & 0 & 1 & 0 & 1 \\ 0 & 0 & 1 & 1 & 0 & 1 & 0 \\ 0 & 1 & 1 & 0 & 1 & 0 & 1 \\ 1 & 1 & 0 & 1 & 0 & 1 & 1 \\ \hline & & & & & & \text{free variables} \end{pmatrix} \quad (8)$$

### 3.2 Improved Triangulation Algorithm with Structured Gaussian Elimination

**Structured Gaussian elimination (SGE).** At 1990 and 1999, LaMacchia *et al.* [37] and Bender *et al.* [6] proposed the structured Gaussian elimination (SGE) paradigm, which solves the large and sparse linear system efficiently. Consider the linear system of equations of the form  $M\mathbf{x} = \mathbf{0}$ , where  $M$  is the coefficient matrix of the linear system. The SGE steps of LaMacchia *et al.* [37] can be summarized roughly as follows:

1. Delete all the columns that have a single non-zero coefficient and the rows in which those columns have non-zero coefficients (this step is similar to step 3 of Khovratovich *et al.*'s TA).
  2. For any row which has only a single non-zero coefficient, subtract appropriate multiples of that row from all other rows that have non-zero coefficients on that column so as to make those coefficients 0. This step can reduce the matrix without introducing new non-zero coefficients for other rows.
- However, for nonlinear system, this step usually does not help. E.g. in Eq. (8), the matrix is different from the coefficient matrix of the linear system. In Eq. (8), the non-zero entry of the matrix means the variable exists in the corresponding nonlinear equation, *i.e.*, the variable may exist in multiple linear or nonlinear terms in that equation. Therefore, one cannot apply similar step to reduce the rows for nonlinear system.

- 353 3. Delete some rows which have the largest number of non-zero elements. Apply  
 354 this step when steps 1 and 2 are not possible.  
 355 We apply this step when the Khovratovich *et al.*'s TA cannot proceed.

356 **Improved TA with the idea of SGE.** The improvements happen to Step 3 to  
 357 Step 5 of Khovratovich *et al.*'s TA by a similar approach of the SGD [37,6], *i.e.*,  
 358 when we are stuck and cannot determine any new dependent variable, greedily  
 359 remove the biggest equation that have the largest number of non-zero element  
 360 (that we will have to satisfy stochastically) and until we can make progress.  
 361 Specifically, we introduce a new rule to process the system (highlighted in italics),  
 362 and the modified algorithm proceeds as follows.

- 363 1. **Construct the system of equations:** Given the system of equations, fix  
 364 the predefined values to constants.
- 365 2. **Initialize all variables and equations as unprocessed:** Mark all vari-  
 366 ables and all equations as unprocessed.
- 367 3. **Find the variable involved in only one unprocessed equation:**
  - 368 (a) Search for a variable that appears in only one unprocessed equation. If  
 369 such a variable exists, mark the equation and the variable as processed.
  - 370 (b) *If no such variable can be found, perform the following steps:*
    - 371 i. *Count the number of variables present in each unprocessed equation.*
    - 372 ii. *Identify the unprocessed equations that contain the largest number of*  
 373 *variables.*
    - 374 iii. *Remove one of the equations in (ii) from the system and mark it as*  
 375 *processed. This reduces the scale of the remaining system.*
- 376 4. **Repeat Step 3 until all equations have been processed:** *Continue*  
 377 *searching for variables involved in a single equation or removing equations*  
 378 *with the maximum number of variables until no unprocessed equations exist.*
- 379 5. **Assign free variables:** After all equations are processed, mark all remain-  
 380 ing unprocessed variables as free.
- 381 6. **Solve the system:** Assign random values to the free variables. Using these  
 382 values, compute the remaining variables by substituting them back into the  
 383 processed equations.

384 This enhancement ensures that the system is further simplified even when no  
 385 variable appears in a single equation. By strategically removing the equation with  
 386 the largest number of variables, we reduce the remaining system and maximize  
 387 the opportunities for variable elimination. At last, fewer variables are marked as  
 388 free, leading to a more efficient solution process.

389 Now let's continue to consider the example in Eq. (8), the whole process is  
 390 illustrated in Eq. (9). After extracting  $y$ , instead of immediately marking the  
 391 remaining variables as free, we analyze the number of variables included in each  
 392 remaining unprocessed equation and prioritize the equations with the largest  
 393 number of variables (4-th and 6-th row in the first matrix of Eq. (9)), which  
 394 are highlighted in **bold**. Label one of them as processed and remove it from



---

**Algorithm 3:** Computing the value space of the neutral words with New TA and a memory-aided precomputation

---

**Input:**  $(I^{\mathcal{E}}[\mathcal{G}^{\mathcal{E}}], I^{\mathcal{K}}[\mathcal{G}^{\mathcal{K}}]) \in \mathbb{F}_2^{w \cdot (|\mathcal{G}^{\mathcal{E}}| + |\mathcal{G}^{\mathcal{K}}|)}$

```

1 for  $(b_2, b_6, b_5, b_3, b_1) \in \mathbb{F}_2^{8 \times 5}$  do
2    $V \leftarrow [], U \leftarrow []$ 
3   for  $(x, s) \in \mathbb{F}_2^{8 \times 2}$  do
4     Compute  $v$  from  $\pi_1^-()$ 
5     Compute  $u$  from  $\pi_3^-()$ 
6     Compute  $t$  from  $\pi_5^-()$ 
7     Compute  $z$  from  $\pi_6^-()$ 
8     Compute  $y$  from  $\pi_2^-()$ 
9     Compute  $\mathbf{u} = b_4$  by equations marked by cyan
10    Store  $U[\mathbf{u}] \leftarrow (x, s, v, u, t, z, y)$ 
11  end
12  Similarly, we can prepare  $V$ 
13  Then, under each index  $i, j$ , compute the values from  $U[i]$  backward, and
    independently, compute the values from  $V[j]$  forward, and filter the
    states by the matching point.
14 end

```

---

Eq. (10). After all variables are determined, compute  $b_4$  by  $\pi_4^-()$  as the index  $\mathbf{u}$ . In Algorithm 3, the  $2^8$  solution spaces of  $\mathbb{R}(I^{\mathcal{E}}[\mathcal{G}^{\mathcal{E}}], I^{\mathcal{K}}[\mathcal{G}^{\mathcal{K}}], \mathbf{c}^-)$ , with  $|\mathbb{R}(I^{\mathcal{E}}[\mathcal{G}^{\mathcal{E}}], I^{\mathcal{K}}[\mathcal{G}^{\mathcal{K}}], \mathbf{c}^-)| = 2^{8 \cdot (\lambda^- - \ell^-)} = 2^8$ , are stored in  $U$  in Line 10. Therefore, only the lower 5 nonlinear equations in the right system of Eq. (10) are actually solved, whose solutions are all stored in  $U$  under different index  $\mathbf{u}$ . We call this method to prepare the solution space of neutral words as a combination of improved TA with memory-aided precomputation. At last, the size to store  $U$  is about  $2^{16} \cdot 7$  bytes. Compared to Dong *et al.*'s method, the memory is significantly reduced from  $2^{56} \cdot 7$  bytes to  $2^{16} \cdot 7$  bytes.

### 3.4 Automatic Triangulating MitM

The full search framework of our attacks consists of two steps:

1. The first step is to use the existing MILP models for MitM attacks on AES and other primitives to find massive MitM paths.  
E.g., for AES we use Dong *et al.*'s model [26] to search potential MitM paths, and more than 1000 MitM paths are found for 5-round AES-128.
2. The second step is to apply the improved TA to each MitM path to solve the systems of the nonlinear constrained neutral words (e.g., Eq. (2) and (1)) and recognize the good MitM path with improved memory complexity.

**Comparison with the guess-and-determine approach in [11].** At CRYPTO 2011, Bouillaguet, Derbez, and Fouque [11] introduced a powerful automatic tool

for searching guess-and-determine and MitM attacks on byte-oriented symmetric primitives by programming techniques such as knowledge propagation and some pruning techniques. The tool automatically and exhaustively searches all possible sets of “free variables” to find a good one, leading to the exploration of a large search tree. The complexity of the exhaustive search is inherently exponential and exploring the whole space might not be feasible.

Our improved TA developed from the structured Gaussian elimination [37,6] does not explore the full space. Therefore, for certain nonlinear byte-equation systems, our algorithm may output weaker solutions than Bouillaguet *et al.*’s tool. However, as shown in our search framework, we first automatically find massive MitM paths and then solve many nonlinear systems for those MitM paths. Hence, the method used to solve nonlinear systems should be very efficient. The time complexity of our improved TA is linear with the number of equations, which is very suitable for our search framework. The guess-and-determine algorithm in [11] exhausted all possible solutions, but it can be slow because so many nonlinear systems should be solved. Moreover, our improved TA is also efficient when the system is huge (e.g., 299 nonlinear equations with 316 variables in Supplementary Material I.3), where the algorithm in [11] may not output solutions in a reasonable time.

Furthermore, in our triangulating MitM attacks, we are not solving the full nonlinear system to get the solution space of the neutral words. As explained in Sect. 3.3, we actually combine the improved TA with the memory-aided precomputation to compute the solution space of neutral words. This core idea is well explained in our 5-round attack on AES-128 in Sect. 4.1. For example, in Eq. (13)-(f), our triangulating MitM first automatically selects a system of 5 byte-equations and solves it for each value of the 5-byte value  $(\widehat{A}^{(2)}[4], \widehat{RK}^{(2)}[12, 13], \widehat{A}^{(1)}[3, 4])$ . Then, store all the solutions in a hash table under the index of 4-byte value  $\mathbf{u} = (\widehat{SR}^{(3)}[1, 4], \widehat{RK}^{(5)}[0], \widehat{A}^{(1)}[14])$  (see Line 7-9 in Algorithm 4). Therefore, all the solutions of the 5 byte-equations are stored under different index of the table  $U$  and no solutions are filter out, since they are all useful in the following MitM procedures. Our improved TA is very suitable for the memory-aided precomputation, since it directly identifies these 5 byte-equations.

## 4 Attacks on Reduced AES with One/Two Plaintexts

### 4.1 Single-Plaintext Key-Recovery Attack on 5-round AES-128

The 5-round MitM characteristic is shown in Figure 5, where green cells  $\blacksquare$  mean linear combinations of  $\blacksquare$  and  $\blacksquare$ . In the MitM path, the starting state  $RK^{(0)}$ , whose bytes are denoted as  $k_0$  to  $k_{15}$ , contains  $\lambda^+ = 4$   $\blacksquare$  bytes and  $\lambda^- = 12$   $\blacksquare$  bytes. In the computation from  $RK^{(0)}$  to  $RK^{(5)}$ , from  $A^{(0)}$  to  $SR^{(2)}$ , and from  $SR^{(4)}$  to  $MC^{(2)}$ , the consumed degrees of freedom (DoFs) of  $\blacksquare$  and  $\blacksquare$  are  $\ell^+ = 3$  and  $\ell^- = 9$  bytes, respectively. Therefore,  $\text{DoF}^+ = 1$ ,  $\text{DoF}^- = 3$ , and there is  $\text{DoM} = 1$  matching byte in round 2. The 9 consumed DoFs of  $\blacksquare$  on  $A^{(1)}[3]$ ,  $A^{(1)}[4]$ ,



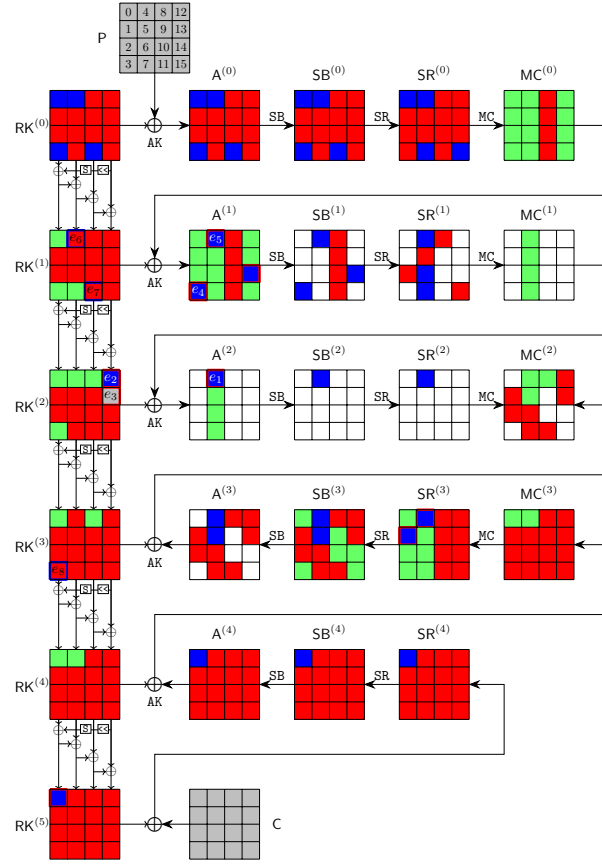


Fig. 5: 5-round attack on AES-128

483  $A^{(1)}[14]$ ,  $RK^{(2)}[12]$ ,  $RK^{(2)}[13]$ ,  $A^{(2)}[4]$ ,  $SR^{(3)}[1]$ ,  $SR^{(3)}[4]$ , and  $RK^{(5)}[0]$  marked by  
 484  $\blacksquare/\blacksquare$  in Figure 5 are a system on the byte-variables of  $RK^{(0)}$  in Eq. (11).

$$\left\{ \begin{array}{l} A^{(1)}[3] = S(k_5) \oplus S(k_{10}) \oplus 2 \cdot S(k_{15}) \oplus S(k_{12}) \oplus 3 \cdot S(k_0) \oplus k_3 \\ A^{(1)}[4] = 3 \cdot S(k_9) \oplus S(k_{14}) \oplus S(k_{13}) \oplus 2 \cdot S(k_4) \oplus k_4 \oplus S(k_3) \oplus k_0 \\ A^{(1)}[14] = S(k_{12}) \oplus S(k_1) \oplus 2 \cdot S(k_6) \oplus k_{14} \oplus k_{10} \oplus k_6 \oplus k_2 \oplus S(k_{15}) \oplus 3 \cdot S(k_{11}) \\ A^{(2)}[4] = 3 \cdot S(S(k_8) \oplus 2 \cdot S(k_{13}) \oplus 3 \cdot S(k_2) \oplus S(k_7) \oplus k_9 \oplus k_5 \oplus k_1 \oplus S(k_{14})) \oplus \\ \quad S(k_{13} \oplus k_9 \oplus k_5 \oplus k_1 \oplus S(k_{14})) \oplus k_4 \oplus S(A^{(1)}[3]) \oplus 2 \cdot S(A^{(1)}[4]) \oplus S(A^{(1)}[14]) \\ RK^{(2)}[12] = k_{12} \oplus S(k_{13} \oplus k_9 \oplus k_5 \oplus k_1 \oplus S(k_{14})) \oplus k_4 \\ RK^{(2)}[13] = k_{13} \oplus k_5 \oplus S(k_{14} \oplus k_{10} \oplus k_6 \oplus k_2 \oplus S(k_{15})) \\ SR^{(3)}[1] = 9 \cdot (S(RK^{(0)}[13]) \oplus S(RK^{(1)}[13]) \oplus S(RK^{(2)}[13]) \oplus S(RK^{(3)}[13])) \oplus \\ \quad e \cdot (MC^{(3)}[1]) \oplus b \cdot (MC^{(3)}[2]) \oplus d \cdot (MC^{(3)}[3]) \oplus 9 \cdot (RK^{(0)}[0] \oplus A^{(4)}[0]) \\ SR^{(3)}[4] = e \cdot (S(RK^{(0)}[13]) \oplus S(RK^{(1)}[13]) \oplus S(RK^{(2)}[13]) \oplus S(RK^{(3)}[13]) \oplus RK^{(3)}[4] \oplus A^{(4)}[4]) \\ \quad \oplus b \cdot (MC^{(3)}[5]) \oplus d \cdot (MC^{(3)}[6]) \oplus 9 \cdot (MC^{(3)}[7]) \oplus e \cdot (RK^{(0)}[0]) \\ RK^{(5)}[0] = S(RK^{(0)}[13]) \oplus S(RK^{(1)}[13]) \oplus S(RK^{(2)}[13]) \oplus S(RK^{(3)}[13]) \oplus S(RK^{(4)}[13]) \oplus RK^{(0)}[0] \end{array} \right. \quad (11)$$

485 Excluding the parts of Eq. (11) related to blue bytes, we get Eq. (12) which is  
 486 only related to the red bytes, where the boxed parts are deleted<sup>5</sup>.

$$\left\{ \begin{array}{l} \hat{A}^{(1)}[3] = S(k_5) \oplus S(k_{10}) \oplus 2 \cdot S(k_{15}) \oplus S(k_{12}) \oplus 3 \cdot S(k_0) \oplus k_3 \\ \hat{A}^{(1)}[4] = 3 \cdot S(k_9) \oplus S(k_{14}) \oplus S(k_{13}) \oplus 2 \cdot S(k_4) \oplus k_4 \oplus S(k_3) \oplus k_0 \\ \hat{A}^{(1)}[14] = S(k_{12}) \oplus S(k_1) \oplus 2 \cdot S(k_6) \oplus k_{14} \oplus k_{10} \oplus k_6 \oplus k_2 \oplus S(k_{15}) \oplus 3 \cdot S(k_{11}) \\ \hat{A}^{(2)}[4] = 3 \cdot S(S(k_8) \oplus 2 \cdot S(k_{13}) \oplus 3 \cdot S(k_2) \oplus S(k_7) \oplus k_9 \oplus k_5 \oplus k_1 \oplus S(k_{14})) \oplus S(k_{13} \oplus k_9 \oplus k_5 \\ \quad \oplus k_1 \oplus S(k_{14})) \oplus k_4 \oplus S(\hat{A}^{(1)}[3] \oplus B_1) \oplus 2 \cdot S(\hat{A}^{(1)}[4] \oplus B_2) \oplus S(\hat{A}^{(1)}[14] \oplus B_3) \\ \widehat{RK}^{(2)}[12] = k_{12} \oplus S(k_{13} \oplus k_9 \oplus k_5 \oplus k_1 \oplus S(k_{14})) \oplus k_4 \\ \widehat{RK}^{(2)}[13] = k_{13} \oplus k_5 \oplus S(k_{14} \oplus k_{10} \oplus k_6 \oplus k_2 \oplus S(k_{15})) \\ \widehat{SR}^{(3)}[1] = 9 \cdot (S(RK^{(0)}[13]) \oplus S(RK^{(1)}[13]) \oplus S(\widehat{RK}^{(2)}[13]) \oplus S(RK^{(3)}[13])) \oplus \\ \quad e \cdot (MC^{(3)}[1]) \oplus b \cdot (MC^{(3)}[2]) \oplus d \cdot (MC^{(3)}[3]) \oplus 9 \cdot (RK^{(0)}[0] \oplus A^{(4)}[0]) \\ \widehat{SR}^{(3)}[4] = e \cdot (S(RK^{(0)}[13]) \oplus S(RK^{(1)}[13]) \oplus S(\widehat{RK}^{(2)}[13]) \oplus S(RK^{(3)}[13]) \oplus RK^{(3)}[4] \oplus A^{(4)}[4]) \\ \quad \oplus b \cdot (MC^{(3)}[5]) \oplus d \cdot (MC^{(3)}[6]) \oplus 9 \cdot (MC^{(3)}[7]) \oplus e \cdot (RK^{(0)}[0]) \\ \widehat{RK}^{(5)}[0] = S(RK^{(0)}[13]) \oplus S(RK^{(1)}[13]) \oplus S(\widehat{RK}^{(2)}[13]) \oplus S(RK^{(3)}[13]) \oplus S(RK^{(4)}[13]) \oplus RK^{(0)}[0] \end{array} \right. \quad (12)$$

487 where  $B_1 = 3 \cdot S(k_0) \oplus k_3$ ,  $B_2 = 2 \cdot S(k_4) \oplus k_4 \oplus S(k_3) \oplus k_0$ ,  $B_3 = 3 \cdot S(k_{11})$ .  
 488 The Eq. (12) is first expressed as the matrix (a) in Eq. (13), where the rows  
 489 correspond to the equations and the columns to variables. Apply our new TA:

- 490 1. At the beginning, in matrix (a), no variable appears in only one unprocessed  
 491 equation. Count the number of variables present in each unprocessed equa-  
 492 tion; there are 3 unprocessed equations that contain 12 variables, which are  
 493 highlighted in **bold**.
- 494 2. Remove the 3 bold rows and label them as processed by moving them to the  
 495 top of the matrix highlighted in cyan. We get the matrix (b).

<sup>5</sup>In our MitM attack (see Line 14 to 27 of Algorithm 4), we need the 9 bytes  $(A^{(1)}[3], A^{(1)}[4], \dots)$  on the left side of Eq. (11) (the bytes marked in red border in Figure 5) to depend only on the blue/gray bytes. Therefore, we specify the red parts in Eq. (12) as global constants  $(\hat{A}^{(1)}[3], \hat{A}^{(1)}[4], \dots)$ , so that the red bytes have a constant effect on the 9 bytes  $(A^{(1)}[3], A^{(1)}[4], \dots)$ .

- 496 3. Process the last 6 rows of (b) with TA and extract a dependent variable  $k_7$   
497 marked by green. We get the matrix (c).  
498 4. Process the last 5 rows of (c). No variable appears in only one unprocessed  
499 equation, we count and remove the unprocessed equation that contains the  
500 most number of variables, *i.e.*, row  $\widehat{A}^{(1)}[14]$  and get the matrix (d).  
501 5. Process the last 4 rows of matrix (d) and extract  $k_1, k_2, k_5, k_9$  sequentially  
502 to get the matrix (f).

$$\begin{aligned}
& \left( \begin{array}{c|cccccccccccccc} & k_1 & k_2 & k_5 & k_6 & k_7 & k_8 & k_9 & k_{10} & k_{12} & k_{13} & k_{14} & k_{15} \\ \hline \widehat{A}^{(1)}[3] & 0 & 0 & 1 & 0 & 0 & 0 & 0 & 1 & 1 & 0 & 0 & 1 \\ \widehat{A}^{(1)}[4] & 0 & 0 & 0 & 0 & 0 & 0 & 1 & 0 & 0 & 1 & 1 & 0 \\ \widehat{A}^{(1)}[14] & 1 & 1 & 0 & 1 & 0 & 0 & 0 & 1 & 1 & 0 & 1 & 1 \\ \widehat{A}^{(2)}[4] & 1 & 1 & 1 & 0 & 1 & 1 & 1 & 0 & 0 & 1 & 1 & 0 \\ \widehat{RK}^{(2)}[12] & 1 & 0 & 1 & 0 & 0 & 0 & 1 & 0 & 1 & 1 & 1 & 0 \\ \widehat{RK}^{(2)}[13] & 0 & 1 & 1 & 1 & 0 & 0 & 0 & 1 & 0 & 1 & 1 & 1 \\ \widehat{SR}^{(3)}[1] & 1 & 1 & 1 & 1 & 1 & 1 & 1 & 1 & 1 & 1 & 1 & 1 \\ \widehat{SR}^{(3)}[4] & 1 & 1 & 1 & 1 & 1 & 1 & 1 & 1 & 1 & 1 & 1 & 1 \\ \widehat{RK}^{(5)}[0] & 1 & 1 & 1 & 1 & 1 & 1 & 1 & 1 & 1 & 1 & 1 & 1 \end{array} \right) & \left( \begin{array}{c|cccccccccccccc} & k_1 & k_2 & k_5 & k_6 & k_7 & k_8 & k_9 & k_{10} & k_{12} & k_{13} & k_{14} & k_{15} \\ \hline \widehat{SR}^{(3)}[1] & 1 & 1 & 1 & 1 & 1 & 1 & 1 & 1 & 1 & 1 & 1 & 1 \\ \widehat{SR}^{(3)}[4] & 1 & 1 & 1 & 1 & 1 & 1 & 1 & 1 & 1 & 1 & 1 & 1 \\ \widehat{RK}^{(5)}[0] & 1 & 1 & 1 & 1 & 1 & 1 & 1 & 1 & 1 & 1 & 1 & 1 \\ \hline \widehat{A}^{(1)}[3] & 0 & 0 & 1 & 0 & 0 & 0 & 0 & 1 & 1 & 0 & 0 & 1 \\ \widehat{A}^{(1)}[4] & 0 & 0 & 0 & 0 & 0 & 0 & 1 & 0 & 0 & 1 & 1 & 0 \\ \widehat{A}^{(1)}[14] & 1 & 1 & 0 & 1 & 0 & 0 & 0 & 1 & 1 & 0 & 1 & 1 \\ \widehat{A}^{(2)}[4] & 1 & 1 & 1 & 0 & 1 & 1 & 1 & 0 & 0 & 1 & 1 & 0 \\ \widehat{RK}^{(2)}[12] & 1 & 0 & 1 & 0 & 0 & 0 & 1 & 0 & 1 & 1 & 1 & 0 \\ \widehat{RK}^{(2)}[13] & 0 & 1 & 1 & 1 & 0 & 0 & 0 & 1 & 0 & 1 & 1 & 1 \end{array} \right) \\
& \quad (a) & \quad (b) \\
& \left( \begin{array}{c|cccccccccccccc} & k_7 & k_1 & k_2 & k_5 & k_6 & k_8 & k_9 & k_{10} & k_{12} & k_{13} & k_{14} & k_{15} \\ \hline \widehat{SR}^{(3)}[1] & 1 & 1 & 1 & 1 & 1 & 1 & 1 & 1 & 1 & 1 & 1 & 1 \\ \widehat{SR}^{(3)}[4] & 1 & 1 & 1 & 1 & 1 & 1 & 1 & 1 & 1 & 1 & 1 & 1 \\ \widehat{RK}^{(5)}[0] & 1 & 1 & 1 & 1 & 1 & 1 & 1 & 1 & 1 & 1 & 1 & 1 \\ \hline \widehat{A}^{(2)}[4] & 1 & 1 & 1 & 1 & 0 & 1 & 1 & 0 & 0 & 1 & 1 & 0 \\ \widehat{A}^{(1)}[3] & 0 & 0 & 0 & 1 & 0 & 0 & 0 & 1 & 1 & 0 & 0 & 1 \\ \widehat{A}^{(1)}[4] & 0 & 0 & 0 & 0 & 0 & 0 & 1 & 0 & 0 & 1 & 1 & 0 \\ \widehat{A}^{(1)}[14] & 0 & 1 & 1 & 0 & 1 & 0 & 0 & 1 & 1 & 0 & 1 & 1 \\ \widehat{RK}^{(2)}[12] & 0 & 1 & 0 & 1 & 0 & 0 & 1 & 0 & 1 & 1 & 1 & 0 \\ \widehat{RK}^{(2)}[13] & 0 & 0 & 1 & 1 & 1 & 0 & 0 & 1 & 0 & 1 & 1 & 1 \end{array} \right) & \left( \begin{array}{c|cccccccccccccc} & k_7 & k_1 & k_2 & k_5 & k_6 & k_8 & k_9 & k_{10} & k_{12} & k_{13} & k_{14} & k_{15} \\ \hline \widehat{SR}^{(3)}[1] & 1 & 1 & 1 & 1 & 1 & 1 & 1 & 1 & 1 & 1 & 1 & 1 \\ \widehat{SR}^{(3)}[4] & 1 & 1 & 1 & 1 & 1 & 1 & 1 & 1 & 1 & 1 & 1 & 1 \\ \widehat{RK}^{(5)}[0] & 1 & 1 & 1 & 1 & 1 & 1 & 1 & 1 & 1 & 1 & 1 & 1 \\ \hline \widehat{A}^{(1)}[14] & 0 & 1 & 1 & 0 & 1 & 0 & 0 & 1 & 1 & 0 & 1 & 1 \\ \hline \widehat{A}^{(2)}[4] & 1 & 1 & 1 & 1 & 0 & 1 & 1 & 0 & 0 & 1 & 1 & 0 \\ \widehat{A}^{(1)}[3] & 0 & 0 & 0 & 1 & 0 & 0 & 0 & 1 & 1 & 0 & 0 & 1 \\ \widehat{A}^{(1)}[4] & 0 & 0 & 0 & 0 & 0 & 0 & 1 & 0 & 0 & 1 & 1 & 0 \\ \widehat{RK}^{(2)}[12] & 0 & 1 & 0 & 1 & 0 & 0 & 1 & 0 & 1 & 1 & 1 & 0 \\ \widehat{RK}^{(2)}[13] & 0 & 0 & 1 & 1 & 1 & 0 & 0 & 1 & 0 & 1 & 1 & 1 \end{array} \right) \\
& \quad (c) & \quad (d) \\
& \left( \begin{array}{c|cccccccccccccc} & k_7 & k_1 & k_2 & k_5 & k_6 & k_8 & k_9 & k_{10} & k_{12} & k_{13} & k_{14} & k_{15} \\ \hline \widehat{SR}^{(3)}[1] & 1 & 1 & 1 & 1 & 1 & 1 & 1 & 1 & 1 & 1 & 1 & 1 \\ \widehat{SR}^{(3)}[4] & 1 & 1 & 1 & 1 & 1 & 1 & 1 & 1 & 1 & 1 & 1 & 1 \\ \widehat{RK}^{(5)}[0] & 1 & 1 & 1 & 1 & 1 & 1 & 1 & 1 & 1 & 1 & 1 & 1 \\ \hline \widehat{A}^{(1)}[14] & 0 & 1 & 1 & 0 & 1 & 0 & 0 & 1 & 1 & 0 & 1 & 1 \\ \hline \widehat{A}^{(2)}[4] & 1 & 1 & 1 & 1 & 0 & 1 & 1 & 0 & 0 & 1 & 1 & 0 \\ \widehat{RK}^{(2)}[12] & 0 & 1 & 0 & 1 & 0 & 0 & 1 & 0 & 1 & 1 & 1 & 0 \\ \widehat{A}^{(1)}[3] & 0 & 0 & 0 & 1 & 0 & 0 & 0 & 1 & 1 & 0 & 0 & 1 \\ \widehat{A}^{(1)}[4] & 0 & 0 & 0 & 0 & 0 & 0 & 1 & 0 & 0 & 1 & 1 & 0 \\ \widehat{RK}^{(2)}[13] & 0 & 0 & 1 & 1 & 1 & 0 & 0 & 1 & 0 & 1 & 1 & 1 \end{array} \right) & \left( \begin{array}{c|cccc|cccccc} & k_7 & k_1 & k_2 & k_5 & k_9 & k_6 & k_8 & k_{10} & k_{12} & k_{13} & k_{14} & k_{15} \\ \hline \widehat{SR}^{(3)}[1] & 1 & 1 & 1 & 1 & 1 & 1 & 1 & 1 & 1 & 1 & 1 & 1 \\ \widehat{SR}^{(3)}[4] & 1 & 1 & 1 & 1 & 1 & 1 & 1 & 1 & 1 & 1 & 1 & 1 \\ \widehat{RK}^{(5)}[0] & 1 & 1 & 1 & 1 & 1 & 1 & 1 & 1 & 1 & 1 & 1 & 1 \\ \hline \widehat{A}^{(1)}[14] & 0 & 1 & 1 & 0 & 1 & 0 & 0 & 1 & 1 & 0 & 1 & 1 \\ \hline \widehat{A}^{(2)}[4] & 1 & 1 & 1 & 1 & 1 & 1 & 0 & 1 & 0 & 0 & 1 & 1 & 0 \\ \widehat{RK}^{(2)}[12] & 0 & 1 & 0 & 1 & 1 & 1 & 0 & 0 & 0 & 1 & 1 & 1 & 0 \\ \widehat{RK}^{(2)}[13] & 0 & 0 & 1 & 1 & 0 & 1 & 0 & 1 & 0 & 1 & 1 & 1 & 1 \\ \hline \widehat{A}^{(1)}[3] & 0 & 0 & 0 & 1 & 0 & 1 & 0 & 0 & 0 & 1 & 1 & 0 & 0 & 1 \\ \widehat{A}^{(1)}[4] & 0 & 0 & 0 & 0 & 0 & 1 & 0 & 0 & 0 & 1 & 1 & 0 & 0 & 1 \end{array} \right) \\
& \quad (e) & \quad (f) \quad \text{free variables}
\end{aligned}$$

503 Finally, we extract 5 dependent variables  $\widehat{RK}^{(0)}[7, 1, 2, 5, 9] = (k_7, k_1, k_2, k_5, k_9)$   
504 marked in green in Eq. (13)-(f) from the rows of  $\widehat{A}^{(2)}[4]$ ,  $\widehat{RK}^{(2)}[12]$ ,  $\widehat{RK}^{(2)}[13]$ ,  
505  $\widehat{A}^{(1)}[3]$ , and  $\widehat{A}^{(1)}[4]$ . The others are 7 free variables  $\widehat{RK}^{(0)}[6, 8, 10, 12, 13, 14, 15] =$   
506  $(k_6, k_8, k_{10}, k_{12}, k_{13}, k_{14}, k_{15})$ . The values  $(e_1, e_2, e_3, e_4, e_5) \in \mathbb{F}_2^{40}$  are assigned  
507 to the expressions for the red bytes of  $(\widehat{A}^{(2)}[4], \widehat{RK}^{(2)}[12], \widehat{RK}^{(2)}[13], \widehat{A}^{(1)}[3],$   
508  $\widehat{A}^{(1)}[4])$ , then given the values of the seven free variables, the dependent variables  
509  $(k_9, k_5, k_2, k_1, k_7)$  are deduced in sequence. Thereafter, the values of  $\widehat{SR}^{(3)}[1],$   
510  $\widehat{SR}^{(3)}[4], \widehat{RK}^{(5)}[0]$  and  $\widehat{A}^{(1)}[14]$  are deduced directly.

511 In the 3 consumed DoFs of blue byte ■ on  $RK^{(1)}[4]$ ,  $RK^{(1)}[11]$ , and  $RK^{(3)}[3]$ ,  
 512 the expressions are

$$\begin{cases} RK^{(1)}[4] = k_4 \oplus k_0 \oplus S(k_{13}) \\ RK^{(1)}[11] = k_{11} \oplus k_3 \oplus k_7 \oplus S(k_{12}) \\ RK^{(3)}[3] = k_3 \oplus S(k_4 \oplus e_2) \oplus S(k_4 \oplus k_0 \oplus S(k_{13}) \oplus k_8 \oplus k_{12}) \oplus S(k_{12}) \end{cases} . \quad (14)$$

513 After assigning the following formulas as constants ( $e_6, e_7, e_8$ ),

$$\begin{cases} k_4 \oplus k_0 = e_6 \\ k_{11} \oplus k_3 = e_7 \\ k_3 \oplus S(k_4 \oplus e_2) = e_8 \end{cases} , \quad (15)$$

514 the bytes  $RK^{(1)}[4]$ ,  $RK^{(1)}[11]$ ,  $RK^{(3)}[3]$  will be ■, *i.e.*, only determined by the red  
 515 cells. By applying the TA to Eq. (15), 1 free variable  $k_0$  is obtained, the other 3  
 516 variables  $RK^{(0)}[3, 4, 11] = (k_3, k_4, k_{11})$  are deduced directly for any value of the  
 517 free variable  $k_0$ . The 5-round MitM attack is given in Algorithm 4.

518 *Analysis of Algorithm 4.* In Line 12 to 27,  $2^{\zeta+24+16+32+8+8} = 2^{128}$  states should  
 519 be tested to recover the 128-bit key; therefore,  $\zeta = 40$ . According to Eq. (3),  $\mathcal{T}_{pre}$   
 520 corresponds to the time complexity of Line 7-9, which is about  $2^{\zeta+24+16+40} =$   
 521  $2^{120}$  1-round AES. Therefore, the first part of Eq. (3) dominates the overall  
 522 complexity, which is about  $2^{128-8 \cdot \min\{\text{DoF}^+, \text{DoF}^-, \text{DoM}\}} = 2^{120}$  5-round AES. The  
 523 memory complexity to store  $U$  is about  $2^{40}$ .

## 524 4.2 Practical-Memory Key-Recovery Attack on 4-full-round AES-128

525 The attack leverages the new representation of AES's key schedule by Leurent  
 526 and Pernot [39]. They introduced a new basis  $S^{(i)}$  to derive the round keys, *i.e.*,  
 527  $RK^{(i)} = C_0 \cdot S^{(i)}$  as shown in Figure 6, where  $C_0$  is a  $16 \times 16$  binary matrix given  
 528 Eq. (26) in Supplementary Material B.

529 The MitM path is shown in Figure 6. The starting state  $S^{(2)}$ , whose bytes  
 530 are denoted by  $k_0$  to  $k_{15}$ , contains  $\lambda^+ = 1$  ■ byte and  $\lambda^- = 6$  ■ bytes. The  
 531 consumed DoFs of ■ and ■ are  $\ell^+ = 0$  and  $\ell^- = 5$  bytes, respectively. The  
 532  $\ell^- = 5$  constraints (marked by ■/■) form a system of 5 nonlinear equations in  
 533 Eq. (17) (deleting the boxed parts). Therefore,  $\text{DoF}^+ = 1$ ,  $\text{DoF}^- = 1$ , and there  
 534 is  $\text{DoM} = 1$  matching byte in round 1. Using new TA, we get 3 free variables  
 535  $S^{(2)}[7, 10, 13] = (k_7, k_{10}, k_{13})$  and 3 dependent variables  $S^{(2)}[0, 1, 4] = (k_0, k_1, k_4)$ .  
 536 The matrices before and after the improved TA are shown in Eq. (16). The steps  
 537 for the MitM attack are given in Algorithm 5. The time complexity is about

---

**Algorithm 4:** Key-recovery attack on 5-round AES-128 with 1  $(P, C)$ 


---

```

1  for  $2^\zeta$  values of  $(e_1, e_2, e_3, e_4, e_5) \in \mathbb{F}_2^{40}$  do
2      for  $(e_6, e_7, e_8) \in \mathbb{F}_2^{24}$  do
3          for  $RK^{(0)}[14, 15] \in \mathbb{F}_2^{16}$  do
4               $U \leftarrow []$ 
5               $(\widehat{A}^{(1)}[4], \widehat{RK}^{(2)}[12], \widehat{RK}^{(2)}[13], \widehat{A}^{(1)}[3], \widehat{A}^{(2)}[4]) \leftarrow (e_1, e_2, e_3, e_4, e_5)$ 
6              for  $RK^{(0)}[6, 8, 10, 12, 13] \in \mathbb{F}_2^{40}$  do
7                  Compute  $RK^{(0)}[7, 1, 2, 5, 9] = (k_7, k_1, k_2, k_5, k_9)$  by Eq. (13)-(f)
8                  Compute  $\mathbf{u} = (\widehat{SR}^{(3)}[1], \widehat{SR}^{(3)}[4], \widehat{RK}^{(5)}[0], \widehat{A}^{(1)}[14]) \in \mathbb{F}_2^{32}$ 
9                   $U[\mathbf{u}] \leftarrow RK^{(0)}[1, 2, 5 - 10, 12 - 15] \in \mathbb{F}_2^{8 \times 12}$ 
10                 /* The nonlinear system solving and memory-aided
                     precomputation are combined to get the solution
                     space of the neutral words. There are about  $2^8$ 
                     elements in  $U[\mathbf{u}]$  for each  $\mathbf{u}$ . */
11             end
12             for  $\mathbf{u} \in \mathbb{F}_2^{32}$  do
13                  $L \leftarrow []$ 
14                 for  $RK^{(0)}[0] = k_0 \in \mathbb{F}_2^8$  do
15                     Compute  $RK^{(0)}[3, 4, 11] = (k_3, k_4, k_{11})$  by Eq. (15)
16                     Compute the 1-byte matching point
17                      $v = \text{SR}^{(2)}[4] \oplus e \cdot \text{MC}^{(2)}[4] \oplus b \cdot \text{MC}^{(2)}[5]$ 
18                      $L[v] \leftarrow (k_0, k_3, k_4, k_{11})$ 
19                 end
20                 for values in  $U[\mathbf{u}]$  do
21                     Compute the 1-byte matching point
22                      $v' = e \cdot \text{MC}^{(2)}[4] \oplus b \cdot \text{MC}^{(2)}[5] \oplus d \cdot \text{MC}^{(2)}[6] \oplus 9 \cdot \text{MC}^{(2)}[7]$ 
23                     for values in  $L[v']$  do
24                         if  $E(\text{Key} = RK^{(0)}, P) = C$  then
25                             return  $RK^{(0)}$ 
26                         end
27                     end
28                 end
29             end
30         end
31     end
32 end

```

---

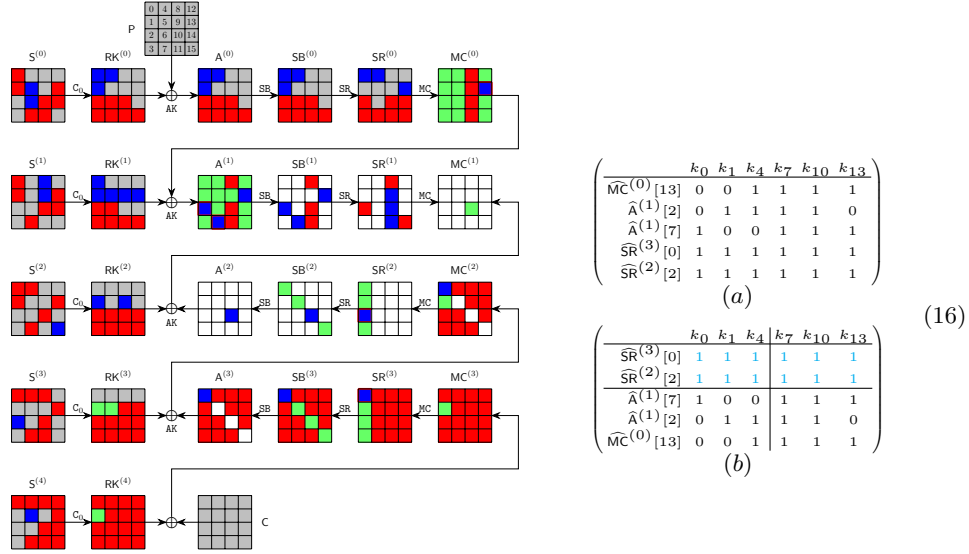


Fig. 6: 4-round attack on AES-128

538  $2^{128-8 \cdot \min\{\text{DoF}^+, \text{DoF}^-, \text{DoM}\}} = 2^{120}$ . The memory is  $2^{24}$  to store  $U$ .

$$\begin{cases}
 \widehat{MC}^{(0)}[13] = 3 \cdot S(k_{14} \oplus k_4 \oplus S(k_7)) \oplus S(k_{10} \oplus k_{13}) \oplus 2 \cdot \widehat{SR}^{(0)}[13] \oplus \widehat{SR}^{(0)}[12] \\
 \widehat{A}^{(1)}[2] = 2 \cdot S(k_{14} \oplus k_1) \oplus 3 \cdot S(k_{10}) \oplus k_4 \oplus S(k_7) \oplus k_1 \oplus \widehat{SR}^{(0)}[0] \oplus k_{11} \oplus k_{14} \oplus \widehat{SR}^{(0)}[1] \\
 \widehat{A}^{(1)}[7] = 2 \cdot S(k_{10} \oplus k_{13} \oplus k_0 \oplus S(k_3) \oplus k_7 \oplus S(k_6)) \oplus k_7 \oplus k_{13} \oplus 3 \cdot (\widehat{SR}^{(0)}[4] \oplus \widehat{SR}^{(0)}[5] \oplus \widehat{SR}^{(0)}[6]) \\
 \widehat{SR}^{(2)}[2] = 9 \cdot (\widehat{A}^{(3)}[1] \oplus \widehat{S}^{(3)}[5] \oplus \widehat{S}^{(3)}[8] \oplus \widehat{S}^{(3)}[15]) \oplus e \cdot \widehat{MC}^{(2)}[2] \oplus b \cdot \widehat{MC}^{(2)}[3] \oplus 9 \cdot \widehat{S}^{(3)}[2] \oplus d \cdot \widehat{MC}^{(2)}[0] \\
 \widehat{SR}^{(3)}[0] = e \cdot \widehat{RK}^{(4)}[0] \oplus b \cdot (\widehat{S}^{(4)}[2] \oplus \widehat{S}^{(4)}[8] \oplus \widehat{S}^{(4)}[15]) \oplus d \cdot \widehat{RK}^{(4)}[2] \oplus 9 \cdot \widehat{RK}^{(4)}[3] \oplus b \cdot \widehat{S}^{(4)}[5]
 \end{cases}
 \quad (17)$$

539 **Partial Experiment of the Key-Recovery Attack.** We give an experiment  
 540 of a 4-byte partial-key-recovery attack as follows:

- 541 1. Data collection: encrypt the plaintext  $P = 0$  with key  $S^{(2)} = 0$  to get the  
 542 ciphertext  $C$ .
  - 543 2. Given  $(P = 0, C)$  and 12-byte key information to recover the other 4-byte key  
 544  $S^{(2)}[7, 10, 13, 15]$ . If the recovered  $S^{(2)}[7, 10, 13, 15] = 0$ , the attack succeeds.  
 545 The 12-byte key information includes 9 bytes  $S^{(2)}[2, 3, 5, 6, 8, 9, 11, 12, 14] =$   
 546  $0$  and 3-byte key relations of  $(\widehat{MC}^{(0)}[13], \widehat{A}^{(1)}[2, 7]) = (e_1, e_2, e_3)$  on the 6 red  
 547 key bytes of  $S^{(2)}$ , i.e., assign  $(e_1, e_2, e_3)$  to the last 3 expressions of Eq.  
 548 (16)-(b). From  $(P, C)$  and  $S^{(2)} = 0$ , pre-compute the 3-byte  $(e_1, e_2, e_3) =$   
 549  $(0x75, 0x00, 0xc6)$ .
- 550 In our experiment,  $(P = 0, C)$  and 12-byte key information  $(S^{(2)}[2, 3, 5, 6,$   
 551  $8, 9, 11, 12, 14] = 0, (e_1, e_2, e_3) = (0x75, 0x00, 0xc6))$  are given, the goal is

552 to recover  $S^{(2)}[7, 10, 13, 15] = 0$ . In brute-force search, the time will be  $2^{32}$ .  
 553 With the given information, we actually conduct the experiment from Line  
 554 3 to Line 20 according to Algorithm 5. The time is  $2^{24}$  with  $2^{24}$  memory<sup>6</sup>.

555 We successfully recover the 4-byte partial key  $S^{(2)}[7, 10, 13, 15] = 0$ , and the  
 556 source codes and results are available via

557 <https://github.com/boxindex/Triangulation-MitM>

558 We implemented the experiment on a computer with an i9-13900KF CPU  
 559 and 32GB of memory. It takes about 200 seconds, while the brute force needs  
 560  $2^{32}$  evaluations of 4-round AES-128, which takes about 3200 seconds in the same  
 561 platform using the same code for AES.

---

**Algorithm 5:** Practical-memory attack on 4-full-round AES-128

---

```

1 for  $S^{(2)}[2, 3, 5, 6, 8, 9, 11, 12, 14] \in \mathbb{F}_2^{8 \times 9}$  and  $(e_1, e_2, e_3) \in \mathbb{F}_2^{24}$  do
2    $(\widehat{MC}^{(0)}[13], \widehat{A}^{(1)}[2, 7]) \leftarrow (e_1, e_2, e_3), U \leftarrow []$ 
3   for  $S^{(2)}[7, 10, 13] \in \mathbb{F}_2^{24}$  do
4     Compute  $S^{(2)}[0, 1, 4]$  by Eq. (16)-(b) and  $u = (\widehat{SR}^{(2)}[2], \widehat{SR}^{(3)}[0]) \in \mathbb{F}_2^{16}$ 
5      $U[u] \leftarrow S^{(2)}[0, 1, 4, 7, 10, 13] \in \mathbb{F}_2^{8 \times 7}$ 
6   end
7   for  $u \in \mathbb{F}_2^{16}$  do
8      $L \leftarrow []$ 
9     for  $S^{(2)}[15] \in \mathbb{F}_2^8$  do
10      Compute the 1-byte matching point  $v, L[v] \leftarrow S^{(2)}[15]$ 
11    end
12    for values in  $U[u]$  do
13      Compute the 1-byte matching point  $v'$ 
14      for values in  $L[v']$  do
15        if  $E(Key = S^{(2)}, P) = C$  then
16          return  $S^{(2)}$ 
17        end
18      end
19    end
20  end
21 end
```

---

562 **4.3 New Attack on 4-full-round AES-128 with  $2^{112}$  Complexity**

563 As shown in Figure 7, the starting state  $S^{(3)} = (k_0, k_1, \dots, k_{15})$  contains  $\lambda^+ = 2$   
 564 ■ bytes (i.e.,  $k_{10}$  and  $k_{14}$ ) and  $\lambda^- = 14$  ■ bytes. The consumed DoFs of ■

<sup>6</sup>In our experiment, we use the data structure “map<uint32\_t, vector<vector<uint8\_t>>>” to store  $U$ , which needs about 300 MB memory.

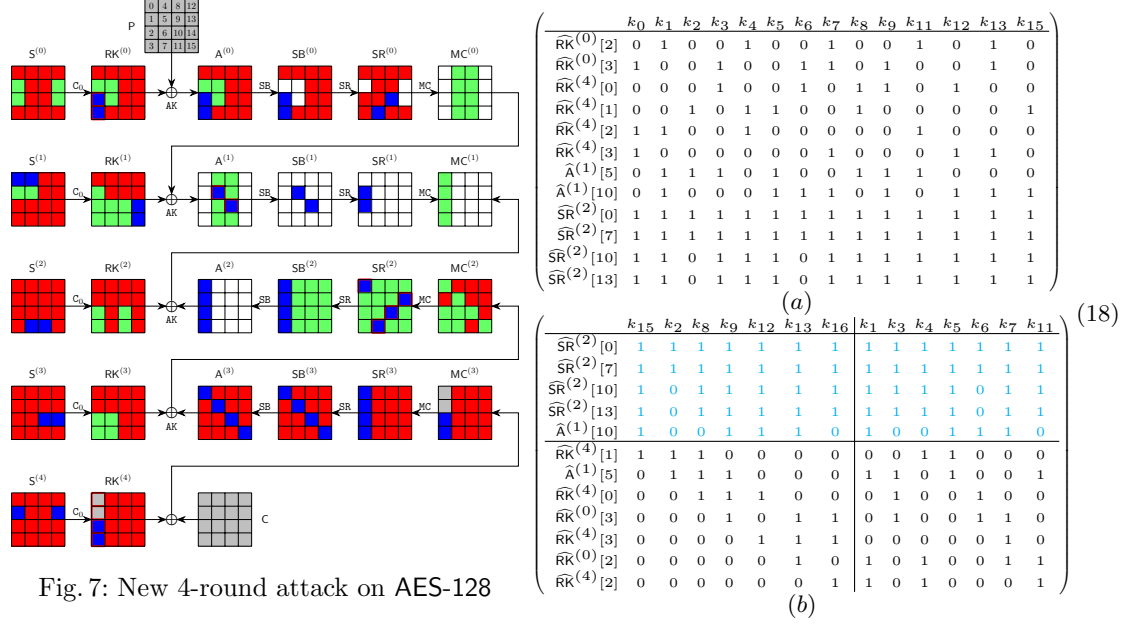


Fig. 7: New 4-round attack on AES-128

565 and  $\blacksquare$  are  $\ell^+ = 0$  and  $\ell^- = 12$  bytes, respectively. The  $\ell^- = 12$  constraints  
 566 (marked by  $\blacksquare/\blacksquare$  in Figure 7) form a system of 12 equations in Eq. (19). There-  
 567 fore,  $\text{DoF}^+ = 2$ ,  $\text{DoF}^- = 2$ , and  $\text{DoM} = 2$ . Using new TA, we get 7 free variables  
 568  $S^{(3)}[1, 3, 4, 5, 6, 7, 11]$  and 7 dependent variables  $S^{(3)}[0, 2, 8, 9, 12, 13, 15]$ . The mat-  
 569 rices before and after TA are given in Eq. (18). The steps for the MitM attack are  
 570 given in Algorithm 6. The time complexity is about  $2^{128-8 \cdot \min\{\text{DoF}^+, \text{DoF}^-, \text{DoM}\}} =$   
 571  $2^{112}$ . The memory is  $2^{56}$  to store  $U$ .



$$\begin{cases}
\widehat{RK}^{(0)}[2] = k_1 \oplus S(k_{13}) \oplus k_4 \oplus S(k_7) \oplus k_{11} \oplus S(k_{10}) \oplus k_{14} \\
\widehat{RK}^{(0)}[3] = k_{13} \oplus k_0 \oplus S(k_3) \oplus k_7 \oplus S(k_6) \oplus S(k_9) \oplus k_{10} \\
\widehat{RK}^{(4)}[0] = k_{12} \oplus k_3 \oplus k_6 \oplus k_9 \oplus S(k_8) \\
\widehat{RK}^{(4)}[1] = k_{15} \oplus k_2 \oplus k_5 \oplus S(k_4) \oplus k_8 \\
\widehat{RK}^{(4)}[2] = k_1 \oplus S(k_0) \oplus k_4 \oplus k_{11} \oplus k_{14} \\
\widehat{RK}^{(4)}[3] = k_{13} \oplus S(k_{12}) \oplus k_0 \oplus k_7 \oplus k_{10} \\
\widehat{A}^{(1)}[5] = S(k_3 \oplus S(k_2) \oplus k_9) \oplus 2 \cdot S(k_5 \oplus k_8 \oplus S(k_{11})) \oplus 3 \cdot S(k_1) \oplus k_8 \oplus S(k_{11}) \\
\quad \oplus k_2 \oplus SR^{(0)}[7] \\
\widehat{A}^{(1)}[10] = S(k_{12} \oplus S(k_{15}) \oplus k_9) \oplus S(k_5) \oplus 3 \cdot S(k_{13} \oplus k_7 \oplus S(k_6)) \oplus k_1 \\
\quad \oplus 2 \cdot SR^{(0)}[10] \oplus k_{14} \\
\widehat{SR}^{(2)}[0] = e \cdot RK^{(3)}[0] \oplus b \cdot (RK^{(3)}[1] \oplus A^{(3)}[1]) \oplus d \cdot (k_1 \oplus k_4 \oplus k_{11} \oplus A^{(3)}[2]) \oplus 9 \cdot (k_0 \\
\quad \oplus k_7 \oplus k_{13} \oplus A^{(3)}[3]) \oplus e \cdot A^{(3)}[0] \oplus d \cdot k_{14} \oplus 9 \cdot k_{10} \\
\widehat{SR}^{(2)}[7] = b \cdot (RK^{(3)}[4] \oplus A^{(3)}[4]) \oplus d \cdot RK^{(3)}[5] \oplus 9 \cdot (k_4 \oplus A^{(3)}[6]) \oplus e \cdot (k_0 \oplus A^{(3)}[7]) \\
\quad \oplus d \cdot A^{(3)}[5] \oplus 9 \cdot k_{14} \oplus e \cdot k_{10} \\
\widehat{SR}^{(2)}[10] = d \cdot MC^{(2)}[8] \oplus 9 \cdot MC^{(2)}[9] \oplus e \cdot RK^{(3)}[10] \oplus b \cdot MC^{(2)}[11] \oplus e \cdot A^{(3)}[10] \\
\widehat{SR}^{(2)}[13] = 9 \cdot MC^{(2)}[12] \oplus e \cdot MC^{(2)}[13] \oplus b \cdot MC^{(2)}[14] \oplus d \cdot RK^{(3)}[15] \oplus d \cdot A^{(3)}[15]
\end{cases} \tag{19}$$

---

**Algorithm 6:** New Attack on 4-full-round AES-128 with  $2^{112}$  time

---

```

1 for  $(e_1, e_2, e_3, e_4, e_5, e_6, e_7) \in \mathbb{F}_2^{56}$  do
2    $(\widehat{A}^{(1)}[5], \widehat{RK}^{(0)}[2, 3], \widehat{RK}^{(4)}[0, 1, 2, 3]) \leftarrow (e_1, e_2, e_3, e_4, e_5, e_6, e_7), U \leftarrow []$ 
3   for  $S^{(3)}[1, 3, 4, 5, 6, 7, 11] \in \mathbb{F}_2^{56}$  do
4     Compute  $S^{(3)}[0, 2, 8, 9, 12, 13, 16]$  by Eq. (18)-(b)
5     Compute  $u = (\widehat{A}^{(1)}[10], \widehat{SR}^{(2)}[0, 7, 10, 13]) \in \mathbb{F}_2^{40}$ 
6      $U[u] \leftarrow S^{(3)}[0 - 9, 11 - 13, 15] \in \mathbb{F}_2^{8 \times 14}$ 
7   end
8   for  $u \in \mathbb{F}_2^{40}$  do
9      $L \leftarrow []$ 
10    for  $S^{(3)}[10, 14] \in \mathbb{F}_2^{16}$  do
11      Compute the 2-byte matching point  $v, L[v] \leftarrow S^{(3)}[10, 14]$ 
12    end
13    for values in  $U[u]$  do
14      Compute the 2-byte matching point  $v'$  for values in  $L[v']$  do
15        if  $E(Key = S^{(3)}, P) = C$  then
16          return  $S^{(3)}$ 
17        end
18      end
19    end
20  end
21 end

```

---

#### 572 4.4 Two-Plaintext Key-Recovery Attack on 6-round AES-192

573 The MitM attack on 6-round AES-192 needs two plaintext-ciphertext pairs. One  
 574 plaintext-ciphertext pair is used in the MitM phase, and the other pair is used to  
 575 identify the unique correct 192-bit key. Similar situation happens to the 7-round  
 576 attack on AES-256 in Sect. 4.5.

577 The 6-round MitM path is given in Figure 8, where the starting state  $S^{(3)}$ ,  
 578 whose bytes are denoted as  $k_0, k_1, \dots, k_{23}$ , contains  $\lambda^+ = 2$  blue bytes and  $\lambda^- = 21$   
 579 red bytes. The consumed degrees of freedom (DoFs) of blue and red are  $\ell^+ = 0$  and  
 580  $\ell^- = 19$  bytes, respectively. Therefore,  $\text{DoF}^+ = 2$ ,  $\text{DoF}^- = 2$ , and there are  
 581  $\text{DoM} = 2$  matching bytes in round 2. We get 19 equations as Eq. (20) (deleting  
 582 the boxed parts) on the red bytes of  $S^{(3)}$  for the 19 consumed DoFs of red marked  
 583 by red/blue in Figure 8.

584 Using the new TA, we get 9 free variables  $S^{(3)}[0, 3, 4, 13, 14, 15, 16, 21, 23]$   
 585 and 12 dependent variables  $S^{(3)}[1, 2, 5, 6, 7, 11, 12, 17, 18, 19, 20, 22]$ . The matrices  
 586 after TA are given in Eq. (21). The 6-round MitM attack is given in Al-  
 587 gorithm 10 in Supplementary Material C. The total time complexity is about  
 588  $2^{192-8 \cdot \min\{\text{DoF}^+, \text{DoF}^-, \text{DoM}\}} = 2^{176}$ . The memory is  $2^{72}$  to store  $U$ .

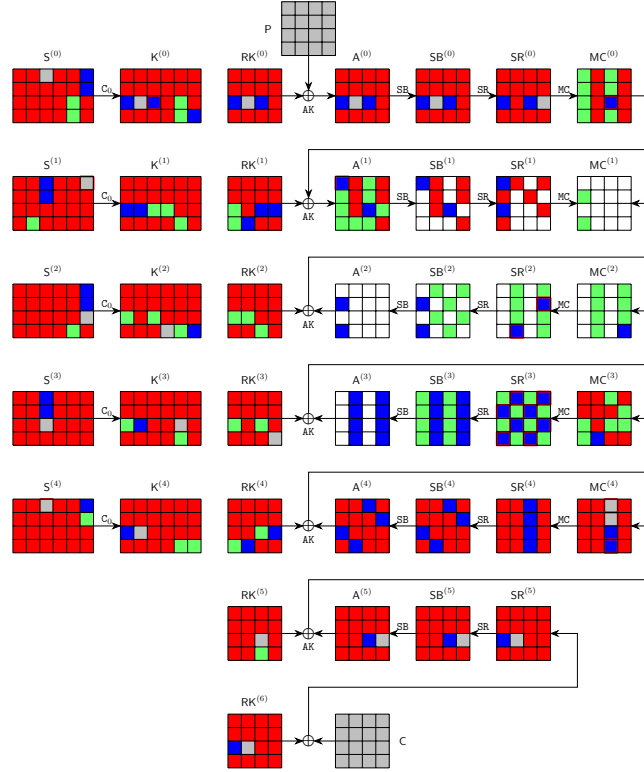


Fig. 8: The 6-round attack on AES-192

$$\begin{cases}
\widehat{S}^{(1)}[20] = k_{20} \oplus S(k_{21} \oplus k_{22}); \widehat{S}^{(4)}[8] = k_{20} \oplus S(k_{21}); \widehat{K}^{(0)}[10] = k_{19} \oplus k_{20} \oplus k_7 \oplus S(k_9); \widehat{K}^{(3)}[18] = k_6 \oplus k_{18} \\
\widehat{MC}^{(0)}[10] = S(k_{13} \oplus k_{14} \oplus k_1 \oplus S(k_3)) \oplus S(k_4 \oplus k_5) \oplus 3 \cdot S(k_{11} \oplus S(k_0 \oplus k_1)) \oplus 2 \cdot \widehat{SR}^{(0)}[10] \\
\widehat{A}^{(1)}[0] = 2 \cdot S(k_{14} \oplus S(k_{15} \oplus k_{16}) \oplus k_2 \oplus S(k_3) \oplus S(k_3 \oplus k_4)) \oplus 3 \cdot S(k_5 \oplus S(k_6 \oplus k_7)) \\
\quad \oplus S(k_{10} \oplus k_{11}) \oplus k_{12} \oplus k_{13} \oplus k_0 \oplus k_2 \oplus \widehat{SR}^{(0)}[2] \\
\widehat{MC}^{(4)}[8] = S^{-1}(k_{13} \oplus k_{14} \oplus S(k_{15}) \oplus k_1) \oplus k_0 \oplus k_{12}; \widehat{MC}^{(4)}[9] = S^{-1}(k_5 \oplus S(k_6)) \oplus k_3 \oplus k_{15} \\
\widehat{MC}^{(4)}[11] = S^{-1}(k_{10} \oplus k_{11} \oplus S(k_0)) \oplus k_{21} \oplus k_9 \\
\widehat{SR}^{(3)}[1] = 9 \cdot \widehat{MC}^{(3)}[0] \oplus e \cdot \widehat{MC}^{(3)}[0] \oplus b \cdot \widehat{RK}^{(4)}[2] \oplus d \cdot (k_{21} \oplus k_{22} \oplus A^{(4)}[3]) \oplus b \cdot A^{(4)}[2] \oplus d \cdot k_9 \\
\widehat{SR}^{(3)}[3] = b \cdot \widehat{MC}^{(3)}[0] \oplus d \cdot \widehat{MC}^{(3)}[1] \oplus 9 \cdot \widehat{RK}^{(4)}[2] \oplus e \cdot (k_{21} \oplus k_{22} \oplus A^{(4)}[3]) \oplus 9 \cdot A^{(4)}[2] \oplus e \cdot k_9 \\
\widehat{SR}^{(3)}[4] = e \cdot \widehat{MC}^{(3)}[4] \oplus b \cdot \widehat{MC}^{(3)}[5] \oplus d \cdot \widehat{MC}^{(3)}[6] \oplus 9 \cdot \widehat{MC}^{(3)}[7] \\
\widehat{SR}^{(3)}[6] = d \cdot \widehat{MC}^{(3)}[4] \oplus 9 \cdot \widehat{MC}^{(3)}[5] \oplus e \cdot \widehat{MC}^{(3)}[6] \oplus b \cdot \widehat{MC}^{(3)}[7] \\
\widehat{SR}^{(3)}[9] = 9 \cdot \widehat{MC}^{(4)}[8] \oplus e \cdot \widehat{MC}^{(3)}[9] \oplus b \cdot (k_{20} \oplus A^{(4)}[10]) \oplus d \cdot \widehat{MC}^{(3)}[11] \oplus 9 \cdot A^{(4)}[8] \oplus b \cdot k_8 \\
\widehat{SR}^{(3)}[11] = b \cdot \widehat{MC}^{(4)}[8] \oplus d \cdot \widehat{MC}^{(3)}[9] \oplus 9 \cdot (k_{20} \oplus A^{(4)}[10]) \oplus e \cdot \widehat{MC}^{(3)}[11] \oplus b \cdot A^{(4)}[8] \oplus 9 \cdot k_8 \\
\widehat{SR}^{(3)}[12] = e \cdot \widehat{MC}^{(3)}[12] \oplus b \cdot \widehat{RK}^{(4)}[13] \oplus d \cdot A^{(4)}[14] \oplus 9 \cdot \widehat{MC}^{(3)}[15] \oplus b \cdot A^{(4)}[13] \oplus d \cdot \widehat{RK}^{(4)}[14] \\
\widehat{SR}^{(3)}[14] = d \cdot \widehat{MC}^{(3)}[12] \oplus 9 \cdot \widehat{RK}^{(4)}[13] \oplus e \cdot A^{(4)}[14] \oplus b \cdot \widehat{MC}^{(3)}[15] \oplus 9 \cdot A^{(4)}[13] \oplus e \cdot \widehat{RK}^{(4)}[14] \\
\widehat{SR}^{(2)}[7] = b \cdot k_{14} \oplus d \cdot k_5 \oplus 9 \cdot k_{20} \oplus e \cdot k_{11} \oplus b \cdot A^{(3)}[4] \oplus d \cdot A^{(3)}[5] \oplus 9 \cdot A^{(3)}[6] \oplus e \cdot A^{(3)}[7] \\
\widehat{SR}^{(2)}[13] = 9 \cdot k_{13} \oplus e \cdot k_4 \oplus b \cdot k_{19} \oplus 9 \cdot A^{(3)}[12] \oplus e \cdot A^{(3)}[13] \oplus b \cdot A^{(3)}[14] \oplus d \cdot (A^{(3)}[15] \oplus k_{10})
\end{cases} \quad (20)$$

$$\begin{pmatrix}
& k_{18} & k_{17} & k_{22} & k_2 & k_6 & k_7 & k_{12} & k_{19} & k_1 & k_5 & k_{11} & k_{20} & k_0 & k_3 & k_4 & k_{13} & k_{14} & k_{15} & k_{16} & k_{21} & k_{23} \\
\widehat{SR}^{(3)}[1] & 1 \\
\widehat{SR}^{(3)}[3] & 1 \\
\widehat{SR}^{(3)}[4] & 1 \\
\widehat{SR}^{(3)}[6] & 1 \\
\widehat{SR}^{(3)}[9] & 0 & 1 & 1 & 1 & 1 & 1 & 0 & 1 & 1 & 1 & 1 & 1 & 1 & 0 & 1 & 1 & 1 & 1 & 1 & 1 \\
\widehat{SR}^{(3)}[11] & 0 & 1 & 1 & 1 & 1 & 1 & 0 & 1 & 1 & 1 & 1 & 1 & 1 & 1 & 0 & 1 & 1 & 1 & 1 & 1 \\
\widehat{SR}^{(3)}[12] & 0 & 1 & 1 & 1 & 1 & 1 & 0 & 1 & 1 & 1 & 1 & 1 & 1 & 1 & 0 & 1 & 1 & 1 & 1 & 1 \\
\widehat{K}^{(3)}[18] & 1 & 0 & 0 & 0 & 1 & 0 & 0 & 0 & 0 & 0 & 0 & 0 & 0 & 0 & 0 & 0 & 0 & 0 & 0 & 0 \\
\widehat{SR}^{(3)}[14] & 0 & 1 & 1 & 1 & 1 & 1 & 0 & 1 & 1 & 1 & 1 & 1 & 1 & 1 & 1 & 1 & 1 & 1 & 1 & 1 \\
\widehat{S}^{(1)}[20] & 0 & 0 & 1 & 0 & 0 & 0 & 0 & 0 & 0 & 0 & 0 & 0 & 1 & 0 & 0 & 0 & 0 & 0 & 1 & 0 \\
\widehat{A}^{(1)}[0] & 0 & 0 & 0 & 1 & 1 & 1 & 1 & 0 & 0 & 1 & 1 & 0 & 0 & 1 & 1 & 1 & 1 & 1 & 0 & 0 \\
\widehat{MC}^{(4)}[9] & 0 & 0 & 0 & 0 & 1 & 0 & 0 & 0 & 0 & 1 & 0 & 0 & 0 & 1 & 0 & 0 & 0 & 0 & 0 & 0 \\
\widehat{K}^{(0)}[10] & 0 & 0 & 0 & 0 & 0 & 1 & 0 & 1 & 0 & 0 & 0 & 1 & 0 & 0 & 0 & 0 & 0 & 0 & 0 & 0 \\
\widehat{MC}^{(4)}[8] & 0 & 0 & 0 & 0 & 0 & 0 & 1 & 0 & 1 & 0 & 0 & 0 & 0 & 1 & 0 & 0 & 0 & 0 & 0 & 0 \\
\widehat{SR}^{(2)}[13] & 0 & 0 & 0 & 0 & 0 & 0 & 0 & 1 & 0 & 0 & 0 & 0 & 0 & 0 & 1 & 1 & 0 & 0 & 0 & 0 \\
\widehat{MC}^{(0)}[10] & 0 & 0 & 0 & 0 & 0 & 0 & 0 & 0 & 1 & 1 & 1 & 0 & 0 & 1 & 1 & 1 & 1 & 0 & 0 & 0 & 0 \\
\widehat{SR}^{(2)}[7] & 0 & 0 & 0 & 0 & 0 & 0 & 0 & 0 & 0 & 1 & 1 & 1 & 1 & 0 & 0 & 0 & 0 & 1 & 0 & 0 & 0 \\
\widehat{MC}^{(4)}[11] & 0 & 0 & 0 & 0 & 0 & 0 & 0 & 0 & 0 & 0 & 0 & 1 & 0 & 1 & 0 & 0 & 0 & 0 & 1 & 0 & 0 \\
\widehat{S}^{(4)}[8] & 0 & 0 & 0 & 0 & 0 & 0 & 0 & 0 & 0 & 0 & 0 & 1 & 0 & 0 & 0 & 0 & 0 & 1 & 0 & 0 & 0
\end{pmatrix} \quad (21)$$

#### 4.5 Two-Plaintext Key-Recovery Attack on 7-round AES-256

Figure 19 in Supplementary Material D is the 7-round MitM path, where the starting state  $S^{(1)}$  contains  $\lambda^+ = 1$  bytes and  $\lambda^- = 23$  bytes. The consumed DoFs of  $\blacksquare$  and  $\blacksquare$  are  $\ell^+ = 0$  and  $\ell^- = 22$  bytes, respectively. Therefore,  $\text{DoF}^+ = 1$ ,  $\text{DoF}^- = 1$ , and there is  $\text{DoM} = 1$  matching byte in round 3. Compute 22 expressions, given in Eq. (29) (by deleting the boxed parts) in Supplementary Material D, for the 22 consumed DoFs of  $\blacksquare$  (marked by  $\blacksquare/\blacksquare$  in Figure 19) on the red bytes of  $S^{(1)}$ . Using the new TA, we get 9 free variables

597  $S^{(1)}[0, 6, 14, 18, 20, 22, 27, 28, 30]$  and 14 dependent variables  $S^{(1)}[1, 2, 3, 4, 5, 7, 9,$   
598  $10, 11, 16, 17, 21, 29, 31]$ . The matrices after TA is given in Eq. (22). The steps for  
599 the 7-round MitM attack are given in Algorithm 11 in Supplementary Material  
600 D. The total time complexity is about  $2^{256-8 \cdot \min\{\text{DoF}^+, \text{DoF}^-, \text{DoM}\}} = 2^{248}$ . The  
601 memory is  $2^{72}$  to store  $U$ .

$$\begin{pmatrix}
& k_5 & k_{21} & k_{17} & k_{11} & k_{16} & k_{10} & k_{31} & k_9 & k_{29} & k_1 & k_3 & k_4 & k_7 & k_2 & k_0 & k_6 & k_{14} & k_{18} & k_{20} & k_{22} & k_{27} & k_{28} & k_{30} \\
\text{SR}^{(4)}[1] & 1 \\
\text{SR}^{(4)}[4] & 1 \\
\text{SR}^{(4)}[11] & 1 \\
\text{SR}^{(4)}[14] & 1 \\
\text{MC}^{(1)}[4] & 1 & 1 & 0 & 0 & 0 & 1 & 1 & 0 & 0 & 1 & 0 & 1 & 1 & 1 & 1 & 1 & 1 & 1 & 1 & 1 & 1 & 1 \\
\text{MC}^{(1)}[14] & 1 & 1 & 1 & 1 & 1 & 1 & 1 & 0 & 0 & 0 & 0 & 0 & 0 & 1 & 0 & 1 & 1 & 1 & 1 & 0 & 1 & 1 \\
\hat{A}^{(2)}[9] & 0 & 0 & 0 & 0 & 1 & 0 & 0 & 0 & 0 & 0 & 0 & 1 & 1 & 1 & 1 & 1 & 1 & 1 & 1 & 1 & 1 & 1 \\
\text{MC}^{(0)}[14] & 0 & 0 & 0 & 0 & 0 & 0 & 0 & 0 & 0 & 0 & 0 & 0 & 0 & 1 & 0 & 1 & 1 & 1 & 0 & 1 & 0 & 0 \\
\text{MC}^{(5)}[9] & 1 & 0 & 1 & 0 & 0 & 1 & 0 & 1 & 0 & 1 & 1 & 1 & 0 & 1 & 0 & 0 & 0 & 0 & 0 & 0 & 0 & 0 \\
\text{MC}^{(5)}[11] & 0 & 1 & 1 & 0 & 0 & 0 & 0 & 0 & 0 & 0 & 0 & 0 & 0 & 0 & 0 & 0 & 0 & 1 & 1 & 0 & 0 & 0 \\
\text{MC}^{(5)}[8] & 0 & 0 & 1 & 1 & 0 & 1 & 0 & 1 & 0 & 0 & 0 & 0 & 0 & 0 & 0 & 0 & 0 & 0 & 0 & 0 & 0 & 0 \\
\hat{A}^{(2)}[3] & 0 & 0 & 0 & 1 & 0 & 1 & 1 & 0 & 0 & 0 & 0 & 1 & 1 & 0 & 1 & 1 & 1 & 1 & 1 & 0 & 1 & 1 \\
\hat{K}^{(0)}[1] & 0 & 0 & 0 & 0 & 1 & 1 & 0 & 0 & 0 & 0 & 0 & 1 & 0 & 0 & 0 & 0 & 0 & 0 & 0 & 0 & 0 & 1 \\
\hat{A}^{(1)}[2] & 0 & 0 & 0 & 0 & 0 & 1 & 1 & 1 & 0 & 1 & 0 & 0 & 0 & 0 & 0 & 1 & 1 & 1 & 0 & 1 & 0 & 1 \\
\hat{A}^{(1)}[13] & 0 & 0 & 0 & 0 & 0 & 0 & 1 & 0 & 0 & 0 & 0 & 0 & 0 & 1 & 0 & 1 & 1 & 0 & 1 & 0 & 0 & 0 \\
\hat{K}^{(3)}[18] & 0 & 0 & 0 & 0 & 0 & 0 & 0 & 1 & 1 & 1 & 1 & 0 & 0 & 1 & 0 & 0 & 0 & 0 & 0 & 1 & 1 & 0 \\
\hat{A}^{(1)}[10] & 0 & 0 & 0 & 0 & 0 & 0 & 0 & 0 & 0 & 1 & 0 & 0 & 0 & 0 & 1 & 0 & 1 & 1 & 0 & 0 & 1 & 1 \\
\hat{K}^{(3)}[10] & 0 & 0 & 0 & 0 & 0 & 0 & 0 & 0 & 0 & 1 & 0 & 0 & 0 & 1 & 0 & 0 & 0 & 0 & 0 & 1 & 1 & 0 \\
\hat{A}^{(1)}[6] & 0 & 0 & 0 & 0 & 0 & 0 & 0 & 0 & 0 & 0 & 0 & 1 & 1 & 1 & 0 & 1 & 1 & 1 & 1 & 0 & 0 & 1 \\
\hat{A}^{(2)}[8] & 0 & 0 & 0 & 0 & 0 & 0 & 0 & 0 & 0 & 0 & 0 & 1 & 1 & 1 & 1 & 1 & 1 & 1 & 1 & 1 & 1 & 1 \\
\hat{A}^{(1)}[12] & 0 & 0 & 0 & 0 & 0 & 0 & 0 & 0 & 0 & 0 & 0 & 0 & 0 & 1 & 1 & 0 & 1 & 1 & 0 & 0 & 0 & 0 \\
\text{MC}^{(0)}[15] & 0 & 0 & 0 & 0 & 0 & 0 & 0 & 0 & 0 & 0 & 0 & 0 & 0 & 0 & 1 & 0 & 1 & 1 & 0 & 1 & 0 & 0
\end{pmatrix} \quad (22)$$

#### 602 4.6 Improved Preimage Attack on 10-round AES-256-DM

603 In addition to the key-recovery attacks, we also significantly reduce the memory  
604 complexity of Dong *et al.*'s 10-round preimage attack on DM hashing mode with  
605 AES-256 from the impractical  $2^{56}$  [26] to the practical  $2^8$ , with the same time  
606 complexity. The compression function of AES-256-DM is  $h_i = \text{AES-256}_{m_{i-1}}(h_{i-1}) \oplus$   
607  $h_{i-1}$ , where  $h_i$  is the 128-bit chaining variable and the 256-bit message block  
608  $m_{i-1}$  acts as the encryption key of AES-256. Given a 128-bit target  $h_i$ , the preim-  
609 age attack is to generate a preimage  $(m_{i-1}, h_{i-1})$  satisfying the target with time  
610 complexity lower than  $2^{128}$ .

611 We reuse the 10-round MitM characteristic in [26] as shown in Figure 20 in  
612 Supplementary Material E. In the MitM path, the starting states are  $A^{(4)}$  and  
613  $S^{(3)}$ . The 1-byte matching occurs in the MC operation in round 8. In  $S^{(3)}$ , there  
614 are 19 ■ cells, 1 ■ cell and 12 ■ cells. In  $A^{(4)}$ , there are 8 ■ cells, 8 ■ cells. Hence,  
615 the total initial DoFs are  $\lambda^+ = 19 + 8 = 27$  cells for ■ cells, and  $\lambda^- = 1 + 8 = 9$   
616 for ■ cells. The consumed DoFs of ■ and DoFs of ■ are  $\ell^+ = 26$  and  $\ell^- = 8$   
617 bytes, respectively. Therefore,  $\text{DoF}^+ = 1$ ,  $\text{DoF}^- = 1$ , and there is  $\text{DoM} = 1$   
618 matching byte.

619 We obtain the 18 equations on ■ bytes of  $S^{(3)}$  for the consumed DoFs of blue  
620 bytes in  $S^{(1)}[13, 14]$ ,  $S^{(2)}[12, 13, 14, 15]$ ,  $S^{(4)}[1]$ ,  $K^{(2)}[0, 3, 4, 5, 9]$ ,  $\text{SR}^{(1)}[3, 6, 9, 12]$   
621 and  $\text{SR}^{(9)}[6, 12]$ , where the expressions of  $\text{SR}^{(1)}[3, 6, 9, 12]$  are obtained by  $\text{MC}^{-1}(\text{RK}^{(1)})$ ,  
622 and assign  $a_i (0 \leq i < 18)$  to them. Using the new TA, we get 4 free variables  
623  $S^{(3)}[8, 16, 18, 24]$  and 15 dependent variables  $S^{(3)}[0, 1, 2, 3, 4, 5, 6, 7, 9, 10, 11, 17, 27,$

28, 31]. The matrices before and after TA are shown in Eq. (31) in Supplementary Material E, where the bytes of  $S^{(3)}$  are denoted as  $k_0, k_1, \dots, k_{31}$ .

Since we try to find a 128-bit preimage, the 128-bit encryption data path and 256-bit key-schedule path provide enough degrees of freedom, we do not need to traverse all the cells to find the 128-bit preimage. The steps for the 10-round MitM attack are given in Algorithm 12 in Supplementary Material E. The total time complexity is about  $2^{120}$ . The memory is  $2^8$  to store  $U$ .

**Experiment of Preimage Attack.** We conduct an experiment of the 5-byte partial target preimage attack by fixing the 5 target bytes  $T[0, 1, 2, 6, 12] = 0$ . According to Algorithm 12, we first fix all gray bytes  $\blacksquare$  in  $S^{(3)}$  as 0 in Line 1, and 15  $a_i$  as 0 in Line 2. Traverse 4 free variables  $\blacksquare S^{(3)}[8, 16, 18, 24]$  and deduce the other 3 ( $a_8, a_{16}, a_{18}$ ), only store the bytes that satisfy  $a_8 = a_{16} = a_{18} = 0$ , where about  $2^8$  values of blue bytes can be obtained and need  $2^8$  memory.

In Line 10 to 22, set all the  $\blacksquare$  bytes in  $MC^{(3)}, MC^{(4)}$  except  $MC^{(4)}[0]$  to 0 and traverse 3-byte  $A^{(5)}[2, 6]$  and  $MC^{(4)}[0]$ , where  $2^{32}$  time complexity is needed to get a preimage of the 5-byte partial target  $T[0, 1, 2, 6, 12] = 0$ . Obviously, to find a preimage of a 5-byte target, a brute-force search takes  $2^{8 \cdot 5=40}$  time. The source codes and results are available via

<https://github.com/boxindex/Triangulation-MitM>

We deploy the experiment on a computer with an i9-13900KF CPU and 32GB memory. In each experiment, the time of precomputation from Line 4 to 8 is about 500 seconds. Then, the process from Line 10 to 22 takes about 35000 seconds, and 4 preimages are produced with  $T[0, 1, 2, 6, 12] = 0$ , which are listed in Table 3 in Supplementary Material E. The brute force search for 40-bit target preimage needs  $2^{40}$  evaluations of 10-round AES-256, which takes about 5888000 seconds using the same AES-256 code in the same platform.

Our 4-round attack on AES-128 with  $2^{24}$  memory in Sect. 4.2 is about 16 times faster than brute force, but the 10-round attack with  $2^8$  memory is about 168 times faster than brute force. The reason behind may be that accessing a larger memory needs more time in practical implementations. This phenomenon also proves that the attacks we proposed with significantly reduced memory complexities are very important in practical attacks.

## 5 Single-Plaintext Key-Recovery on Reduced Rijndael-EM

FAEST [5] additionally uses Rijndael in the Even-Mansour (EM) mode shown in Figure 9, *i.e.*, Rijndael-EM-128/-192/-256, where Rijndael with block sizes of 128/192/256 bits acts as the ideal permutations. Given a plaintext-ciphertext pair  $(P, C)$ , suppose  $X = P \oplus k$ , then Rijndael-EM in Figure 9 can be transformed into Figure 10, *i.e.*,  $Rijndael(X) \oplus X = P \oplus C$ . Therefore, the key-recovery problem turns into the preimage attack on DM-like hashing mode, *i.e.*, given the target  $P \oplus C$  and find the preimage  $X$ . Then, find the key  $k = X \oplus P$ .



Fig. 9: Rijndael-EM

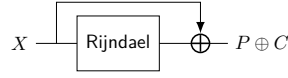


Fig. 10: Equivalent Form

### 5.1 Key-Recovery Attack on 7-round Rijndael-EM-128

The 7-round MitM characteristic is shown in Figure 11. The starting states  $A^{(1)}$  contains  $\lambda^+ = 6$  blue bytes and  $\lambda^- = 2$  red bytes. In the computation from  $A^{(1)}$  to  $SR^{(2)}$  and  $MC^{(2)}$ , the consumed DoFs of blue and red are  $\ell^+ = 4$  and  $\ell^- = 0$  bytes, respectively. Therefore,  $DoF^+ = 2$ ,  $DoF^- = 2$ , and there are  $DoM = 4$  matching bytes in round 2. The steps for the 7-round MitM attack are given in Algorithm 7. The time complexity is about  $2^{128-8 \cdot \min\{DoF^+, DoF^-, DoM\}} = 2^{112}$ . The memory is  $2^{32}$  to store  $U$ .

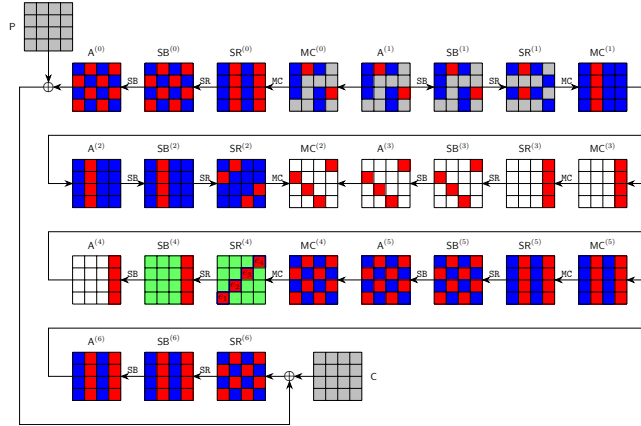


Fig. 11: The 7-round attack on Rijndael-EM-128

### 5.2 Key-Recovery Attack on 8-round Rijndael-EM-192

The 8-round MitM characteristic is shown in Figure 12. The starting state  $A^{(1)}$  contains  $\lambda^+ = 4$  blue bytes and  $\lambda^- = 8$  red bytes. In the computation from  $A^{(1)}$  to  $SR^{(4)}$  and  $MC^{(4)}$ , the consumed DoFs of blue and red are  $\ell^+ = 2$  and  $\ell^- = 6$  bytes, respectively. Therefore,  $DoF^+ = 2$ ,  $DoF^- = 2$ , and there are  $DoM = 2$  matching bytes.

The steps for the 8-round MitM attack are given in Algorithm 8. The time complexity is about  $2^{192-8 \cdot \min\{DoF^+, DoF^-, DoM\}} = 2^{176}$ . The memory is  $2^{16}$  to store the table  $L$ .

---

**Algorithm 7:** Attack on 7-round Rijndael-EM-128

---

```

1 for  $A^{(1)}[5, 6, 7, 12, 13, 15] \in \mathbb{F}_2^{48}$  do
2   for  $(e_1, e_2, e_3, e_4) \in \mathbb{F}_2^{32}$  do
3      $U \leftarrow []$ 
4     for  $MC^{(4)}[0, 5, 8, 13] \in \mathbb{F}_2^{32}$  do
5       Compute  $MC^{(4)}[2, 7, 10, 15]$  according to  $(e_1, e_2, e_3, e_4)$ 
6       /* e.g.,  $b \cdot MC^{(4)}[0] \oplus 9 \cdot MC^{(4)}[2] = e_1$  */
7       Compute  $u = MC^{(0)}[3, 9] \in \mathbb{F}_2^{16}$ 
8        $U[u] \leftarrow MC^{(4)}[0, 2, 5, 7, 8, 10, 13, 15]$ 
9     end
10    for  $u \in \mathbb{F}_2^{16}$  do
11       $L \leftarrow []$ 
12      for  $A^{(1)}[4, 14] \in \mathbb{F}_2^{16}$  do
13        Compute the 4-byte matching point  $v$ ,  $L[v] \leftarrow A^{(1)}[4, 14]$ 
14      end
15      for values in  $U[u]$  do
16        Compute the 4-byte matching point  $v'$ 
17        for values in  $L[v']$  do
18          Check if the target  $P \oplus C$  is satisfied
19        end
20      end
21    end
22  end
23 end

```

---



---

**Algorithm 8:** Attack on 8-round Rijndael-EM-192

---

```

1 for  $A^{(1)}[5, 6, 7, 10, 11, 12, 15, 16, 17, 20, 21, 22] \in \mathbb{F}_2^{96}$  do
2   for  $SR^{(0)}[1, 2] \in \mathbb{F}_2^{16}$  do
3     for  $MC^{(1)}[4, 7, 8, 9] \in \mathbb{F}_2^{32}$  do
4       for  $(e_1, e_2) \in \mathbb{F}_2^{16}$  do
5          $L \leftarrow []$ 
6         for  $A^{(1)}[0, 1] \in \mathbb{F}_2^{16}$  do
7           Compute  $A^{(1)}[2, 3]$  according to  $SR^{(0)}[1, 2]$ 
8           Compute the 2-byte matching point  $v$ 
9            $L[v] \leftarrow A^{(1)}[0, 1, 2, 3]$ 
10        end
11        for  $SR^{(2)}[1, 22] \in \mathbb{F}_2^{16}$  do
12          Compute  $SR^{(2)}[2, 23]$  according to  $(e_1, e_2)$ 
13          /* e.g.,  $3 \cdot SR^{(2)}[1] \oplus SR^{(2)}[2] = e_1$  */
14          Compute the 2-byte matching point  $v'$ 
15          for values in  $L[v']$  do
16            Check if the target  $P \oplus C$  is satisfied
17          end
18        end
19      end
20    end
21  end
22 end

```

---

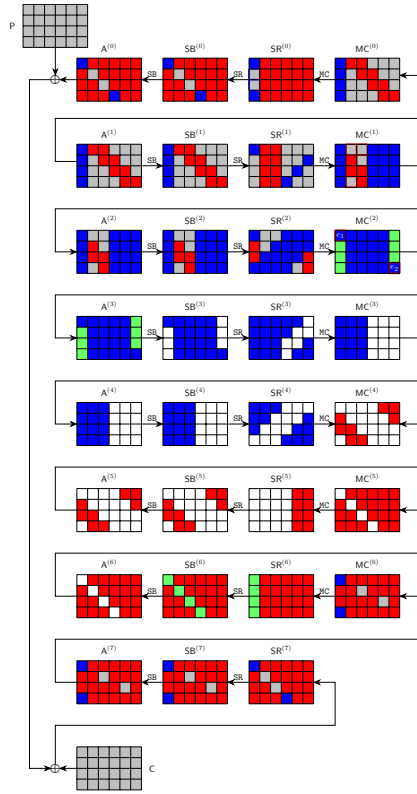


Fig. 12: 8-round Rijndael-EM-192

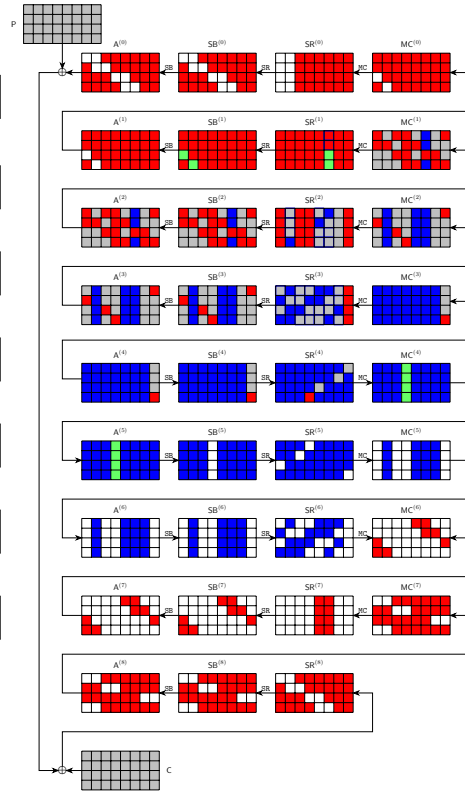


Fig. 13: 9-round Rijndael-EM-256



### 5.3 Key-Recovery Attack on 9-round Rijndael-EM-256

The 9-round MitM characteristic is shown in Figure 13. The starting state  $A^{(4)}$  contains  $\lambda^+ = 28$  blue bytes and  $\lambda^- = 1$  red byte. In the computation from  $A^{(4)}$  to  $SR^{(6)}$  and  $MC^{(6)}$ , the consumed degrees of freedom (DoFs) of blue and red are  $\ell^+ = 27$  and  $\ell^- = 0$  bytes, respectively. Therefore,  $DoF^+ = 1$ ,  $DoF^- = 1$ , and there is  $DoM = 1$  matching byte.

The steps for the 9-round MitM attack are given in Algorithm 9. The time complexity is about  $2^{256-8 \cdot \min\{DoF^+, DoF^-, DoM\}} = 2^{248}$ . The memory is  $2^8$  to store table  $L$ .

---

#### Algorithm 9: Attack on 9-round Rijndael-EM-256

---

```

1  for  $A^{(4)}[28, 29, 30] \in \mathbb{F}_2^{24}$  do
2      for  $SR^{(1)}[20, 21] \in \mathbb{F}_2^{16}$  do
3          for  $SR^{(2)}[4, 5, 6, 16, 18, 19, 21, 22, 23] \in \mathbb{F}_2^{72}$  do
4              for  $SR^{(3)}[0, 2, 5, 8, 9, 11, 12, 14, 15, 18, 19, 21, 22, 24, 25, 27] \in \mathbb{F}_2^{128}$  do
5                   $L \leftarrow []$ 
6                  for  $MC^{(1)}[20] \in \mathbb{F}_2^8$  do
7                      Compute  $MC^{(1)}[21, 23]$  according to  $SR^{(1)}[20, 21]$ 
8                      Compute forward and backward to the 1-byte matching point  $v$ 
9                       $L[v] \leftarrow MC^{(1)}[20, 21, 23]$ 
10                 end
11                 for  $A^{(4)}[31] \in \mathbb{F}_2^8$  do
12                     Compute forward and backward to the 2-byte matching point  $v'$ 
13                     for values in  $L[v']$  do
14                         Check if  $E(Key = A^{(0)} \oplus P, P) = C$ 
15                     end
16                 end
17             end
18         end
19     end
20 end

```

---

## 6 Further Applications and Conclusion

This paper introduces the *triangulating Meet-in-the-Middle attack* to reduce the memory complexity when considering MitM paths with nonlinearly constrained neutral words. We achieve this goal by leveraging and improving the Triangulation Algorithm (TA) of Khovratovich *et al.* to solve nonlinear systems of the MitM efficiently.

For AES, we reduce the memory complexities of the 4-/5-round single-plaintext key-recovery attacks on AES-128 and propose new attacks on 6-round AES-192 and 7-round AES-256. For Rijndael-EM, we convert key-recovery attack into preimage attack on its hashing mode and give new key recovery attacks Rijndael-EM-128/192/256 with a single plaintext-ciphertext pair.

For sponge functions like Keccak[1024], Keccak[768], Xoodyak-XOF, Ascon-XOF, Gimli-XOF, and Subterranean 2.0, we either reduce the memory complexity

of existing attacks or introduce new attacks with better time complexity in  
Supplementary Material **G**, **H**, **I**, **J**, and **K**.

**Acknowledgements.** We would like to thank Yu Sasaki and the anonymous reviewers from CRYPTO 2025 for their excellent guidance in improving the paper. This work is supported by the National Key R&D Program of China (2024YFA1013000), the Natural Science Foundation of China (62272257, 62302250), the Young Elite Scientists Sponsorship Program by CAST (2023QNRC001), and the Zhongguancun Laboratory.

## References

1. Kazumaro Aoki and Yu Sasaki. Preimage attacks on one-block MD4, 63-step MD5 and more. In *SAC 2008*, volume 5381, pages 103–119. Springer, 2008.
2. Zhenzhen Bao, Xiaoyang Dong, Jian Guo, Zheng Li, Danping Shi, Siwei Sun, and Xiaoyun Wang. Automatic search of meet-in-the-middle preimage attacks on AES-like hashing. In *EUROCRYPT 2021, Part I*, volume 12696, pages 771–804.
3. Zhenzhen Bao, Jian Guo, Danping Shi, and Yi Tu. Superposition meet-in-the-middle attacks: Updates on fundamental security of AES-like hashing. In Yevgeniy Dodis and Thomas Shrimpton, editors, *CRYPTO 2022, Proceedings, Part I*, volume 13507 of *LNCS*, pages 64–93. Springer, 2022.
4. Achiya Bar-On, Orr Dunkelman, Nathan Keller, Eyal Ronen, and Adi Shamir. Improved key recovery attacks on reduced-round AES with practical data and memory complexities. In Hovav Shacham and Alexandra Boldyreva, editors, *Advances in Cryptology - CRYPTO 2018 - 38th Annual International Cryptology Conference, Santa Barbara, CA, USA, August 19-23, 2018, Proceedings, Part II*, volume 10992 of *Lecture Notes in Computer Science*, pages 185–212. Springer, 2018.
5. Carsten Baum, Lennart Braun, Cyprien Delpech de Saint Guilhem, Michael Kloof, Christian Majenz, Shibam Mukherjee, Emmanuela Orsini, Sebastian Ramacher, Christian Rechberger, Lawrence Roy, et al. Faest: algorithm specifications. Technical report, Technical report, National Institute of Standards and Technology, 2023.
6. Edward A. Bender and E. Rodney Canfield. An approximate probabilistic model for structured gaussian elimination. *J. Algorithms*, 31(2):271–290, 1999.
7. Guido Bertoni, Joan Daemen, Michaël Peeters, and Gilles Van Assche. Keccak sponge function family main document. *Submission to NIST*, 3(30):320–337, 2009.
8. Andrey Bogdanov, Dmitry Khovratovich, and Christian Rechberger. Biclique cryptanalysis of the full AES. In *ASIACRYPT 2011, Proceedings*, pages 344–371.
9. Andrey Bogdanov and Christian Rechberger. A 3-subset meet-in-the-middle attack: Cryptanalysis of the lightweight block cipher KTANTAN. In *SAC 2010*, volume 6544, pages 229–240. Springer, 2010.
10. Charles Bouillaguet, Patrick Derbez, Orr Dunkelman, Pierre-Alain Fouque, Nathan Keller, and Vincent Rijmen. Low-data complexity attacks on aes. *IEEE transactions on information theory*, 58(11):7002–7017, 2012.
11. Charles Bouillaguet, Patrick Derbez, and Pierre-Alain Fouque. Automatic search of attacks on round-reduced AES and applications. In Phillip Rogaway, editor, *Advances in Cryptology - CRYPTO 2011 - 31st Annual Cryptology Conference, Santa Barbara, CA, USA, August 14-18, 2011. Proceedings*, volume 6841 of *Lecture Notes in Computer Science*, pages 169–187. Springer, 2011.

- 749 12. Christina Boura, Nicolas David, Patrick Derbez, Gregor Leander, and María Naya-  
750 Plasencia. Differential meet-in-the-middle cryptanalysis. In Helena Handschuh and  
751 Anna Lysyanskaya, editors, *CRYPTO 2023, Proceedings, Part III*, volume 14083  
752 of *Lecture Notes in Computer Science*, pages 240–272. Springer, 2023.
- 753 13. Anne Canteaut, María Naya-Plasencia, and Bastien Vayssière. Sieve-in-the-middle:  
754 Improved MITM attacks. In *CRYPTO 2013, Proceedings, Part I*, pages 222–240.
- 755 14. Shiyao Chen, Jian Guo, Eik List, Danping Shi, and Tianyu Zhang. Diving deep  
756 into the preimage security of aes-like hashing. In Marc Joye and Gregor Leander,  
757 editors, *Advances in Cryptology - EUROCRYPT 2024 - 43rd Annual International  
758 Conference on the Theory and Applications of Cryptographic Techniques, Zurich,  
759 Switzerland, May 26-30, 2024, Proceedings, Part I*, volume 14651 of *Lecture Notes  
760 in Computer Science*, pages 398–426. Springer, 2024.
- 761 15. Joan Daemen, Seth Hoffert, Michaël Peeters, Gilles Van Assche, and Ronny Van  
762 Keer. Xoodyak, a lightweight cryptographic scheme. *IACR Trans. Symmetric  
763 Cryptol.*, 2020(S1):60–87, 2020.
- 764 16. Joan Daemen, Pedro Maat Costa Massolino, Alireza Mehrdad, and Yann  
765 Rotella. The subterranean 2.0 cipher suite. *IACR Trans. Symmetric Cryptol.*,  
766 2020(S1):262–294, 2020.
- 767 17. Joan Daemen and Vincent Rijmen. *The Design of Rijndael: AES - The Advanced  
768 Encryption Standard*. Information Security and Cryptography. Springer, 2002.
- 769 18. Mathieu Degré, Patrick Derbez, Lucie Lahaye, and André Schrottenloher. New  
770 models for the cryptanalysis of ASCON. *IACR Cryptol. ePrint Arch.*, page 298,  
771 2024.
- 772 19. Patrick Derbez. *Meet-in-the-middle attacks on AES*. PhD thesis, Ecole Normale  
773 Supérieure de Paris-ENS Paris, 2013.
- 774 20. Patrick Derbez and Pierre-Alain Fouque. Automatic search of meet-in-the-middle  
775 and impossible differential attacks. In *CRYPTO 2016, Proceedings, Part II*, volume  
776 9815, pages 157–184. Springer, 2016.
- 777 21. Whitfield Diffie and Martin E. Hellman. Special feature exhaustive cryptanalysis  
778 of the NBS data encryption standard. *Computer*, 10(6):74–84, 1977.
- 779 22. Itai Dinur. Cryptanalytic applications of the polynomial method for solving mul-  
780 tivariate equation systems over  $\text{GF}(2)$ . In *EUROCRYPT 2021, Proceedings, Part  
781 I*, volume 12696, pages 374–403. Springer, 2021.
- 782 23. Itai Dinur, Orr Dunkelman, Nathan Keller, and Adi Shamir. Efficient dissection  
783 of composite problems, with applications to cryptanalysis, knapsacks, and combi-  
784 natorial search problems. In *CRYPTO 2012*, volume 7417, pages 719–740.
- 785 24. Christoph Dobraunig, Maria Eichlseder, Florian Mendel, and Martin Schläffer. As-  
786 con v1.2: Lightweight authenticated encryption and hashing. *J. Cryptol.*, 34(3):33,  
787 2021.
- 788 25. Xiaoyang Dong, Jian Guo, Shun Li, and Phuong Pham. Triangulating rebound  
789 attack on aes-like hashing. In Yevgeniy Dodis and Thomas Shrimpton, editors,  
790 *Advances in Cryptology - CRYPTO 2022 - 42nd Annual International Cryptol-  
791 ogy Conference, CRYPTO 2022, Santa Barbara, CA, USA, August 15-18, 2022,  
792 Proceedings, Part I*, volume 13507 of *Lecture Notes in Computer Science*, pages  
793 94–124. Springer, 2022.
- 794 26. Xiaoyang Dong, Jialiang Hua, Siwei Sun, Zheng Li, Xiaoyun Wang, and Lei Hu.  
795 Meet-in-the-middle attacks revisited: Key-recovery, collision, and preimage attacks.  
796 In *CRYPTO 2021, Proceedings, Part III*, volume 12827, pages 278–308. Springer.
- 797 27. Xiaoyang Dong, Boxin Zhao, Lingyue Qin, Qingliang Hou, Shun Zhang, and Xi-  
798 aoyun Wang. Generic mitm attack frameworks on sponge constructions. In Leonid

- 799 Reyzin and Douglas Stebila, editors, *Advances in Cryptology - CRYPTO 2024 -*  
800 *44th Annual International Cryptology Conference, Santa Barbara, CA, USA, Au-*  
801 *gust 18-22, 2024, Proceedings, Part IV*, volume 14923 of *Lecture Notes in Computer*  
802 *Science*, pages 3–37. Springer, 2024.
- 803 28. Orr Dunkelman, Nathan Keller, Eyal Ronen, and Adi Shamir. The retracing  
804 boomerang attack, with application to reduced-round AES. *J. Cryptol.*, 37(3):32,  
805 2024.
- 806 29. Orr Dunkelman, Gautham Sekar, and Bart Preneel. Improved meet-in-the-middle  
807 attacks on reduced-round DES. In *INDOCRYPT 2007, Proceedings*, volume 4859,  
808 pages 86–100. Springer, 2007.
- 809 30. Thomas Espitau, Pierre-Alain Fouque, and Pierre Karpman. Higher-order differ-  
810 ential meet-in-the-middle preimage attacks on SHA-1 and BLAKE. In *CRYPTO*  
811 *2015, Proceedings, Part I*, volume 9215, pages 683–701. Springer, 2015.
- 812 31. Thomas Fuhr and Brice Minaud. Match box meet-in-the-middle attack against  
813 KATAN. In *FSE 2014*, pages 61–81, 2014.
- 814 32. Jian Guo, San Ling, Christian Rechberger, and Huaxiong Wang. Advanced meet-  
815 in-the-middle preimage attacks: First results on full Tiger, and improved results on  
816 MD4 and SHA-2. In *ASIACRYPT 2010, Proceedings*, volume 6477, pages 56–75.
- 817 33. Hosein Hadipour and Maria Eichlseder. Autoguess: A tool for finding guess-and-  
818 determine attacks and key bridges. In Giuseppe Ateniese and Daniele Venturi,  
819 editors, *Applied Cryptography and Network Security - 20th International Confer-*  
820 *ence, ACNS 2022, Rome, Italy, June 20-23, 2022, Proceedings*, volume 13269 of  
821 *Lecture Notes in Computer Science*, pages 230–250. Springer, 2022.
- 822 34. Dmitry Khovratovich, Alex Biryukov, and Ivica Nikolic. Speeding up collision  
823 search for byte-oriented hash functions. In Marc Fischlin, editor, *Topics in Crypt-*  
824 *ology - CT-RSA 2009, The Cryptographers’ Track at the RSA Conference 2009,*  
825 *San Francisco, CA, USA, April 20-24, 2009. Proceedings*, volume 5473 of *Lecture*  
826 *Notes in Computer Science*, pages 164–181. Springer, 2009.
- 827 35. Dmitry Khovratovich, Gaëtan Leurent, and Christian Rechberger. Narrow-  
828 bicliques: Cryptanalysis of full IDEA. In David Pointcheval and Thomas Johans-  
829 son, editors, *EUROCRYPT 2012, Proceedings*, volume 7237, pages 392–410.
- 830 36. Simon Knellwolf and Dmitry Khovratovich. New preimage attacks against reduced  
831 SHA-1. In *CRYPTO 2012, Proceedings*, volume 7417, pages 367–383.
- 832 37. Brian A. LaMacchia and Andrew M. Odlyzko. Solving large sparse linear systems  
833 over finite fields. In Alfred Menezes and Scott A. Vanstone, editors, *Advances*  
834 *in Cryptology - CRYPTO ’90, 10th Annual International Cryptology Conference,*  
835 *Santa Barbara, California, USA, August 11-15, 1990, Proceedings*, volume 537 of  
836 *Lecture Notes in Computer Science*, pages 109–133. Springer, 1990.
- 837 38. Charlotte Lefevre and Bart Mennink. Tight preimage resistance of the sponge  
838 construction. In Yevgeniy Dodis and Thomas Shrimpton, editors, *Advances in*  
839 *Cryptology - CRYPTO 2022 - 42nd Annual International Cryptology Conference,*  
840 *CRYPTO 2022, Santa Barbara, CA, USA, August 15-18, 2022, Proceedings, Part*  
841 *IV*, volume 13510 of *Lecture Notes in Computer Science*, pages 185–204. Springer,  
842 2022.
- 843 39. Gaëtan Leurent and Clara Pernot. New Representations of the AES Key Schedule.  
844 Cryptology ePrint Archive, Report 2020/1253, 2020.
- 845 40. Gaëtan Leurent and Clara Pernot. New representations of the AES key schedule.  
846 In Anne Canteaut and François-Xavier Standaert, editors, *Advances in Cryptology*  
847 *- EUROCRYPT 2021 - 40th Annual International Conference on the Theory and*  
848 *Applications of Cryptographic Techniques, Zagreb, Croatia, October 17-21, 2021,*

- 849 *Proceedings, Part I*, volume 12696 of *Lecture Notes in Computer Science*, pages  
850 54–84. Springer, 2021.
- 851 41. Fukang Liu, Takanori Isobe, and Willi Meier. Exploiting weak diffusion of gimli:  
852 Improved distinguishers and preimage attacks. *IACR Trans. Symmetric Cryptol.*,  
853 2021(1):185–216, 2021.
- 854 42. Fukang Liu, Takanori Isobe, Willi Meier, and Zhonghao Yang. Algebraic attacks on  
855 round-reduced Keccak. In *ACISP 2021, Proceedings*, volume 13083, pages 91–110.
- 856 43. Florian Mendel, Christian Rechberger, Martin Schl  ffer, and S  ren S. Thomsen.  
857 The rebound attack: Cryptanalysis of reduced whirlpool and gr  stl. In *FSE 2009,*  
858 *2009*, pages 260–276, 2009.
- 859 44. Pawel Morawiecki, Josef Pieprzyk, and Marian Srebrny. Rotational cryptanalysis  
860 of round-reduced Keccak. In *FSE 2013,*, volume 8424, pages 241–262.
- 861 45. Lingyue Qin, Jialiang Hua, Xiaoyang Dong, Hailun Yan, and Xiaoyun Wang. Meet-  
862 in-the-middle preimage attacks on sponge-based hashing. In Carmit Hazay and  
863 Martijn Stam, editors, *Advances in Cryptology - EUROCRYPT 2023 - 42nd An-  
864 nual International Conference on the Theory and Applications of Cryptographic  
865 Techniques, Lyon, France, April 23-27, 2023, Proceedings, Part IV*, volume 14007  
866 of *Lecture Notes in Computer Science*, pages 158–188. Springer, 2023.
- 867 46. Lingyue Qin, Jialiang Hua, Xiaoyang Dong, Hailun Yan, and Xiaoyun Wang. Meet-  
868 in-the-middle preimage attacks on sponge-based hashing. In *EUROCRYPT 2023,*  
869 *Proceedings, Part IV*, volume 14007, pages 158–188. Springer, 2023.
- 870 47. Sondre R  njom, Navid Ghaedi Bardeh, and Tor Hellese  th. Yoyo tricks with AES.  
871 In Tsuyoshi Takagi and Thomas Peyrin, editors, *Advances in Cryptology - ASI-  
872 ACRYPT 2017 - 23rd International Conference on the Theory and Applications  
873 of Cryptology and Information Security, Hong Kong, China, December 3-7, 2017,*  
874 *Proceedings, Part I*, volume 10624 of *Lecture Notes in Computer Science*, pages  
875 217–243. Springer, 2017.
- 876 48. Yu Sasaki. Integer linear programming for three-subset meet-in-the-middle attacks:  
877 Application to GIFT. In *IWSEC 2018*, volume 11049, pages 227–243.
- 878 49. Yu Sasaki. Meet-in-the-middle preimage attacks on AES hashing modes and an  
879 application to whirlpool. In Antoine Joux, editor, *Fast Software Encryption -  
880 18th International Workshop, FSE 2011, Lyngby, Denmark, February 13-16, 2011,*  
881 *Revised Selected Papers*, volume 6733 of *Lecture Notes in Computer Science*, pages  
882 378–396. Springer, 2011.
- 883 50. Yu Sasaki and Kazumaro Aoki. Finding preimages in full MD5 faster than exhaus-  
884 tive search. In *EUROCRYPT 2009, Proceedings*, volume 5479, pages 134–152.
- 885 51. Yu Sasaki, Lei Wang, Shuang Wu, and Wenling Wu. Investigating fundamental  
886 security requirements on whirlpool: Improved preimage and collision attacks. In  
887 Xiaoyun Wang and Kazue Sako, editors, *Advances in Cryptology - ASIACRYPT  
888 2012 - 18th International Conference on the Theory and Application of Cryptology  
889 and Information Security, Beijing, China, December 2-6, 2012. Proceedings*, vol-  
890 ume 7658 of *Lecture Notes in Computer Science*, pages 562–579. Springer, 2012.
- 891 52. Andr   Schrottenloher and Marc Stevens. Simplified MITM modeling for permuta-  
892 tions: New (quantum) attacks. In *CRYPTO 2022, Proceedings, Part III*, volume  
893 13509, pages 717–747. Springer, 2022.
- 894 53. Andr   Schrottenloher and Marc Stevens. Simplified modeling of MITM attacks  
895 for block ciphers: new (quantum) attacks. *IACR Cryptol. ePrint Arch.*, page 816,  
896 2023.
- 897 54. Tyge Tiessen. Polytopic cryptanalysis. In Marc Fischlin and Jean-S  bastien Coron,  
898 editors, *Advances in Cryptology - EUROCRYPT 2016 - 35th Annual International*

- 899      *Conference on the Theory and Applications of Cryptographic Techniques, Vienna,*  
900      *Austria, May 8-12, 2016, Proceedings, Part I*, volume 9665 of *Lecture Notes in*  
901      *Computer Science*, pages 214–239. Springer, 2016.
- 902    55. Michael Tunstall. Improved "partial sums"-based square attack on AES. In  
903      Pierangela Samarati, Wenjing Lou, and Jianying Zhou, editors, *SECRYPT 2012 -*  
904      *Proceedings of the International Conference on Security and Cryptography, Rome,*  
905      *Italy, 24-27 July, 2012, SECRYPT is part of ICETE - The International Joint*  
906      *Conference on e-Business and Telecommunications*, pages 25–34. SciTePress, 2012.

## 908

000



912

## 913

014

917 The  $\text{MC}^{(3)}[0-3]$  are chosen as neutral bytes (marked by blue) for the for-  
 918 ward chunk and the  $\text{SR}^{(4)}[1-6, 8, 9, 11, 12, 14, 15]$  (marked by red) are chosen  
 919 as neutral bytes for the backward chunk. The intersection of the forward and  
 920 backward computations occurs at states  $\text{SR}^{(1)}$  and  $\text{MC}^{(1)}$ , where a partial match  
 921 is verified.

922 **Constraints on the Initial Structure** The constraints are applied to the  
 923 neutral bytes in the forward computation to ensure the two chunks operate  
 924 independently. Specifically, three constraints are added to the bytes  $\text{MC}^{(3)}[0-3]$   
 925 to prevent interference with the backward propagation.

926 The constants for  $\text{SR}_{\{1,2,3\}}^{(3)}$  are precomputed as follows:

$$\begin{cases} c_0 = 9 \cdot \text{MC}^{(3)}[0] \oplus e \cdot \text{MC}^{(3)}[1] \oplus b \cdot \text{MC}^{(3)}[2] \oplus d \cdot \text{MC}^{(3)}[3] \\ c_1 = d \cdot \text{MC}^{(3)}[0] \oplus 9 \cdot \text{MC}^{(3)}[1] \oplus e \cdot \text{MC}^{(3)}[2] \oplus b \cdot \text{MC}^{(3)}[3] \\ c_2 = b \cdot \text{MC}^{(3)}[0] \oplus d \cdot \text{MC}^{(3)}[1] \oplus 9 \cdot \text{MC}^{(3)}[2] \oplus e \cdot \text{MC}^{(3)}[3] \end{cases} \quad (23)$$

927 There are  $2^8$  possibilities for the values of  $\text{MC}^{(3)}[0-3]$  given the constraints.  
 928 Similarly, the backward chunk imposes 8 additional constraints on the bytes  
 929  $\text{MC}^{(4)}[0, 2, 5, 7, 8, 10, 13, 15]$ .

930 **Partial Matching Through MixColumns** The MitM approach relies on  
 931 the MixColumns operation to validate matches. Since each column in  $\text{SR}^{(1)}$  and  
 932  $\text{MC}^{(1)}$  contains five known bytes, one match is derived per column.

933 For example, the first column match involves deriving  $\text{SR}^{(1)}[0, 2]$  in the for-  
 934 ward direction and  $\text{MC}^{(1)}[1, 2, 3]$  in the backward computation. The relationship  
 935 can be expressed as:

$$\begin{aligned} & d \cdot \text{SR}^{(1)}[0] \oplus e \cdot \text{SR}^{(1)}[2] \\ &= d \cdot (b \cdot \text{MC}^{(1)}[1] \oplus d \cdot \text{MC}^{(1)}[2] \oplus 9 \cdot \text{MC}^{(1)}[3]) \oplus e \cdot (9 \cdot \text{MC}^{(1)}[1] \\ & \quad \oplus e \cdot \text{MC}^{(1)}[2] \oplus b \cdot \text{MC}^{(1)}[3]). \end{aligned} \quad (24)$$

## 936 Forward and Backward Computations

- 937 1. **Forward Computation:** The neutral bytes from  $\text{MC}^{(3)}$  propagate forward  
 938 to  $\text{SR}^{(1)}$ . By traversing all  $2^8$  possibilities of  $\text{MC}^{(3)}[0-3]$ , the resulting values  
 939 of  $\text{SR}^{(1)}$  are stored in table  $L_1$ , by the value of  $\text{SR}^{(1)}$  as the left part of Eq. (24)  
 940 (*i.e.*  $d \cdot \text{SR}^{(1)}[0] \oplus e \cdot \text{SR}^{(1)}[2]$ ).
- 941 2. **Backward Computation:** Similarly, the red neutral bytes from  $\text{SR}^{(4)}$  prop-  
 942 agate backward to  $\text{MC}^{(1)}$ . These values are stored in table  $L_2$ , indexed by  
 943  $\text{MC}^{(1)}$  as the right part of Eq. (24).
- 944 3. **Partial Matching:** The two tables  $L_1$  and  $L_2$  are compared to identify  
 945 32-bit partial matches based on the indices, allowing the preimage to be  
 946 recovered efficiently.



947 **B New Representation of AES's Key Schedule**

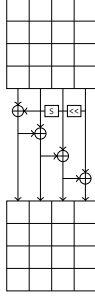


Fig. 15: AES-128

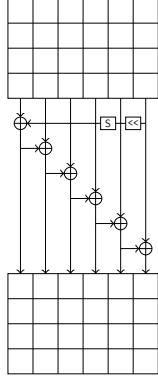


Fig. 16: AES-192

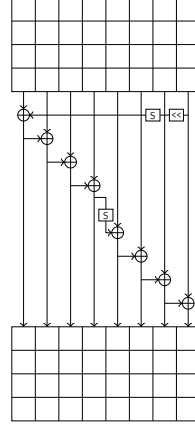


Fig. 17: AES-256

$$\text{MC} = \begin{bmatrix} 2 & 3 & 1 & 1 \\ 1 & 2 & 3 & 1 \\ 1 & 1 & 2 & 3 \\ 3 & 1 & 1 & 2 \end{bmatrix} \quad \text{MC}^{-1} = \begin{bmatrix} \text{e} & \text{b} & \text{d} & 9 \\ 9 & \text{e} & \text{b} & \text{d} \\ \text{d} & 9 & \text{e} & \text{b} \\ \text{b} & \text{d} & 9 & \text{e} \end{bmatrix} \quad (25)$$

948 At EUROCRYPT 2021, Leurent and Pernot introduced the new representa-  
 949 tion of AES's key schedule [40]. For AES-128, denote the 16-byte round key by  
 950  $\text{RK}^{(i)} = (a_0, a_1, \dots, a_{15})$ . Leurent *et al.* derived a new basis  $\text{S}^{(i)} = (s_0, s_1, \dots, s_{15})$ .  
 951 The relations between  $\text{RK}^{(i)}$  and  $\text{S}^{(i)}$  are  $\text{S}^{(i)} = A \cdot (\text{RK}^{(i)})^\dagger$  and  $\text{RK}^{(i)} =$   
 952  $C_0 \cdot (\text{S}^{(i)})^\dagger$ , where  $A$  is a matrix in Eq. (26) and  $C_0 = A^{-1}$ . Denote the state of  
 953 next round by  $\text{S}^{(i)} = (s'_0, s'_1, \dots, s'_{15})$ , the update process is illustrated in Figure  
 954 18, and the details listed in Eq. (27). For more details of AES-192/256, please  
 955 refer to [40].

$$A = \begin{pmatrix} 0 & 0 & 0 & 0 & 0 & 0 & 0 & 0 & 0 & 0 & 0 & 0 & 0 & 0 & 0 & 1 \\ 0 & 0 & 1 & 0 & 0 & 0 & 1 & 0 & 0 & 0 & 1 & 0 & 0 & 0 & 0 & 0 \\ 0 & 0 & 0 & 0 & 0 & 1 & 0 & 0 & 0 & 0 & 0 & 0 & 0 & 1 & 0 & 0 \\ 0 & 0 & 0 & 0 & 0 & 0 & 0 & 0 & 0 & 0 & 0 & 0 & 1 & 0 & 0 & 0 \\ 0 & 0 & 0 & 0 & 0 & 0 & 0 & 0 & 0 & 0 & 0 & 0 & 0 & 0 & 1 & 0 \\ 0 & 1 & 0 & 0 & 0 & 1 & 0 & 0 & 0 & 1 & 0 & 0 & 0 & 1 & 0 & 0 \\ 0 & 0 & 0 & 0 & 1 & 0 & 0 & 0 & 0 & 0 & 0 & 0 & 0 & 0 & 1 & 0 \\ 0 & 0 & 0 & 0 & 0 & 0 & 0 & 0 & 0 & 0 & 1 & 0 & 0 & 0 & 0 & 1 \\ 1 & 0 & 0 & 0 & 0 & 0 & 0 & 0 & 0 & 0 & 0 & 0 & 0 & 1 & 0 & 0 \\ 0 & 0 & 0 & 0 & 0 & 0 & 0 & 0 & 0 & 0 & 0 & 0 & 0 & 0 & 1 & 0 \\ 0 & 0 & 0 & 0 & 0 & 0 & 0 & 0 & 0 & 0 & 1 & 0 & 0 & 0 & 0 & 1 \\ 0 & 0 & 0 & 0 & 0 & 0 & 0 & 0 & 0 & 0 & 0 & 1 & 0 & 0 & 0 & 1 \\ 0 & 0 & 0 & 0 & 0 & 0 & 0 & 0 & 0 & 0 & 0 & 0 & 1 & 0 & 0 & 0 \\ 0 & 0 & 0 & 0 & 0 & 0 & 0 & 0 & 0 & 0 & 0 & 0 & 0 & 1 & 0 & 0 \\ 0 & 0 & 0 & 0 & 0 & 0 & 0 & 0 & 0 & 0 & 0 & 0 & 0 & 0 & 1 & 0 \\ 0 & 0 & 0 & 0 & 0 & 0 & 0 & 0 & 0 & 0 & 0 & 0 & 0 & 0 & 0 & 1 \end{pmatrix} \quad C_0 = \begin{pmatrix} 0 & 0 & 0 & 1 & 0 & 0 & 1 & 0 & 0 & 1 & 0 & 0 & 0 & 0 & 0 & 0 \\ 0 & 0 & 1 & 0 & 0 & 1 & 0 & 0 & 0 & 0 & 0 & 0 & 0 & 0 & 0 & 1 \\ 0 & 1 & 0 & 0 & 1 & 0 & 0 & 0 & 0 & 0 & 0 & 0 & 1 & 0 & 0 & 1 & 0 \\ 1 & 0 & 0 & 0 & 0 & 0 & 1 & 0 & 0 & 1 & 0 & 0 & 1 & 0 & 0 & 0 & 0 \\ 0 & 0 & 0 & 0 & 0 & 0 & 1 & 0 & 0 & 0 & 0 & 0 & 1 & 0 & 0 & 0 & 0 \\ 0 & 0 & 1 & 0 & 0 & 0 & 0 & 0 & 0 & 0 & 0 & 0 & 0 & 0 & 0 & 0 & 0 \\ 1 & 0 & 0 & 0 & 0 & 0 & 0 & 0 & 0 & 0 & 1 & 0 & 0 & 0 & 0 & 0 & 0 \\ 0 & 0 & 0 & 0 & 1 & 0 & 0 & 0 & 0 & 0 & 0 & 0 & 0 & 0 & 0 & 0 & 1 \\ 1 & 0 & 0 & 0 & 0 & 0 & 0 & 0 & 0 & 0 & 0 & 1 & 0 & 0 & 0 & 0 & 0 \\ 0 & 0 & 0 & 0 & 0 & 0 & 0 & 0 & 0 & 0 & 0 & 0 & 1 & 0 & 0 & 0 & 0 \\ 0 & 0 & 0 & 0 & 0 & 0 & 0 & 0 & 0 & 0 & 0 & 0 & 0 & 1 & 0 & 0 & 0 \\ 0 & 0 & 0 & 0 & 0 & 0 & 0 & 0 & 0 & 0 & 0 & 0 & 0 & 0 & 1 & 0 & 0 \\ 0 & 0 & 0 & 0 & 0 & 0 & 0 & 0 & 0 & 0 & 0 & 0 & 0 & 0 & 0 & 1 & 0 \\ 0 & 0 & 0 & 0 & 0 & 0 & 0 & 0 & 0 & 0 & 0 & 0 & 0 & 0 & 0 & 0 & 1 \end{pmatrix} \quad (\text{S}^{(i)})^\dagger = \begin{pmatrix} s_0 \\ s_1 \\ s_2 \\ s_3 \\ s_4 \\ s_5 \\ s_6 \\ s_7 \\ s_8 \\ s_9 \\ s_{10} \\ s_{11} \\ s_{12} \\ s_{13} \\ s_{14} \\ s_{15} \end{pmatrix} \quad (26)$$

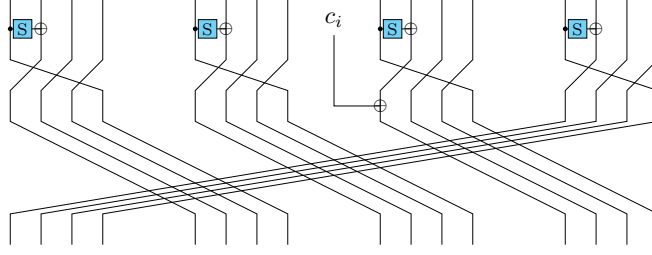


Fig. 18: New Representations of AES-128's key schedule [40]

$$\left\{ \begin{array}{ll} s'_0 = s_{13} \oplus S(s_{12}) & s'_8 = s_5 \oplus S(s_4) \\ s'_1 = s_{14} & s'_9 = s_6 \\ s'_2 = s_{15} & s'_{10} = s_7 \\ s'_3 = s_{12} & s'_{11} = s_4 \\ s'_4 = s_1 \oplus S(s_0) & s'_{12} = s_9 \oplus S(s_8) \oplus c_i \\ s'_5 = s_2 & s'_{13} = s_{10} \\ s'_6 = s_3 & s'_{14} = s_{11} \\ s'_7 = s_0 & s'_{15} = s_8 \end{array} \right. \quad (27)$$

## 956 C Key-Recovery Attack on 6-round AES-192 with Two 957 Plaintext-Ciphertext Pairs

958 The 6-round MitM characteristic is shown in Figure 8. Denote the bytes of the  
959 starting state  $S^{(3)}$  by  $k_0, k_1, \dots, k_{23}$ . The 19 expressions on the red bytes of  
960  $S^{(3)}$  for the 19 consumed DoFs of  $\blacksquare$  are shown as Eq. (20) (deleting the boxed  
961 parts). The matrices before and after TA are shown in Eq. (28). The steps for  
962 the 6-round MitM attack are given in Algorithm 10.

$$\begin{pmatrix}
\begin{array}{c}
\widehat{S}^{(1)}[20] \\
\widehat{S}^{(4)}[8] \\
\widehat{R}^{(0)}[10] \\
\widehat{R}^{(3)}[18] \\
\widehat{MC}^{(0)}[10] \\
\widehat{A}^{(1)}[0] \\
\widehat{MC}^{(4)}[8] \\
\widehat{MC}^{(4)}[9] \\
\widehat{MC}^{(4)}[11] \\
\widehat{SR}^{(3)}[1] \\
\widehat{SR}^{(3)}[3] \\
\widehat{SR}^{(3)}[4] \\
\widehat{SR}^{(3)}[6] \\
\widehat{SR}^{(3)}[9] \\
\widehat{SR}^{(3)}[11] \\
\widehat{SR}^{(3)}[12] \\
\widehat{SR}^{(3)}[14] \\
\widehat{SR}^{(2)}[7] \\
\widehat{SR}^{(2)}[13]
\end{array}
&
\begin{array}{c}
k_0 \ k_1 \ k_2 \ k_3 \ k_4 \ k_5 \ k_6 \ k_7 \ k_{11} \ k_{12} \ k_{13} \ k_{14} \ k_{15} \ k_{16} \ k_{17} \ k_{18} \ k_{19} \ k_{20} \ k_{21} \ k_{22} \ k_{23} \\
0 \ 0 \ 0 \ 0 \ 0 \ 0 \ 0 \ 0 \ 0 \ 0 \ 0 \ 0 \ 0 \ 0 \ 0 \ 0 \ 0 \ 1 \ 1 \ 1 \ 0 \\
0 \ 0 \ 0 \ 0 \ 0 \ 0 \ 0 \ 0 \ 0 \ 0 \ 0 \ 0 \ 0 \ 0 \ 0 \ 0 \ 0 \ 1 \ 1 \ 0 \ 0 \\
0 \ 0 \ 0 \ 0 \ 0 \ 0 \ 0 \ 0 \ 1 \ 0 \ 0 \ 0 \ 0 \ 0 \ 0 \ 0 \ 0 \ 1 \ 1 \ 0 \ 0 \ 0 \\
0 \ 0 \ 0 \ 0 \ 0 \ 0 \ 0 \ 1 \ 0 \ 0 \ 0 \ 0 \ 0 \ 0 \ 0 \ 0 \ 1 \ 0 \ 0 \ 0 \ 0 \ 0 \\
1 \ 1 \ 0 \ 1 \ 1 \ 1 \ 1 \ 0 \ 0 \ 1 \ 0 \ 1 \ 1 \ 0 \ 0 \ 0 \ 0 \ 0 \ 0 \ 0 \ 0 \ 0 \\
1 \ 0 \ 1 \ 1 \ 1 \ 1 \ 1 \ 1 \ 1 \ 1 \ 1 \ 1 \ 1 \ 1 \ 0 \ 0 \ 0 \ 0 \ 0 \ 0 \ 0 \ 0 \\
1 \ 1 \ 0 \ 0 \ 0 \ 0 \ 0 \ 0 \ 0 \ 0 \ 1 \ 1 \ 1 \ 1 \ 0 \ 0 \ 0 \ 0 \ 0 \ 0 \ 0 \ 0 \\
0 \ 0 \ 0 \ 1 \ 0 \ 1 \ 1 \ 0 \ 0 \ 0 \ 0 \ 0 \ 1 \ 0 \ 0 \ 0 \ 0 \ 0 \ 0 \ 0 \ 0 \ 0 \\
1 \ 0 \ 0 \ 0 \ 0 \ 0 \ 0 \ 0 \ 0 \ 1 \ 0 \ 0 \ 0 \ 0 \ 0 \ 0 \ 0 \ 0 \ 1 \ 0 \ 0 \ 0 \\
1 \ 1 \\
1 \ 1 \\
1 \ 1 \\
1 \ 1 \\
1 \ 1 \ 1 \ 0 \ 1 \ 1 \ 1 \ 1 \ 1 \ 0 \ 1 \ 1 \ 1 \ 1 \ 1 \ 0 \ 1 \ 1 \ 1 \ 1 \ 1 \ 1 \\
1 \ 1 \ 1 \ 0 \ 1 \ 1 \ 1 \ 1 \ 1 \ 0 \ 1 \ 1 \ 1 \ 1 \ 1 \ 0 \ 1 \ 1 \ 1 \ 1 \ 1 \ 1 \\
1 \ 1 \ 1 \ 0 \ 1 \ 1 \ 1 \ 1 \ 1 \ 0 \ 1 \ 1 \ 1 \ 1 \ 1 \ 0 \ 1 \ 1 \ 1 \ 1 \ 1 \ 1 \\
0 \ 0 \ 0 \ 0 \ 0 \ 1 \ 0 \ 0 \ 1 \ 0 \ 0 \ 1 \ 0 \ 0 \ 0 \ 0 \ 0 \ 1 \ 0 \ 0 \ 0 \ 0 \\
0 \ 0 \ 0 \ 0 \ 1 \ 0 \ 0 \ 0 \ 0 \ 0 \ 0 \ 0 \ 1 \ 0 \ 0 \ 0 \ 0 \ 1 \ 0 \ 0 \ 0 \ 0
\end{array}
\end{pmatrix}
\begin{pmatrix}
\begin{array}{c}
\widehat{SR}^{(3)}[1] \\
\widehat{SR}^{(3)}[3] \\
\widehat{SR}^{(3)}[4] \\
\widehat{SR}^{(3)}[6] \\
\widehat{SR}^{(3)}[9] \\
\widehat{SR}^{(3)}[11] \\
\widehat{SR}^{(3)}[12] \\
\widehat{R}^{(3)}[18] \\
\widehat{SR}^{(3)}[14] \\
\widehat{S}^{(1)}[20] \\
\widehat{A}^{(1)}[0] \\
\widehat{MC}^{(4)}[9] \\
\widehat{R}^{(0)}[10] \\
\widehat{MC}^{(4)}[8] \\
\widehat{SR}^{(2)}[13] \\
\widehat{MC}^{(0)}[10] \\
\widehat{SR}^{(2)}[7] \\
\widehat{MC}^{(4)}[11] \\
\widehat{S}^{(4)}[8]
\end{array}
&
\begin{array}{c}
k_{18} \ k_{17} \ k_{22} \ k_2 \ k_6 \ k_7 \ k_{12} \ k_{19} \ k_1 \ k_5 \ k_{11} \ k_{20} \\
1 \ 1 \ 1 \ 1 \ 1 \ 1 \ 1 \ 1 \ 1 \ 1 \ 1 \ 1 \ 1 \\
1 \ 1 \ 1 \ 1 \ 1 \ 1 \ 1 \ 1 \ 1 \ 1 \ 1 \ 1 \ 1 \\
1 \ 1 \ 1 \ 1 \ 1 \ 1 \ 1 \ 1 \ 1 \ 1 \ 1 \ 1 \ 1 \\
1 \ 1 \ 1 \ 1 \ 1 \ 1 \ 1 \ 1 \ 1 \ 1 \ 1 \ 1 \ 1 \\
0 \ 1 \ 1 \ 1 \ 1 \ 1 \ 0 \ 1 \ 1 \ 1 \ 1 \ 1 \ 1 \\
0 \ 1 \ 1 \ 1 \ 1 \ 1 \ 0 \ 1 \ 1 \ 1 \ 1 \ 1 \ 1 \\
0 \ 1 \ 1 \ 1 \ 1 \ 1 \ 0 \ 1 \ 1 \ 1 \ 1 \ 1 \ 1 \\
1 \ 0 \ 0 \ 0 \ 1 \ 0 \ 0 \ 0 \ 0 \ 0 \ 0 \ 0 \\
0 \ 1 \ 1 \ 1 \ 1 \ 1 \ 0 \ 1 \ 1 \ 1 \ 1 \ 1 \\
0 \ 0 \ 1 \ 0 \ 0 \ 0 \ 0 \ 0 \ 0 \ 0 \ 1 \\
0 \ 0 \ 0 \ 1 \ 1 \ 1 \ 1 \ 0 \ 0 \ 1 \ 1 \ 0 \\
0 \ 0 \ 0 \ 0 \ 1 \ 0 \ 0 \ 0 \ 1 \ 0 \ 0 \ 0 \\
0 \ 0 \ 0 \ 0 \ 0 \ 1 \ 0 \ 1 \ 0 \ 0 \ 0 \ 1 \\
0 \ 0 \ 0 \ 0 \ 0 \ 0 \ 1 \ 0 \ 1 \ 0 \ 0 \ 0 \\
0 \ 0 \ 0 \ 0 \ 0 \ 0 \ 0 \ 1 \ 0 \ 0 \ 0 \ 0 \\
0 \ 0 \ 0 \ 0 \ 0 \ 0 \ 0 \ 0 \ 1 \ 1 \ 1 \ 0 \\
0 \ 0 \ 0 \ 0 \ 0 \ 0 \ 0 \ 0 \ 0 \ 1 \ 1 \ 1 \\
0 \ 0 \ 0 \ 0 \ 0 \ 0 \ 0 \ 0 \ 0 \ 1 \ 0 \\
0 \ 0 \ 0 \ 0 \ 0 \ 0 \ 0 \ 0 \ 0 \ 1 \ 0 \\
0 \ 0 \ 0 \ 0 \ 0 \ 0 \ 0 \ 0 \ 0 \ 1
\end{array}
&
\begin{array}{c}
k_0 \ k_3 \ k_4 \ k_{13} \ k_{14} \ k_{15} \ k_{16} \ k_{21} \ k_{23} \\
1 \ 1 \ 1 \ 1 \ 1 \ 1 \ 1 \ 1 \ 1 \\
1 \ 1 \ 1 \ 1 \ 1 \ 1 \ 1 \ 1 \ 1 \\
1 \ 1 \ 1 \ 1 \ 1 \ 1 \ 1 \ 1 \ 1 \\
1 \ 1 \ 1 \ 1 \ 1 \ 1 \ 1 \ 1 \ 1 \\
1 \ 0 \ 1 \ 1 \ 1 \ 1 \ 1 \ 1 \ 1 \\
1 \ 0 \ 1 \ 1 \ 1 \ 1 \ 1 \ 1 \ 1 \\
1 \ 0 \ 0 \ 0 \ 0 \ 0 \ 0 \ 0 \ 0 \\
1 \ 0 \ 1 \ 1 \ 1 \ 1 \ 1 \ 1 \ 1 \\
1 \ 0 \ 1 \ 1 \ 1 \ 1 \ 1 \ 1 \ 1 \\
0 \ 0 \ 0 \ 0 \ 0 \ 0 \ 0 \ 0 \ 0 \\
0 \ 1 \ 0 \ 0 \ 0 \ 1 \ 0 \ 0 \ 0 \\
0 \ 0 \ 0 \ 0 \ 0 \ 0 \ 0 \ 0 \ 0 \\
1 \ 0 \ 0 \ 1 \ 1 \ 1 \ 1 \ 0 \ 0 \ 0 \\
0 \ 0 \ 1 \ 1 \ 0 \ 0 \ 0 \ 0 \ 0 \ 0 \\
1 \ 1 \ 1 \ 1 \ 1 \ 0 \ 0 \ 0 \ 0 \ 0 \\
0 \ 0 \ 0 \ 0 \ 1 \ 0 \ 0 \ 0 \ 0 \ 0 \\
1 \ 0 \ 0 \ 0 \ 0 \ 0 \ 0 \ 0 \ 1 \ 0 \\
0 \ 0 \ 0 \ 0 \ 0 \ 0 \ 0 \ 0 \ 1 \ 0
\end{array}
\end{pmatrix}
\quad (28)$$

## D Key-Recovery Attack on 7-round AES-256 with Two Plaintext-Ciphertext Pairs

The 7-round MitM characteristic is shown in Figure 19. The bytes of the starting state  $S^{(1)}$  are denoted as  $k_0, k_1, \dots, k_{31}$ . The 22 expressions on the red bytes of  $S^{(1)}$  for the 22 consumed DoFs of  $\blacksquare$  are shown as Eq. (29) (deleting the boxed parts). Using TA, we can get 9 free variables  $S^{(1)}[0, 6, 14, 18, 20, 22, 27, 28, 30]$  and 14 dependent variables  $S^{(1)}[1, 2, 3, 4, 5, 7, 9, 10, 11, 16, 17, 21, 29, 31]$ , the matrices before and after TA are shown in Eq. (30). The steps for the 7-round MitM attack are given in Algorithm 11.

---

**Algorithm 10:** Attack on 6-round AES-192 with 2  $(P, C)$ 


---

```

1 for  $2^\zeta$  values of  $S^{(3)}[10] \in \mathbb{F}_2^8$  do
2   for  $(e_1, e_2, \dots, e_{12}) \in \mathbb{F}_2^{96}$  do
3      $U \leftarrow []$ 
4     for  $S^{(3)}[0, 3, 4, 13, 14, 15, 16, 21, 23] \in \mathbb{F}_2^{72}$  do
5       Assign  $(e_1, e_2, \dots, e_{12})$  to the last 12 expressions in Eq. (21) (b)
6       Deduce  $S^{(3)}[1, 2, 5, 6, 7, 11, 12, 17, 18, 19, 20, 22]$ 
7       Compute  $\mathbf{u} = \widehat{SR}^{(3)}[1, 3, 4, 6, 9, 11, 12] \in \mathbb{F}_2^{8 \times 7}$ 
8        $U[\mathbf{u}] \leftarrow S^{(3)}[v_{\mathcal{R}}]$  /*  $v_{\mathcal{R}}$  represents all 21 red indexes */
9     end
10    for  $\mathbf{u} \in \mathbb{F}_2^{56}$  do
11       $L \leftarrow []$ 
12      for  $S^{(3)}[8, 9] \in \mathbb{F}_2^{16}$  do
13        Compute the 2-byte matching point  $v$ ,  $L[v] \leftarrow S^{(3)}[8, 9]$ 
14      end
15      for values in  $U[\mathbf{u}]$  do
16        Compute the 2-byte matching point  $v'$ 
17        for values in  $L[v']$  do
18          if  $E(Key = S^{(3)}, P_1) = C_1$  and  $E(Key = S^{(3)}, P_2) = C_2$ 
19            then
20              return  $S^{(3)}$ 
21            end
22          end
23        end
24      end
25    end

```

---

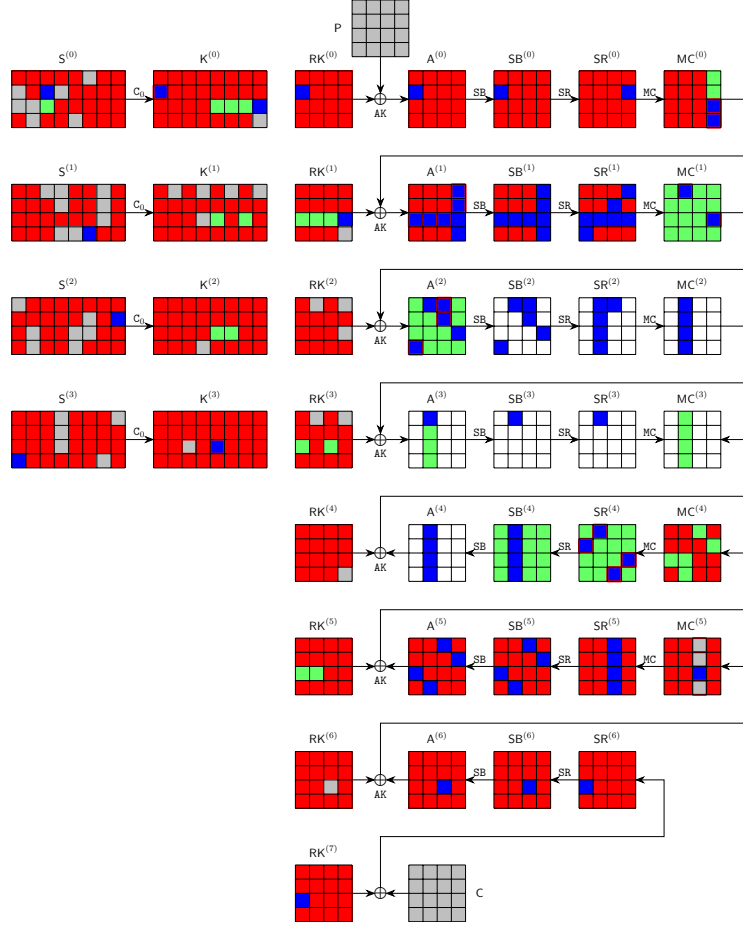


Fig. 19: The 7-round attack on AES-256

$$\begin{aligned}
& \widehat{K}^{(0)}[1] = k_{10} \oplus k_{16} \oplus k_{30} \oplus k_4 \oplus S(k_{23}) \\
& \widehat{K}^{(3)}[10] = k_{28} \oplus S(k_{27} \oplus S(k_{26} \oplus S(k_{25}))) \oplus k_2 \oplus S(k_1) \\
& \widehat{K}^{(3)}[18] = k_{29} \oplus S(k_{28} \oplus S(k_{27} \oplus S(k_{26} \oplus S(k_{25})))) \oplus k_3 \oplus S(k_2 \oplus S(k_1)) \oplus k_9 \oplus k_{23} \\
& \widehat{MC}^{(0)}[14] = S(k_6) \oplus 2 \cdot S(k_{22} \oplus k_2) \oplus 3 \cdot S(k_{14} \oplus k_{20}) \oplus SR^{(0)}[13] \\
& \widehat{MC}^{(0)}[15] = 3 \cdot S(k_6) \oplus S(k_{22} \oplus k_2) \oplus 2 \cdot S(k_{14} \oplus k_{20}) \oplus SR^{(0)}[13] \\
& \widehat{A}^{(1)}[2] = S(k_{12} \oplus k_{18} \oplus k_{24} \oplus S(k_{31}) \oplus k_6) \oplus S(k_{10} \oplus k_{30}) \oplus 2 \cdot S(k_{22} \oplus k_{28}) \oplus 3 \cdot S(k_{14}) \\
& \quad \oplus k_9 \oplus k_{29} \oplus k_3 \oplus S(k_8) \oplus k_{23} \\
& \widehat{A}^{(1)}[6] = S(k_{18} \oplus k_6) \oplus S(k_{30} \oplus k_4) \oplus 2 \cdot S(k_{22}) \oplus 3 \cdot S(k_{14} \oplus k_{20} \oplus k_{26} \oplus k_0 \oplus S(k_7)) \\
& \quad \oplus k_3 \oplus k_{23} \\
& \widehat{A}^{(1)}[10] = S(k_{12} \oplus k_6) \oplus S(k_{30}) \oplus 2 \cdot S(k_8 \oplus S(k_{15}) \oplus k_{22} \oplus k_{28} \oplus k_2) \oplus 3 \cdot S(k_{14} \oplus k_{26}) \\
& \quad \oplus k_{29} \oplus k_{23} \\
& \widehat{A}^{(1)}[12] = 2 \cdot S(k_6) \oplus S(k_{22} \oplus k_2) \oplus S(k_{14} \oplus k_{20}) \oplus k_7 \oplus 3 \cdot SR^{(0)}[13] \\
& \widehat{A}^{(1)}[13] = S(k_6) \oplus 3 \cdot S(k_{22} \oplus k_2) \oplus S(k_{14} \oplus k_{20}) \oplus k_{31} \oplus 2 \cdot SR^{(0)}[13] \\
& \widehat{MC}^{(1)}[4] = 2 \cdot SR^{(1)}[4] \oplus 3 \cdot SR^{(1)}[5] \oplus SR^{(1)}[7] \oplus SR^{(1)}[6] \\
& \widehat{MC}^{(1)}[14] = SR^{(1)}[13] \oplus 3 \cdot SR^{(1)}[6] \oplus SR^{(1)}[12] \oplus 2 \cdot SR^{(1)}[14] \\
& \widehat{A}^{(2)}[3] = 3 \cdot SR^{(1)}[0] \oplus SR^{(1)}[1] \oplus RK^{(2)}[3] \oplus SR^{(1)}[2] \oplus 2 \cdot SR^{(1)}[3] \\
& \widehat{A}^{(2)}[8] = 2 \cdot SR^{(1)}[8] \oplus SR^{(1)}[11] \oplus RK^{(2)}[8] \oplus 3 \cdot SR^{(1)}[9] \oplus SR^{(1)}[10] \\
& \widehat{A}^{(2)}[9] = SR^{(1)}[8] \oplus SR^{(1)}[11] \oplus RK^{(2)}[9] \oplus 2 \cdot SR^{(1)}[9] \oplus 3 \cdot SR^{(1)}[10] \\
& \widehat{MC}^{(5)}[8] = S^{-1}(k_{19} \oplus S(k_{18} \oplus S(k_{17}))) \oplus k_{13} \oplus S(k_{12} \oplus S(k_{11} \oplus S(k_{10} \oplus S(k_9)))) \oplus k_{18} \\
& \quad \oplus S(k_{17}) \oplus S(k_{11} \oplus S(k_{10} \oplus S(k_9))) \oplus k_{12} \\
& \widehat{MC}^{(5)}[9] = S^{-1}(k_{17} \oplus k_5 \oplus S(k_4 \oplus S(k_3 \oplus S(k_2 \oplus S(k_1))))) \oplus k_4 \oplus S(k_3 \oplus S(k_2 \oplus S(k_1))) \\
& \quad \oplus k_{10} \oplus S(k_9) \\
& \widehat{MC}^{(5)}[11] = S^{-1}(k_{21} \oplus S(k_{20} \oplus S(k_{19} \oplus S(k_{18} \oplus S(k_{17})))) \oplus k_{20} \oplus S(k_{19} \oplus S(k_{18} \oplus S(k_{17}))) \\
& \quad \oplus k_{26} \oplus S(k_{25}) \\
& \widehat{SR}^{(4)}[1] = 9 \cdot MC^{(4)}[0] \oplus e \cdot MC^{(4)}[1] \oplus b \cdot (S^{(2)}[3] \oplus S^{(2)}[9] \oplus S^{(2)}[23]) \oplus d \cdot MC^{(4)}[3] \\
& \quad \oplus b \cdot (S^{(2)}[29] \oplus A^{(5)}[2]) \\
& \widehat{SR}^{(4)}[4] = e \cdot MC^{(4)}[4] \oplus b \cdot MC^{(4)}[5] \oplus d \cdot (S^{(2)}[9] \oplus A^{(5)}[6]) \oplus 9 \cdot RK^{(2)}[29] \oplus b \cdot (S^{(2)}[29] \oplus A^{(5)}[7]) \\
& \widehat{SR}^{(4)}[11] = d \cdot RK^{(5)}[8] \oplus 9 \cdot MC^{(4)}[9] \oplus e \cdot MC^{(4)}[10] \oplus b \cdot MC^{(4)}[11] \oplus d \cdot A^{(5)}[8] \\
& \widehat{SR}^{(4)}[14] = b \cdot MC^{(4)}[12] \oplus d \cdot RK^{(5)}[13] \oplus 9 \cdot MC^{(4)}[14] \oplus e \cdot MC^{(4)}[15] \oplus d \cdot A^{(5)}[13]
\end{aligned}$$

(29)



---

**Algorithm 11:** Attack on 7-round AES-256 with 2  $(P, C)$ 


---

```

1  for  $2^\zeta$  values of  $S^{(1)}[8, 12, 13, 15, 19, 24, 25, 26] \in \mathbb{F}_2^{64}$  do
2      for  $(e_1, e_2, \dots, e_{14}) \in \mathbb{F}_2^{112}$  do
3           $U \leftarrow []$ 
4          for  $S^{(1)}[0, 6, 14, 18, 20, 22, 27, 28, 30] \in \mathbb{F}_2^{72}$  do
5              Assign  $(e_1, e_2, \dots, e_{14})$  to the last 14 expressions in Eq. (30) (b)
6              Deduce  $S^{(1)}[1, 2, 3, 4, 5, 7, 9, 10, 11, 16, 17, 21, 29, 31]$ 
7              Compute 8-byte
                   $\mathbf{u} = (\widehat{SR}^{(4)}[1, 4, 11, 14], \widehat{MC}^{(1)}[4, 14], \widehat{A}^{(2)}[9], \widehat{MC}^{(0)}[14]) \in \mathbb{F}_2^{64}$ 
8               $U[\mathbf{u}] \leftarrow S^{(1)}[v_{\mathcal{R}}] /* v_{\mathcal{R}}$  represents all 23 red indexes */
9          end
10         for  $\mathbf{u} \in \mathbb{F}_2^{64}$  do
11              $L \leftarrow []$ 
12             for  $S^{(1)}[23] \in \mathbb{F}_2^8$  do
13                 Compute forward and backward to the 1-byte matching point  $v$ 
14                  $L[v] \leftarrow S^{(1)}[23]$ 
15             end
16             for values in  $U[\mathbf{u}]$  do
17                 Compute forward and backward to the 1-byte matching point  $v'$ 
18                 for values in  $L[v']$  do
19                     if  $E(Key = S^{(1)}, P_1) = C_1$  and  $E(Key = S^{(1)}, P_2) = C_2$  then
20                         return  $S^{(1)}$ 
21                     end
22                 end
23             end
24         end
25     end
26 end

```

---



980 We experiment with the 5-byte partial target preimage attack by fixing  
 981 the 5 target bytes  $T[0,1,2,6,12] = 0$ . The 4 preimages are produced with  
 982  $T[0,1,2,6,12] = 0$ , which are listed in Table 3.

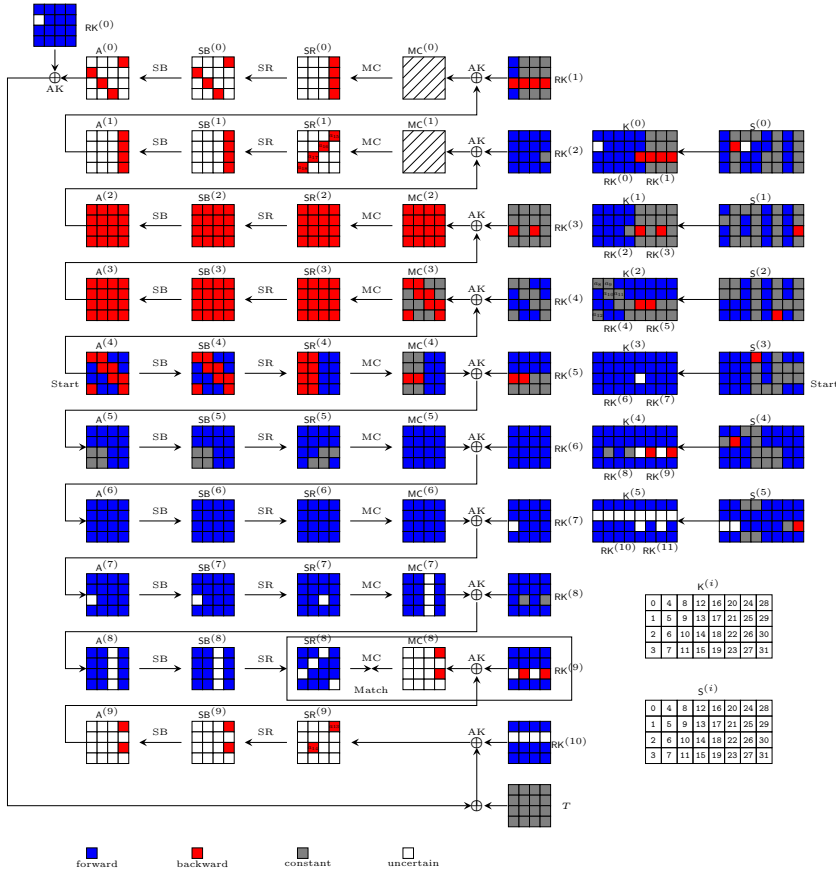


Fig. 20: The MitM attack on 10-round AES-256

[illegible]

983 **F** Details of Specifications on Keccak, Ascon and Xoodyak  
984 Hash functions

## 985 F.1 The Keccak Hash Function

The Keccak [7] family has a  $b = 1600$ -bit state and different sizes of capacity and rate. For example, Keccak[1024] has a 512-bit digest and a capacity  $c = 2 \times 512$ . The 1600-bit state can be viewed as a  $5 \times 5 \times 64$  array of bits. Denote  $A_{\{x,y,z\}}^{(r)}$  as the bit located at the  $x$ -th column,  $y$ -th row and  $z$ -th lane in the round  $r$  ( $r \geq 0$ ), where  $0 \leq x \leq 4$ ,  $0 \leq y \leq 4$ ,  $0 \leq z \leq 63$ . For simplicity, all the coordinates are considered modulo 5 for  $x$  and  $y$ , and modulo 64 for  $z$  in the following paper. The inner permutation consists of 24 rounds, and each round has five operations  $\iota \circ \chi \circ \pi \circ \rho \circ \theta$ . The internal states of round  $r$  are denoted as  $A^{(r)} \xrightarrow{\theta} \theta^{(r)} \xrightarrow{\rho} \rho^{(r)} \xrightarrow{\pi} \pi^{(r)} \xrightarrow{\chi} \chi^{(r)} \xrightarrow{\iota} A^{(r+1)}$ . We list the five operations in each

---

**Algorithm 12:** Preimage Attack on 10-round AES-256-DM
 

---

```

1  Assign 0 to all  $\blacksquare$  in  $S^{(3)}$ ,  $S^{(3)}[13, 14, 15, 19, 20, 21, 22, 23, 25, 26, 29, 30] \leftarrow 0$ .
2   $(a_1, a_2, a_3, a_4, a_5, a_6, a_7, a_9, a_{10}, a_{11}, a_{12}, a_{13}, a_{14}, a_{15}, a_{17}) \leftarrow 0$ 
3   $U \leftarrow []$ 
4  for  $S^{(3)}[8, 16, 18, 24] \in \mathbb{F}_2^{32}$  do
5    Compute  $S^{(3)}[0, 1, 2, 3, 4, 5, 6, 7, 9, 10, 11, 17, 27, 28, 31]$ 
6    Compute  $a_8, a_{16}, a_{18}$  (denoted as  $\mathbf{u} \in \mathbb{F}_2^{24}$ )
7    If  $a_8 = 0, a_{16} = 0$  and  $a_{18} = 0$ , store the 19-byte  $\blacksquare$  of  $S^{(3)}$  in  $U[\mathbf{u}]$ .
8  end
9  /* In the following, we always fix  $a_8 = 0, a_{16} = 0$  and  $a_{18} = 0$  */
10 for  $2^{112}$  values of  $\blacksquare$  in  $MC^{(3)}, MC^{(4)}$  and  $A^{(5)}[2, 6]$  do
11    $L \leftarrow []$ 
12   for  $S^{(3)}[12] \in \mathbb{F}_2^8$  do
13     Compute backward to the 1-byte matching point  $v$ 
14      $L[v] \leftarrow S^{(3)}[12]$ 
15   end
16   for values in  $U[0]$  do
17     Compute forward to the 1-byte matching point  $v'$ 
18     for values in  $L[v']$  do
19       Check the full preimage.
20     end
21   end
22 end

```

---

Rounds	$S^{(3)}$	$A^{(4)}$	Target
10	0x40, 0x09, 0x01, 0x7a, 0x2d, 0x00, 0x50, 0x53, 0x90, 0x60, 0x2d, 0x00, 0x70, 0x00, 0x00, 0x00, 0x30, 0x04, 0x50, 0x00, 0x8e, 0x00, 0x00, 0x00, 0x11, 0x82, 0x23, 0x00, 0x00, 0x00, 0x2d, 0xd8	0xb9, 0x7e, 0xf2, 0xba, 0x89, 0x36, 0x01, 0x23, 0x20, 0x6c, 0x59, 0x8e, 0x50, 0x2d, 0x70, 0x43	0x00, 0x00, 0x00, 0xe9, 0x2d, 0xcf, 0x00, 0x56, 0xde, 0xfa, 0xae, 0xe6, 0x00, 0x7c, 0x3b, 0x83
	0xc7, 0xc6, 0xb4, 0xff, 0xe7, 0x00, 0xb3, 0x6d, 0x5a, 0xbe, 0xe7, 0x00, 0x51, 0x00, 0x00, 0x00, 0xa9, 0xd3, 0xb3, 0x00, 0x4e, 0x00, 0x00, 0x00, 0x73, 0x8f, 0xb5, 0x00, 0x00, 0x00, 0xe7, 0x94	0x57, 0x2d, 0x8d, 0xc3, 0x50, 0x57, 0xb4, 0xb5, 0xe2, 0x75, 0xe3, 0x4e, 0xb3, 0xe7, 0x28, 0x9c	0x00, 0x00, 0x00, 0xb7, 0xb6, 0x05, 0x00, 0x21, 0xda, 0x1e, 0x49, 0x31, 0x00, 0xbd, 0x0d, 0xef
	0xe0, 0xe1, 0xf8, 0x6e, 0xd3, 0x00, 0x34, 0x18, 0x79, 0xb6, 0xd3, 0x00, 0x6c, 0x00, 0x00, 0x00, 0xa0, 0xe0, 0x34, 0x00, 0x8e, 0x00, 0x00, 0x00, 0x5f, 0xcf, 0xc3, 0x00, 0x00, 0xd3, 0x66	0xcd, 0x10, 0xe2, 0x6e, 0x40, 0xd8, 0xf8, 0xc3, 0x58, 0x19, 0x1a, 0x8e, 0x34, 0xd3, 0xb, 0x11	0x00, 0x00, 0x00, 0x5b, 0x4a, 0x26, 0x00, 0x95, 0x94, 0xf4, 0x2d, 0x08, 0x00, 0x48, 0x16, 0x2d
	0xc0, 0xba, 0xf4, 0x17, 0x12, 0x00, 0x5a, 0xbe, 0x91, 0x81, 0x12, 0x00, 0x1a, 0x00, 0x00, 0x00, 0xd5, 0x03, 0x5a, 0x00, 0xf3, 0x00, 0x00, 0x00, 0xc7, 0xc6, 0x9d, 0x00, 0x00, 0x12, 0xc9	0xbf, 0xa4, 0x06, 0x44, 0x87, 0x32, 0xf4, 0x9d, 0x40, 0xde, 0x3c, 0xf3, 0x5a, 0x12, 0x39, 0xf7	0x00, 0x00, 0x00, 0x57, 0xe8, 0x01, 0x00, 0xb7, 0x94, 0x6d, 0xcc, 0xe3, 0x00, 0x9f, 0xfb, 0xa7

Table 3: Preimages of 10-round AFS-256

round as follows:

$$\begin{aligned}
\theta : \theta_{\{x,y,z\}}^{(r)} &= A_{\{x,y,z\}}^{(r)} \oplus D_{\{x,z\}}^{(r)}, D_{\{x,z\}}^{(r)} = C_{\{x-1,z\}}^{(r)} \oplus C_{\{x+1,z-1\}}^{(r)}, C_{\{x,z\}}^{(r)} = \sum_{y'=0}^4 A_{\{x,y',z\}}^{(r)}, \\
\rho : \rho_{\{x,y,z\}}^{(r)} &= \theta_{\{x,y,z-\gamma[x,y]\}}^{(r)}, \\
\pi : \pi_{\{y,2x+3y,z\}}^{(r)} &= \rho_{\{x,y,z\}}^{(r)}, \\
\chi : \chi_{\{x,y,z\}}^{(r)} &= \pi_{\{x,y,z\}}^{(r)} \oplus (\pi_{\{x+1,y,z\}}^{(r)} \oplus 1) \cdot \pi_{\{x+2,y,z\}}^{(r)}, \\
\iota : A^{(r+1)} &= \chi^{(r)} \oplus RC_r, RC_r \text{ is round-dependent constant,}
\end{aligned} \tag{32}$$

where the  $\theta$  operation is divided into three steps. The rotation constants  $\gamma[x, y]$ s are given in Table 4.

This paper focuses on Keccak[1024] and Keccak[768], as well as SHA3-512 and SHA3-384. For Keccak, the message is padded with “10\*1”, which is a single bit 1 followed by the minimum number of 0s and followed by a single bit 1. For SHA3, the message is padded with “0110\*1”.

	$x = 0$	$x = 1$	$x = 2$	$x = 3$	$x = 4$
$y = 0$	0	1	62	28	27
$y = 1$	36	44	6	55	20
$y = 2$	3	10	43	25	39
$y = 3$	41	45	15	21	8
$y = 4$	18	2	61	56	14

Table 4: The offset  $\gamma[x, y]$  in the  $\rho$  operation for Keccak

## F.2 Ascon-Hash and Ascon-XOF

The Ascon family [24] includes the hash functions Ascon-Hash and Ascon-Hasha as well as the extendable output functions Ascon-XOF and Ascon-XOFa with sponge-based modes of operations.

**Ascon Permutation.** The inner permutation applies 12 round functions to a 320-bit state. The state  $A$  is split into five 64-bit words, and denote  $A_{\{x,y\}}^{(r)}$  to be the  $x$ -th (column) bit of the  $y$ -th (row) 64-bit word, where  $0 \leq y \leq 4$ ,  $0 \leq x \leq 63$ . The round function consists of three operations  $p_C$ ,  $p_S$ , and  $p_L$ . Denote the internal states of round  $r$  as  $A^{(r)} \xrightarrow{p_S \circ p_C} S^{(r)} \xrightarrow{p_L} A^{(r+1)}$ .

- **Addition of Constants**  $p_C$ :  $A_{\{*,2\}}^{(r)} = A_{\{*,2\}}^{(r)} \oplus RC_r$ .
- **Substitution Layer**  $p_S$ : For each  $x$ , this step updates the columns  $A_{\{x,*\}}^{(r)}$  using the 5-bit Sbox. Assume the S-box maps  $(a_0, a_1, a_2, a_3, a_4) \in \mathbb{F}_2^5$  to

1014  $(b_0, b_1, b_2, b_3, b_4) \in \mathbb{F}_2^5$ , where  $a_0$  is the most significant bit. The algebraic  
 1015 normal form (ANF) of the Sbox is as follows:

$$\begin{cases} b_0 = a_4a_1 + a_3 + a_2a_1 + a_2 + a_1a_0 + a_1 + a_0 \\ b_1 = a_4 + a_3a_2 + a_3a_1 + a_3 + a_2a_1 + a_2 + a_1 + a_0 \\ b_2 = a_4a_3 + a_4 + a_2 + a_1 + 1 \\ b_3 = a_4a_0 + a_4 + a_3a_0 + a_3 + a_2 + a_1 + a_0 \\ b_4 = a_4a_1 + a_4 + a_3 + a_1a_0 + a_1 \end{cases} \quad (33)$$

1016 – **Linear Diffusion Layer  $p_L$ :**

$$\begin{aligned} A_{\{*,0\}}^{(r+1)} &\leftarrow S_{\{*,0\}}^{(r)} \oplus (S_{\{*,0\}}^{(r)} \ggg 19) \oplus (S_{\{*,0\}}^{(r)} \ggg 28), \\ A_{\{*,1\}}^{(r+1)} &\leftarrow S_{\{*,1\}}^{(r)} \oplus (S_{\{*,1\}}^{(r)} \ggg 61) \oplus (S_{\{*,1\}}^{(r)} \ggg 39), \\ A_{\{*,2\}}^{(r+1)} &\leftarrow S_{\{*,2\}}^{(r)} \oplus (S_{\{*,2\}}^{(r)} \ggg 1) \oplus (S_{\{*,2\}}^{(r)} \ggg 6), \\ A_{\{*,3\}}^{(r+1)} &\leftarrow S_{\{*,3\}}^{(r)} \oplus (S_{\{*,3\}}^{(r)} \ggg 10) \oplus (S_{\{*,3\}}^{(r)} \ggg 17), \\ A_{\{*,4\}}^{(r+1)} &\leftarrow S_{\{*,4\}}^{(r)} \oplus (S_{\{*,4\}}^{(r)} \ggg 7) \oplus (S_{\{*,4\}}^{(r)} \ggg 41). \end{aligned}$$

1017 **Ascon-Hash and Ascon-XOF.** The state  $A$  is composed of the outer part with 64  
 1018 bits  $A_{\{*,0\}}$  and the inner part 256 bits  $A_{\{*,i\}}$  ( $i = 1, 2, 3, 4$ ). For **Ascon-Hash**,  
 1019 the output size is 256 bits, and the security claim is  $2^{128}$ . For **Ascon-XOF**, the  
 1020 output can have arbitrary length and the security claim against preimage attack  
 1021 is  $\min(2^{128}, 2^l)$ , where  $l$  is the output length.

### 1022 F.3 Xoodyak and Xoodoo Permutation

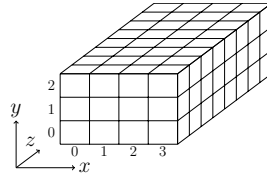


Fig. 21: Toy version of the Xoodoo state. The order in  $y$  is opposite to Keccak

Internally, Xoodyak makes use of the Xoodoo permutation [15], whose state (shown in Figure 21) bit denoted by  $A_{\{x,y,z\}}^{(r)}$  is located at the  $x$ -th column,  $y$ -th row and  $z$ -th lane in the round  $r$ , where  $0 \leq x \leq 3$ ,  $0 \leq y \leq 2$ ,  $0 \leq z \leq 31$ . For Xoodoo, all the coordinates are considered modulo 4 for  $x$ , modulo 3 for  $y$ , and modulo 32 for  $z$ . The permutation consists of the iteration of a round function  $R = \rho_{\text{east}} \circ \chi \circ \iota \circ \rho_{\text{west}} \circ \theta$ . The number of rounds is a parameter, which is 12 in Xoodyak. Denote the internal states of the round  $r$  as

$$A^{(r)} \xrightarrow{\theta} \theta^{(r)} \xrightarrow{\rho_{\text{west}}} \rho^{(r)} \xrightarrow{\iota} \iota^{(r)} \xrightarrow{\chi} \chi^{(r)} \xrightarrow{\rho_{\text{east}}} A^{(r+1)}.$$

1023

$$\begin{aligned}
\theta : \theta_{\{x,y,z\}}^{(r)} &= A_{\{x,y,z\}}^{(r)} \oplus \sum_{y'=0}^2 (A_{\{x-1,y',z-5\}}^{(r)} \oplus A_{\{x-1,y',z-14\}}^{(r)}), \\
\rho_{\text{west}} : \rho_{\{x,0,z\}}^{(r)} &= \theta_{\{x,0,z\}}^{(r)}, \rho_{\{x,1,z\}}^{(r)} = \theta_{\{x-1,1,z\}}^{(r)}, \rho_{\{x,2,z\}}^{(r)} = \theta_{\{x,2,z-11\}}^{(r)}, \\
\iota : \iota_{\{0,0,z\}}^{(r)} &= \rho_{\{0,0,z\}}^{(r)} \oplus RC_r, \text{ where } RC_r \text{ is round-dependent constant,} \\
\chi : \chi_{\{x,y,z\}}^{(r)} &= \iota_{\{x,y,z\}}^{(r)} \oplus (\iota_{\{x,y+1,z\}}^{(r)} \oplus 1) \cdot \iota_{\{x,y+2,z\}}^{(r)}, \\
\rho_{\text{east}} : A_{\{x,0,z\}}^{(r+1)} &= \chi_{\{x,0,z\}}^{(r)}, A_{\{x,1,z\}}^{(r+1)} = \chi_{\{x,1,z-1\}}^{(r)}, A_{\{x,2,z\}}^{(r+1)} = \chi_{\{x-2,2,z-8\}}^{(r)}.
\end{aligned} \tag{34}$$

1024 Xoodyak can serve as a XOF, i.e. Xoodyak-XOF, which offers arbitrary output  
1025 length  $l$ . The preimage resistance is  $\min(2^{128}, 2^l)$ . We target on Xoodyak-XOF  
1026 with output of 128-bit hash value and 128-bit absorbed message block.

## 1027 G MITM Attacks on 3-round Xoodyak-XOF

1028 The specification of Xoodyak [15] (one of the finalists of NIST LWC) is given  
1029 in F.3. The Xoodyak-XOF offers an arbitrary output length  $l$  and the preimage  
1030 resistance is  $\min(2^{128}, 2^l)$ . We target Xoodyak-XOF with a 128-bit digest against  
the preimage attack and collision attack.

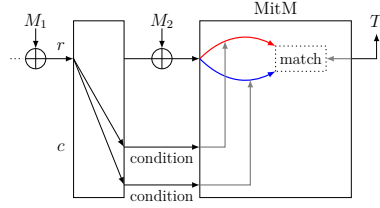


Fig. 22: MitM Preimage Attack [45]

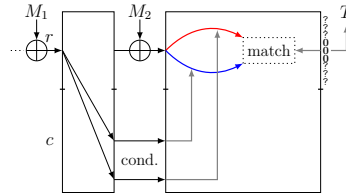


Fig. 23: MitM Collision Attack [27]

1031  
1032

### G.1 MitM Preimage Attack on 3-round Xoodyak-XOF

1033 Following Qin *et al.*'s framework [45] of MitM preimage attack on sponge func-  
1034 tion in Figure 22, we launch a new 3-round MitM preimage attack on Xoodyak-  
1035 XOF with a new 3-round MitM path given in Figure 24.

1036 The starting state  $A^{(0)}$  contains  $\lambda^+ = 7$  ■ bits and  $\lambda^- = 67$  ■ bits. In the  
1037 computation from  $A^{(0)}$  to  $\iota^{(2)}$ , the consumed degrees of freedom (DoFs) of ■ and  
1038 ■ are  $l^+ = 0$  and  $l^- = 60$  bits, respectively. Therefore,  $\text{DoF}^+ = 7$ ,  $\text{DoF}^- = 7$ ,  
1039 and there is  $\text{DoM} = 7$  matching bits as in Eq. (35) with the deterministic relations  
1040 of  $\iota^{(2)}$ :

$$\begin{aligned}
\chi_{\{1,2,8\}}^{(2)} &= \iota_{\{1,2,8\}}^{(2)} \oplus (\iota_{\{1,0,8\}}^{(2)} \oplus 1) \cdot \iota_{\{1,1,8\}}^{(2)}, \chi_{\{1,2,10\}}^{(2)} = \iota_{\{1,2,10\}}^{(2)} \oplus (\iota_{\{1,0,10\}}^{(2)} \oplus 1) \cdot \iota_{\{1,1,10\}}^{(2)}, \\
\chi_{\{2,2,10\}}^{(2)} &= \iota_{\{2,2,10\}}^{(2)} \oplus (\iota_{\{2,0,10\}}^{(2)} \oplus 1) \cdot \iota_{\{2,1,10\}}^{(2)}, \chi_{\{1,2,17\}}^{(2)} = \iota_{\{1,2,17\}}^{(2)} \oplus (\iota_{\{1,0,17\}}^{(2)} \oplus 1) \cdot \iota_{\{1,1,17\}}^{(2)}, \\
\chi_{\{1,2,26\}}^{(2)} &= \iota_{\{1,2,26\}}^{(2)} \oplus (\iota_{\{1,0,26\}}^{(2)} \oplus 1) \cdot \iota_{\{1,1,26\}}^{(2)}, \chi_{\{1,2,31\}}^{(2)} = \iota_{\{1,2,31\}}^{(2)} \oplus (\iota_{\{1,0,31\}}^{(2)} \oplus 1) \cdot \iota_{\{1,1,31\}}^{(2)}, \\
\chi_{\{2,2,31\}}^{(2)} &= \iota_{\{2,2,31\}}^{(2)} \oplus (\iota_{\{2,0,31\}}^{(2)} \oplus 1) \cdot \iota_{\{2,1,31\}}^{(2)}.
\end{aligned} \tag{35}$$

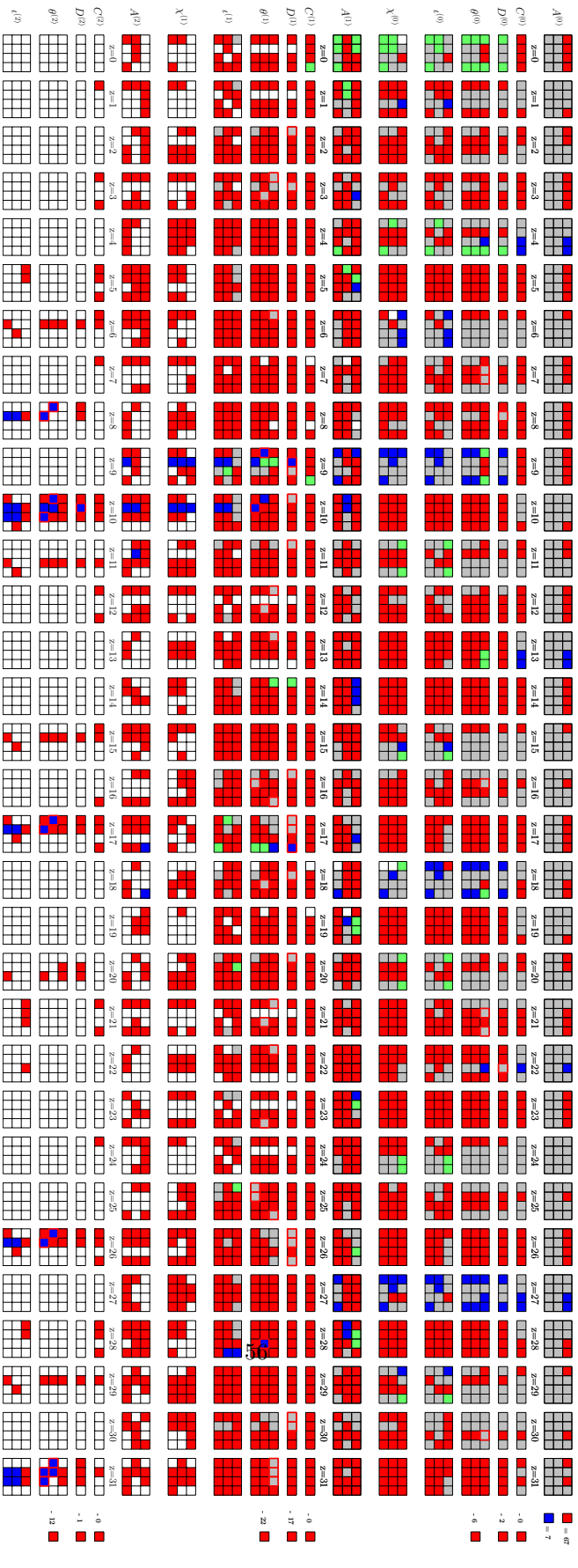


Fig. 24: The improved MitM preimage attack on 3-round Xoodyak-XOF



As shown in Figure 22, we use two message blocks ( $M_1, M_2$ ) to perform the preimage attack, where  $M_2$  has two padding bits. In the 2nd block, 70 conditions on  $\iota^{(0)}$  listed in Table 5 should be satisfied before the MitM process, which form a system of linear equations involving 256 bits of the inner part of the 2nd block and  $128 - 7 - 67 - 2 = 52$  gray bits of  $M_2$ . We calculate the rank of the coefficient matrix of the linear system related to the 52 bits of  $M_2$ , and the result is 32. In other words, through certain linear transformations, there are  $70 - 32 = 38$  equations determined solely by the bits of the inner part. Consequently, randomly given an  $M_1$  (thus 256-bit inner part of the 2nd block is determined), the probability of finding a solution of this system is expected to be  $2^{-38}$ . Then, for a proper 256-bit inner part, there are  $2^{52-32} = 2^{20}$  solutions of  $M_2$  that make all the conditions hold.

---


$$\begin{aligned}
&\iota_{\{2,0,0\}}^{(0)} = 0; \iota_{\{2,0,1\}}^{(0)} = 0; \iota_{\{2,0,6\}}^{(0)} = 0; \iota_{\{2,0,15\}}^{(0)} = 0; \iota_{\{2,0,24\}}^{(0)} = 0; \iota_{\{3,1,0\}}^{(0)} = 0; \iota_{\{3,1,4\}}^{(0)} = 0; \\
&\iota_{\{3,1,9\}}^{(0)} = 0; \iota_{\{3,1,18\}}^{(0)} = 0; \iota_{\{3,1,22\}}^{(0)} = 0; \iota_{\{3,1,27\}}^{(0)} = 0; \iota_{\{0,0,2\}}^{(0)} = 0; \iota_{\{0,0,11\}}^{(0)} = 0; \iota_{\{0,0,16\}}^{(0)} = 0; \\
&\iota_{\{0,0,20\}}^{(0)} = 0; \iota_{\{0,0,25\}}^{(0)} = 0; \iota_{\{0,0,29\}}^{(0)} = 0; \iota_{\{1,2,3\}}^{(0)} = 0; \iota_{\{1,2,6\}}^{(0)} = 0; \iota_{\{1,2,9\}}^{(0)} = 0; \iota_{\{1,2,18\}}^{(0)} = 0; \\
&\iota_{\{1,2,27\}}^{(0)} = 0; \iota_{\{2,1,3\}}^{(0)} = 0; \iota_{\{2,1,8\}}^{(0)} = 0; \iota_{\{0,2,4\}}^{(0)} = 0; \iota_{\{3,0,6\}}^{(0)} = 0; \iota_{\{3,0,11\}}^{(0)} = 0; \iota_{\{3,0,15\}}^{(0)} = 0; \\
&\iota_{\{3,0,20\}}^{(0)} = 0; \iota_{\{3,0,24\}}^{(0)} = 0; \iota_{\{3,0,29\}}^{(0)} = 0; \iota_{\{1,1,12\}}^{(0)} = 0; \iota_{\{1,1,29\}}^{(0)} = 0; \iota_{\{0,1,15\}}^{(0)} = 0; \iota_{\{1,0,30\}}^{(0)} = 0; \\
&\iota_{\{1,0,0\}}^{(0)} = 1; \iota_{\{1,0,3\}}^{(0)} = 1; \iota_{\{1,0,6\}}^{(0)} = 1; \iota_{\{1,0,9\}}^{(0)} = 1; \iota_{\{1,0,18\}}^{(0)} = 1; \iota_{\{1,0,27\}}^{(0)} = 1; \iota_{\{2,1,0\}}^{(0)} = 1; \\
&\iota_{\{2,1,1\}}^{(0)} = 1; \iota_{\{2,1,6\}}^{(0)} = 1; \iota_{\{2,1,15\}}^{(0)} = 1; \iota_{\{2,1,24\}}^{(0)} = 1; \iota_{\{2,1,27\}}^{(0)} = 1; \iota_{\{3,2,0\}}^{(0)} = 1; \iota_{\{3,2,4\}}^{(0)} = 1; \\
&\iota_{\{3,2,9\}}^{(0)} = 1; \iota_{\{3,2,18\}}^{(0)} = 1; \iota_{\{3,2,27\}}^{(0)} = 1; \iota_{\{0,1,2\}}^{(0)} = 1; \iota_{\{0,1,7\}}^{(0)} = 1; \iota_{\{0,1,11\}}^{(0)} = 1; \iota_{\{0,1,16\}}^{(0)} = 1; \\
&\iota_{\{0,1,20\}}^{(0)} = 1; \iota_{\{0,1,29\}}^{(0)} = 1; \iota_{\{2,2,3\}}^{(0)} = 1; \iota_{\{2,2,8\}}^{(0)} = 1; \iota_{\{0,0,4\}}^{(0)} = 1; \iota_{\{3,1,6\}}^{(0)} = 1; \iota_{\{3,1,11\}}^{(0)} = 1; \\
&\iota_{\{3,1,15\}}^{(0)} = 1; \iota_{\{3,1,20\}}^{(0)} = 1; \iota_{\{3,1,24\}}^{(0)} = 1; \iota_{\{3,1,29\}}^{(0)} = 1; \iota_{\{1,2,12\}}^{(0)} = 1; \iota_{\{2,0,22\}}^{(0)} = 1; \iota_{\{1,1,30\}}^{(0)} = 1;
\end{aligned}$$


---

Table 5: Bit Conditions in 3-round Attack on Xoodyak-XOF

Using the new TA, we get 37 free variables and 30 dependent variables. The TA matrices are shown in MATRIX/Xoodyak\_3r.txt at <https://anonymous.4open.science/r/Triangulation-MitM-7373>. The 3-round MitM attack is given in Algorithm 13. In Line 17 to 28, a space of  $2^{7+7} = 2^{14}$  is searched. Assuming  $2^{\zeta_1}$   $M_1$  are needed, to search a 128-bit preimage, we have to search a space of  $2^{\zeta_1-38+\zeta_2+30+30+7+7} = 2^{128}$ , we set  $\zeta_1 = 72$  and  $\zeta_2 = 20$ . The complexity is about  $2^{128-\min\{\text{DoF}^+, \text{DoF}^-, \text{DoM}\}} = 2^{121}$  time and  $2^{37}$  memory.

## G.2 MitM Collision Attack on 3-round Xoodyak-XOF

The characteristic in Figure 24 can also be used to conduct a collision attack for Xoodyak-XOF following Figure 23. In the attack, set the 7 expressions of Eq. (35) as 0. We need to find  $2^{(128-7)/2} = 2^{60.5}$  preimages satisfying the 7-bit 0 target, then we expect to get a collision on average for the other 121-bit target.

The detailed attack is given in Algorithm 14. In Line 20 to 33, we get  $2^{7+7-7} = 2^7$  preimages, so that we need to repeat  $2^{(128-7)/2-7} = 2^{53.5}$  times to build  $2^{60.5}$  preimages. Assume  $2^{\zeta_1}$  possible values of  $M_1$  are required and  $2^{\zeta_2}$  out of  $2^{20}$  solutions of  $M_2$  are required. We set  $\zeta_1 = 38$  and  $\zeta_2 = 0$ . The time and memory complexities are both  $2^{60.5}$ .

---

**Algorithm 13:** Preimage Attack on 3-round Xoodyak-XOF
 

---

```

1 for  $2^{\zeta_1}$  values of  $M_1$  /*  $\zeta_1 = 72$  */
2 do
3   Compute the inner part of the 2nd block
4   Solve the system of 70 linear equations
5   if the equations have solutions /* with probability of  $2^{-38}$  */
6   then
7     for  $2^{\zeta_2}$  solutions of  $M_2$  /*  $\zeta_2 = 20 \leq 20$  */
8     do
9        $U \leftarrow []$ 
10      for  $(e_1, e_2, \dots, e_{30}) \in \mathbb{F}_2^{30}$  do
11        for 37 free variables  $\blacksquare$  in  $A^{(0)} \in 2^{37}$  do
12          Assign  $(e_1, e_2, \dots, e_{30})$  to 30 expressions
13          Deduce the 30 dependent variables
14          Compute forward to other 30-bit  $\blacksquare/\blacksquare$   $\mathbf{u} \in \mathbb{F}_2^{30}$ 
15           $U[\mathbf{u}] \leftarrow A^{(0)}[v_{\mathcal{R}}]$  /*  $v_{\mathcal{R}}$  represents 67 red indexes */
16        end
17      for  $\mathbf{u} \in \mathbb{F}_2^{30}$  do
18         $L \leftarrow []$ 
19        for  $A^{(0)}[v_{\mathcal{B}}] \in 2^7$  /*  $v_{\mathcal{B}}$  represents 7 blue indexes */
20        do
21          Compute forward to the 7-bit matching point  $v$ 
22           $L[v] \leftarrow A^{(0)}[v_{\mathcal{B}}]$ 
23        end
24        for values in  $U[\mathbf{u}]$  do
25          Compute forward the 7-bit matching point  $v'$ 
26          for values in  $L[v']$  do
27            if it leads to the given hash value then
28              Output the preimage
29            end
26          end
27        end
28      end
29    end
30  end
31 end
32 end
33 end
34 end
35 end
36 end

```

---

---

**Algorithm 14:** The MitM Collision Attack on 3-round Xoodyak-Xof with 128-bit Tag

---

```

1 Fix the 7-bit matching point to 0
2 for  $2^{\zeta_1}$  values of  $M_1$  /*  $\zeta = 38$  */
3 do
4   Compute the inner part of the 2nd block
5   Solve the system of 70 linear equations
6   if the equations have solutions /* with probability of  $2^{-38}$  */
7   then
8     for  $2^{\zeta_2}$  solutions of  $M_2$  /*  $\zeta_2 = 0 \leq 20$  */
9     do
10       $U \leftarrow []$ 
11      for  $2^{23.5}$  values of  $(e_1, e_2, \dots, e_{30}) \in \mathbb{F}_2^{30}$  do
12        for 37 free variables  $\blacksquare$  in  $A^{(0)} \in 2^{37}$  do
13          Assign  $(e_1, e_2, \dots, e_{30})$  to 30 expressions
14          Deduce the 30 dependent variables
15          Compute forward to other 30-bit  $\blacksquare/\blacksquare$   $\mathbf{u} \in \mathbb{F}_2^{30}$ 
16           $U[\mathbf{u}] \leftarrow A^{(0)}[v_{\mathcal{R}}]$  /*  $v_{\mathcal{R}}$  represents all 67 red indexes */
17        end
18      for  $\mathbf{u} \in \mathbb{F}_2^{30}$  do
19         $L \leftarrow []$ 
20        for  $A^{(0)}[v_{\mathcal{B}}] \in 2^7$  /*  $v_{\mathcal{B}}$  represents all 7 blue indexes */
21        do
22          Compute forward to the 7-bit matching point  $v$ 
23           $L[v] \leftarrow A^{(0)}[v_{\mathcal{B}}]$ 
24        end
25        for values in  $U[\mathbf{u}]$  do
26          Compute forward the 7-bit matching point  $v'$ 
27          for values in  $L[v']$  do
28            Compute the 128-bit target  $h$  and store the
               $(M_1, M_2, h)$  in  $L_1$  indexed by  $h$ 
29            if the size of  $L_1$  is  $2^{(128-7)/2} = 2^{60.5}$  then
30              Check  $L_1$  and return  $(M_1, M_2)$  and  $(M'_1, M'_2)$ 
                with the same  $h$ 
31            end
32          end
33        end
34      end
35    end
36  end
37 end
38 end

```

---

## 1070 H MITM Preimage Attacks on Ascon-XOF

1071 The description of Ascon-XOF are given in Supplementary Material F.2. The 320-  
 1072 bit state  $A$  of Ascon is divided into five 64-bit words, and denote  $A_{\{x,y\}}^{(r)}$  to be the  
 1073  $x$ -th (column) bit of the  $y$ -th (row) 64-bit word, where  $0 \leq y \leq 4$ ,  $0 \leq x \leq 63$ .

1074 We explore the symmetry in the  $x$ -axis to speed up the search by cutting the  
 1075 full 64-bit word into 32-bit word. Therefore, the linear operation works modular  
 1076 32 instead of 64. For example, the linear operation in the second row changes  
 1077 from the original  $A_{\{*,1\}}^{(r+1)} \leftarrow S_{\{*,1\}}^{(r)} \oplus (S_{\{*,1\}}^{(r)} \ggg 61) \oplus (S_{\{*,1\}}^{(r)} \ggg 39)$  into the current  
 1078  $A_{\{*,1\}}^{(r+1)} \leftarrow S_{\{*,1\}}^{(r)} \oplus (S_{\{*,1\}}^{(r)} \ggg 29) \oplus (S_{\{*,1\}}^{(r)} \ggg 7)$ .

### 1079 H.1 3-round Preimage Attack on Ascon-XOF

1080 The 3-round MitM characteristic is shown in Figure 25. The starting state  $A^{(0)}$   
 1081 in the full MitM path contains  $\lambda^+ = 14$  ■ bits and  $\lambda^- = 24$  ■ bits. There  
 1082 are 48 conditions on ■ bits of  $A^{(0)}$ . In the computation from  $A^{(0)}$  to  $A^{(2)}$ , the  
 1083 consumed DoFs of ■ and ■ are  $l^+ = 0$  and  $l^- = 10$  bits, respectively. Therefore,  
 1084  $\text{DoF}^+ = 14$ ,  $\text{DoF}^- = 14$ , and there are  $\text{DoM} = 14$  matching bits.

1085 Using new TA to system of 10 constraints on red ■ bits, we get 14 free vari-  
 1086 ables and 10 dependent variables, the matrices before and after TA are shown  
 1087 in Eq. (37)<sup>7</sup>. The 3-round attack is given in Algorithm 15. The total time com-  
 1088 plexity is about  $2^{128 - \min\{\text{DoF}^+, \text{DoF}^-, \text{DoM}\}} = 2^{114}$  time and  $2^{14}$  memory.

$$\begin{cases}
 e_1 = A_{\{26,1\}}^{(2)} &= A_{\{29,0\}}^{(0)} \left( A_{\{29,0\}}^{(0)} \oplus A_{\{32,0\}}^{(0)} \oplus A_{\{54,0\}}^{(0)} \right) \oplus A_{\{7,0\}}^{(0)} \oplus A_{\{22,0\}}^{(0)} \oplus A_{\{32,0\}}^{(0)} \\
 e_2 = A_{\{58,1\}}^{(2)} &= A_{\{61,0\}}^{(0)} \left( A_{\{0,0\}}^{(0)} \oplus A_{\{22,0\}}^{(0)} \oplus A_{\{61,0\}}^{(0)} \right) \oplus A_{\{0,0\}}^{(0)} \oplus A_{\{39,0\}}^{(0)} \oplus A_{\{54,0\}}^{(0)} \\
 e_3 = A_{\{2,1\}}^{(2)} &= A_{\{25,0\}}^{(0)} \oplus A_{\{27,0\}}^{(0)} \oplus A_{\{38,0\}}^{(0)} \oplus A_{\{47,0\}}^{(0)} \oplus A_{\{50,0\}}^{(0)} \oplus 1 \\
 e_4 = A_{\{34,1\}}^{(2)} &= A_{\{6,0\}}^{(0)} \oplus A_{\{15,0\}}^{(0)} \oplus A_{\{18,0\}}^{(0)} \oplus A_{\{57,0\}}^{(0)} \oplus A_{\{59,0\}}^{(0)} \oplus 1 \\
 e_5 = A_{\{12,1\}}^{(2)} &= A_{\{15,0\}}^{(0)} \oplus A_{\{18,0\}}^{(0)} \oplus A_{\{37,0\}}^{(0)} \oplus A_{\{60,0\}}^{(0)} \\
 e_6 = A_{\{44,1\}}^{(2)} &= A_{\{5,0\}}^{(0)} \oplus A_{\{28,0\}}^{(0)} \oplus A_{\{47,0\}}^{(0)} \oplus A_{\{50,0\}}^{(0)} \\
 e_7 = A_{\{6,1\}}^{(2)} &= A_{\{6,0\}}^{(0)} \oplus A_{\{60,0\}}^{(0)} \oplus A_{\{6,0\}}^{(0)} \oplus A_{\{32,0\}}^{(0)} \oplus A_{\{54,0\}}^{(0)} \\
 e_8 = A_{\{38,1\}}^{(2)} &= A_{\{28,0\}}^{(0)} \oplus A_{\{38,0\}}^{(0)} \oplus A_{\{0,0\}}^{(0)} \oplus A_{\{22,0\}}^{(0)} \oplus A_{\{38,0\}}^{(0)} \\
 e_9 = A_{\{16,1\}}^{(2)} &= A_{\{0,0\}}^{(0)} \oplus A_{\{22,0\}}^{(0)} \oplus A_{\{61,0\}}^{(0)} \oplus 1 \\
 e_{10} = A_{\{48,1\}}^{(2)} &= A_{\{29,0\}}^{(0)} \oplus A_{\{32,0\}}^{(0)} \oplus A_{\{54,0\}}^{(0)} \oplus 1
 \end{cases} \tag{36}$$

<sup>7</sup>Note that we explore the symmetry in the  $x$ -axis of Ascon by cutting the full 64-bit word into 32-bit word. Therefore, there are two systems of constraints as Eq. (37) totally.

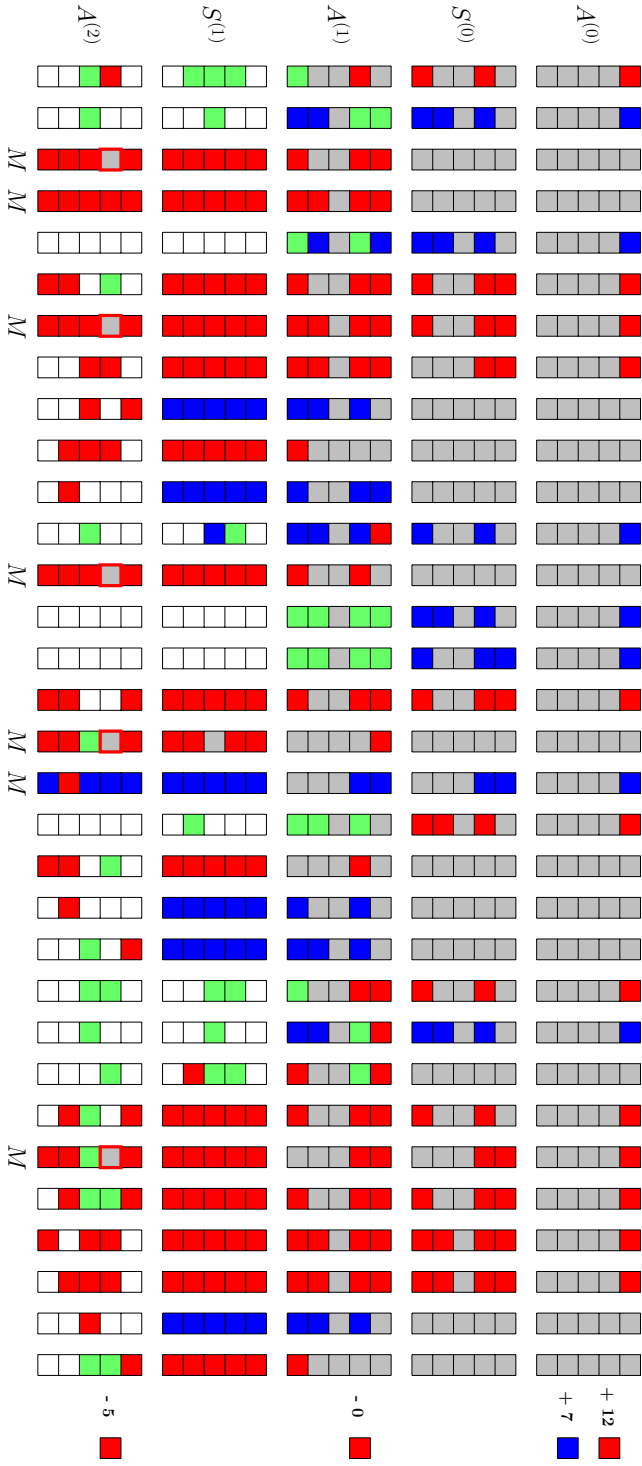


Fig. 25: The 3-round Preimage attack on Ascon-XOF. Since we explore the symmetry in the  $x$ -axis to speed up the search by cutting the full 64-bit word into 32-bit word, only 32-bit state version of Ascon-XOF is displayed here.

$$\begin{pmatrix}
\begin{array}{c|cccccccccccc}
& v_0 & v_5 & v_6 & v_7 & v_{15} & v_{18} & v_{22} & v_{25} & v_{26} & v_{27} & v_{28} & v_{29} \\
\hline
A_{\{2,1\}}^{(2)} & 0 & 1 & 1 & 0 & 1 & 1 & 0 & 1 & 0 & 1 & 1 & 0 \\
A_{\{6,1\}}^{(2)} & 1 & 0 & 1 & 0 & 0 & 0 & 1 & 0 & 0 & 0 & 1 & 1 \\
A_{\{12,1\}}^{(2)} & 0 & 1 & 1 & 0 & 1 & 1 & 0 & 0 & 0 & 0 & 1 & 0 \\
A_{\{16,1\}}^{(2)} & 1 & 0 & 0 & 0 & 0 & 0 & 1 & 0 & 0 & 0 & 0 & 1 \\
A_{\{26,1\}}^{(2)} & 1 & 0 & 0 & 1 & 0 & 0 & 1 & 0 & 1 & 0 & 0 & 1
\end{array}
&
\begin{array}{c|cccccccc|cccccccc}
& v_7 & v_{25} & v_5 & v_6 & v_{22} & v_0 & v_{15} & v_{18} & v_{26} & v_{27} & v_{28} & v_{29} \\
\hline
A_{\{26,1\}}^{(2)} & 1 & 0 & 0 & 0 & 1 & 1 & 0 & 0 & 1 & 0 & 0 & 1 \\
A_{\{2,1\}}^{(2)} & 0 & 1 & 1 & 1 & 0 & 0 & 1 & 1 & 0 & 1 & 1 & 0 \\
A_{\{12,1\}}^{(2)} & 0 & 0 & 1 & 1 & 0 & 0 & 1 & 1 & 0 & 0 & 1 & 0 \\
A_{\{16,1\}}^{(2)} & 0 & 0 & 0 & 1 & 1 & 1 & 0 & 0 & 0 & 0 & 1 & 1 \\
A_{\{26,1\}}^{(2)} & 0 & 0 & 0 & 0 & 1 & 1 & 0 & 0 & 0 & 0 & 0 & 1
\end{array}
\end{pmatrix} \quad (37)$$

(a)
(b)

---

**Algorithm 15:** Preimage Attack on 3-round Ascon-XOF

---

```

1  Compute  $S_{\{*,0\}}^{(3)} = p_L^{-1}(T)$  /*  $T$  is the hash value */
2  for  $2^\zeta$  values of  $(M_1, M_2)$  /*  $\zeta = 114$  */
3  do
4      Compute the inner part of the 3rd block
5      if the 48 conditions are satisfied /* with probability of  $2^{-48}$  */
6      then
7          for  $2^{24}$  values of  $\blacksquare$  bits in  $A^{(0)}$  do
8              for  $(e_1, e_2, \dots, e_{10}) \in \mathbb{F}_2^{10}$  do
9                   $L \leftarrow []$ 
10                 for  $A^{(0)}[v_B] \in 2^{14}$  /*  $v_B$  represents all 14 blue indexes */
11                 do
12                     Compute forward to the 14-bit matching point  $v$ 
13                      $L[v] \leftarrow A^{(0)}[v_B]$ 
14                 end
15                 for 14 free variables  $\blacksquare$  in  $A^{(0)} \in 2^{14}$  do
16                     Assign  $(e_1, e_2, \dots, e_{10})$  to the last 10 expressions in Eq.
17                     (37) (b)
18                     /* Due to symmetry, the complete matrix in Eq. (37)
19                     (b) contains 10 rows and 24 columns. */
20                     Deduce 10 dependent variables
21                     Compute forward to the 14-bit matching point  $v'$ 
22                     for values in  $L[v']$  do
23                         Check if  $T$  is satisfied
24                     end
25                 end
26             end
27         end
28     end
29 end

```

---

1089 **Partial Experiment of the Preimage Attack on 3-round Ascon-XOF.**  
1090 To verify the correctness of the bit-wise triangulating MitM attack, we give

an experiment of a 32-bit partial target preimage attack. Fix the 14-bit target  $S_{\{i,0\}}^{(2)}$  ( $i \in [2, 3, 6, 12, 16, 17, 26, 34, 35, 38, 44, 48, 49, 58]$ ) and another 18-bit target  $S_{\{j,0\}}^{(2)}$  ( $j \in [0, 1, 4, 5, 7, 8, 9, 10, 11, 13, 14, 15, 18, 19, 20, 21, 22, 23]$ ) as zero. Totally, the 32-bit target is fixed as zero and the goal is to find the preimages of the 32-bit 0 target. The procedures are as follows:

1. Set the 256-bit inner part in  $A^{(0)}$  as fixed values, which satisfy the 48-bit condition, *i.e.*,  $A_{\{*,1\}}^{(0)} = 0xc8142340c8142340$ ,  $A_{\{*,3\}}^{(0)} = 0x8713427087134270$ , and  $A_{\{*,2\}}^{(0)} = A_{\{*,4\}}^{(0)} = 0x0$ . In order to simplify the expressions for TA, we set 7  $\blacksquare$  bits  $A_{\{i,0\}}^{(0)} = 1$  for  $i \in [12, 16, 19, 30, 44, 48, 51]$ , and the remaining 17  $\blacksquare$  bits to be 0. The simplified equations are given in Eq. (36).
2. In our experiment, we traverse the values of the first 8-bit expressions ( $e_1, e_2, \dots, e_8$ ) in Eq. (36) and fix  $e_9 = e_{10} = 0$  in Alg. 15, *i.e.*,  $2^{8+14+14} = 2^{36}$  states are tested with MitM approach and  $2^{36-32} = 2^4$  preimages are expected to find.

We finally found  $2^{4.3}$  preimages satisfying the 32-bit all-zero target, which is close to the theoretical expectation. The results are given in Table 6. The experiment is run on a computer with an i9-13900KF CPU and 32 GB of memory in seconds. The source codes are available via <https://anonymous.4open.science/r/Triangulation-MitM-7373>.

Round	First row of preimage $(A_{\{*,0\}}^{(0)})$	32-bit target $S_{\{i,0\}}^{(2)}$ ( $i \in [0 - 23, 26, 34, 35, 38, 44, 48, 49, 58]$ )
$r = 3$	8d0fd306451f902e	00000000
	c61b91524318b242	00000000
	8018936e800ab33e	00000000
	4a1dd34ec81a926a	00000000
	4119b25e461cb142	00000000
	cf0bb302471ed376	00000000
	cb0cb346871b931e	00000000
	c10db24a4318f256	00000000
	c80ab1028e1d9002	00000000
	cf1f924ac11f912e	00000000

Table 6: 32-bit Partial Target Preimage Examples of 3-round ASCON-XOF

## H.2 4-round Preimage Attack on Ascon-XOF

The 4-round MitM characteristic is shown in Figure 26. The starting state  $A^{(0)}$  in the full MitM path contains  $\lambda^+ = 4 \blacksquare$  bits and  $\lambda^- = 34 \blacksquare$  bits. In the computation from  $A^{(0)}$  to  $A^{(3)}$ , the consumed degrees of freedom (DoFs) of  $\blacksquare$  and  $\blacksquare$  are  $l^+ = 0$  and 26 bits, respectively. Additionally, there are 4 consumed DoFs of  $\blacksquare$  to make

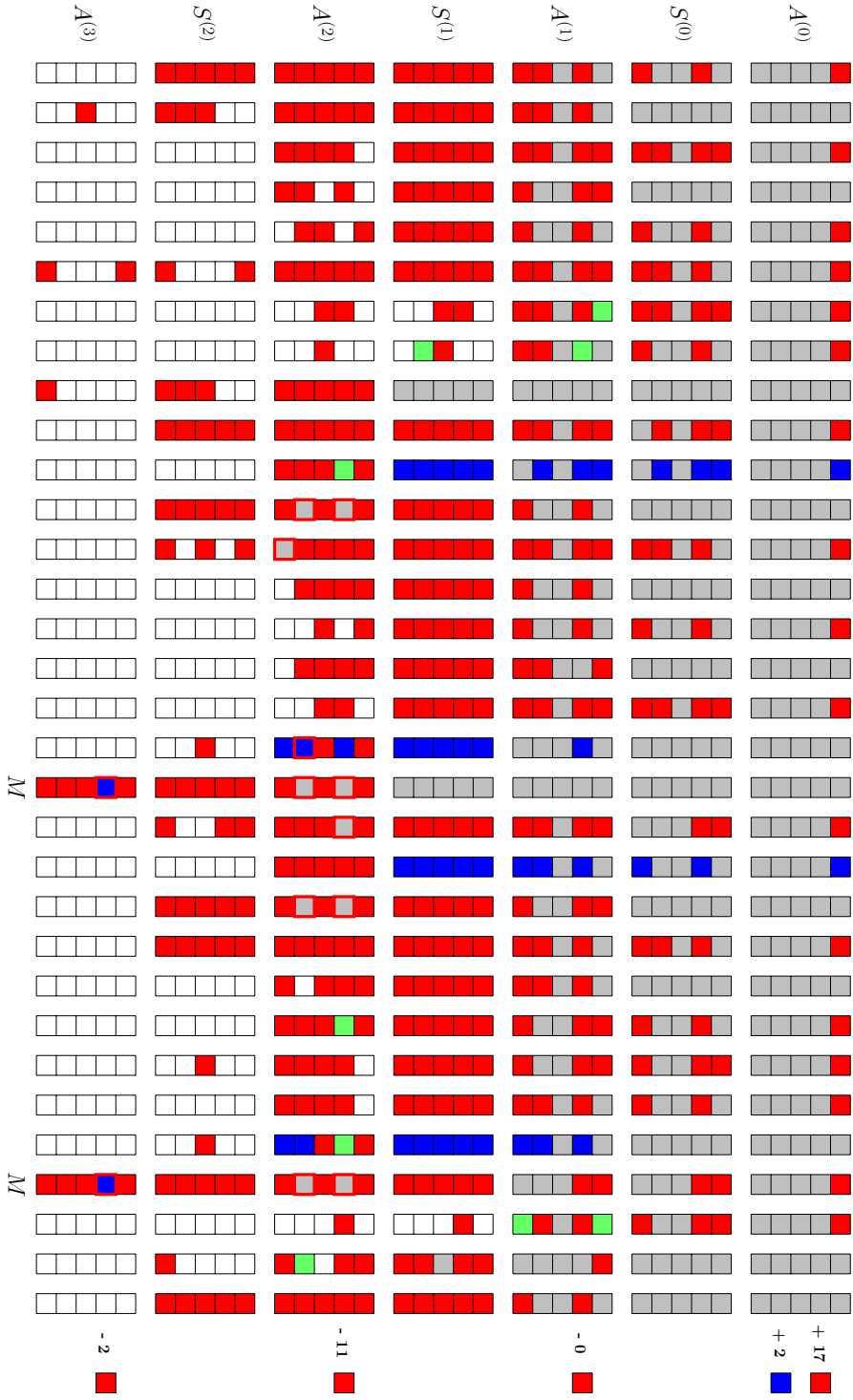


Fig. 26: The 4-round Preimage attack on Ascon-XOF. Since we explore the symmetry in the  $x$ -axis to speed up the search by cutting the full 64-bit word into 32-bit word, only 32-bit state version of Ascon-XOF is displayed here.



1114  $a_0 + a_2 + a_4$  become  $\blacksquare$  for matching points, so that  $l^- = 26 + 4 = 30$ . Therefore,  
1115  $\text{DoF}^+ = 4$ ,  $\text{DoF}^- = 4$ , and there are  $\text{DoM} = 4$  matching bits.  
1116 Using the new TA, we can get 14 free variables and 20 dependent variables,  
1117 the matrices before and after TA are shown in Eq. (38). The 4-round attack is  
1118 given in Algorithm 16. The total time complexity is about  $2^{128 - \min\{\text{DoF}^+, \text{DoF}^-, \text{DoM}\}} =$   
1119  $2^{124}$  time and  $2^{14}$  memory.

$$\begin{aligned}
& \begin{pmatrix} v_0 & v_2 & v_4 & v_5 & v_6 & v_7 & v_9 & v_{12} & v_{14} & v_{16} & v_{19} & v_{22} & v_{24} & v_{25} & v_{26} & v_{28} & v_{29} \\ A_{\{11,1\}}^{(2)} & 0 & 1 & 1 & 1 & 0 & 1 & 0 & 0 & 1 & 0 & 0 & 0 & 0 & 0 & 0 & 1 \\ A_{\{18,1\}}^{(2)} & 0 & 1 & 1 & 0 & 0 & 0 & 0 & 1 & 1 & 0 & 0 & 0 & 1 & 1 & 0 & 0 \\ A_{\{19,1\}}^{(2)} & 0 & 1 & 0 & 1 & 0 & 0 & 1 & 1 & 0 & 1 & 1 & 1 & 0 & 1 & 0 & 0 \\ A_{\{21,1\}}^{(2)} & 0 & 1 & 0 & 1 & 0 & 1 & 0 & 1 & 1 & 0 & 0 & 0 & 1 & 1 & 0 & 1 \\ A_{\{28,1\}}^{(2)} & 0 & 1 & 0 & 0 & 0 & 0 & 1 & 1 & 1 & 0 & 0 & 1 & 1 & 1 & 0 & 1 \\ A_{\{11,3\}}^{(2)} & 0 & 1 & 1 & 0 & 0 & 0 & 1 & 0 & 1 & 1 & 1 & 0 & 1 & 0 & 1 & 0 \\ A_{\{17,3\}}^{(2)} & 1 & 0 & 0 & 0 & 0 & 1 & 0 & 0 & 0 & 0 & 0 & 1 & 0 & 1 & 0 & 0 \\ A_{\{18,3\}}^{(2)} & 0 & 0 & 1 & 0 & 0 & 0 & 0 & 0 & 0 & 1 & 0 & 0 & 1 & 0 & 1 & 0 \\ A_{\{21,3\}}^{(2)} & 0 & 1 & 1 & 0 & 0 & 1 & 0 & 1 & 1 & 0 & 0 & 0 & 1 & 1 & 0 & 0 \\ A_{\{28,3\}}^{(2)} & 0 & 1 & 1 & 0 & 0 & 0 & 1 & 0 & 1 & 0 & 0 & 0 & 0 & 0 & 0 & 1 \\ A_{\{12,4\}}^{(2)} & 0 & 1 & 0 & 1 & 1 & 0 & 1 & 1 & 0 & 1 & 0 & 0 & 0 & 1 & 1 & 1 \\ A_{\{31,4\}}^{(3)} & 1 & 1 & 1 & 1 & 1 & 1 & 1 & 1 & 1 & 1 & 1 & 1 & 1 & 1 & 1 & 1 \\ A_{\{31,4\}}^{(3)} & 1 & 1 & 1 & 1 & 1 & 1 & 1 & 1 & 1 & 1 & 1 & 1 & 1 & 1 & 1 & 1 \end{pmatrix} \\
& \quad (a) \\
& \begin{pmatrix} v_0 & v_6 & v_{19} & v_{22} & v_{26} & v_9 & v_{28} & v_5 & v_7 & v_{12} & v_2 & v_4 & v_{14} & v_{16} & v_{24} & v_{25} & v_{29} \\ A_{\{31,4\}}^{(3)} & 1 & 1 & 1 & 1 & 1 & 1 & 1 & 1 & 1 & 1 & 1 & 1 & 1 & 1 & 1 & 1 \\ A_{\{31,4\}}^{(3)} & 1 & 1 & 1 & 1 & 1 & 1 & 1 & 1 & 1 & 1 & 1 & 1 & 1 & 1 & 1 & 1 \\ A_{\{11,3\}}^{(2)} & 0 & 0 & 1 & 0 & 1 & 1 & 0 & 0 & 0 & 1 & 1 & 1 & 1 & 1 & 0 & 1 \\ A_{\{17,3\}}^{(2)} & 1 & 0 & 0 & 1 & 0 & 0 & 0 & 0 & 1 & 0 & 0 & 0 & 0 & 0 & 1 & 0 \\ A_{\{12,4\}}^{(2)} & 0 & 1 & 0 & 0 & 1 & 1 & 1 & 1 & 0 & 1 & 1 & 0 & 0 & 1 & 0 & 1 \\ A_{\{19,1\}}^{(2)} & 0 & 0 & 1 & 1 & 0 & 1 & 0 & 1 & 0 & 1 & 1 & 0 & 0 & 1 & 0 & 1 \\ A_{\{28,1\}}^{(2)} & 0 & 0 & 0 & 1 & 0 & 1 & 1 & 0 & 0 & 1 & 1 & 0 & 1 & 0 & 1 & 1 \\ A_{\{18,3\}}^{(2)} & 0 & 0 & 0 & 0 & 1 & 0 & 0 & 0 & 0 & 0 & 0 & 1 & 0 & 1 & 1 & 0 \\ A_{\{28,3\}}^{(2)} & 0 & 0 & 0 & 0 & 0 & 1 & 1 & 0 & 0 & 0 & 1 & 1 & 1 & 0 & 0 & 0 \\ A_{\{21,1\}}^{(2)} & 0 & 0 & 0 & 0 & 0 & 0 & 1 & 1 & 1 & 1 & 1 & 0 & 1 & 0 & 1 & 1 \\ A_{\{11,1\}}^{(2)} & 0 & 0 & 0 & 0 & 0 & 0 & 0 & 1 & 1 & 0 & 1 & 1 & 1 & 0 & 0 & 0 \\ A_{\{21,3\}}^{(2)} & 0 & 0 & 0 & 0 & 0 & 0 & 0 & 0 & 1 & 1 & 1 & 1 & 1 & 0 & 1 & 1 \\ A_{\{18,1\}}^{(2)} & 0 & 0 & 0 & 0 & 0 & 0 & 0 & 0 & 0 & 1 & 1 & 1 & 1 & 0 & 1 & 1 \end{pmatrix} \\
& \quad (b)
\end{aligned} \tag{38}$$

1120 **Partial Experiment of the Preimage Attack on 4-round Ascon-XOF.** In  
1121 this practical experiment, we attempt to find a preimage of 24-bit all-zero target.  
1122 That is, the 24-bit  $S_{\{i,0\}}^{(3)}$  ( $i \in [16 - 19, 28 - 31, 48 - 63]$ ) of target are fixed to be  
1123 zero. The attack procedures are as follows:

- 1124 1. Set the 256-bit inner part in  $A^{(0)}$  as fixed values, which satisfied the 50-bit  
1125 condition, *i.e.*,  $A_{\{*,1\}}^{(0)} = 0x8d0a0aa08d0a0aa0$ ,  $A_{\{*,3\}}^{(0)} = 0x890218ec890218ec$ ,  
1126 and  $A_{\{*,2\}}^{(0)} = A_{\{*,4\}}^{(0)} = 0x0$ . In order to simplify the expressions for TA, we

---

**Algorithm 16:** Preimage Attack on 4-round Ascon-XOF
 

---

```

1  Compute  $S_{\{*,0\}}^{(3)} = p_L^{-1}(T)$ 
2  /*  $T$  is the hash value */
3  for  $2^\zeta$  values of  $(M_1, M_2)$  /*  $\zeta = 116$  */
4  do
5    Compute the inner part of the 3rd block
6    if the 50 conditions are satisfied /* with probability of  $2^{-50}$  */
7    then
8      for  $2^{24}$  values of  $\blacksquare$  bits in  $A^{(0)}$  do
9        for  $(e_1, e_2, \dots, e_{20}) \in \mathbb{F}_2^{20}$  do
10          $U \leftarrow []$ 
11         for 14 free variables  $\blacksquare$  in  $A^{(0)} \in 2^{14}$  do
12           Assign  $(e_1, e_2, \dots, e_{20})$  to the last 20 expressions in Eq.
13           (38) (b)
14           Deduce 20 dependent variables
15           Compute forward to other 10-bit  $\blacksquare/\blacksquare \mathbf{u} \in \mathbb{F}_2^{10}$ 
16            $U[\mathbf{u}] \leftarrow A^{(0)}[v_{\mathcal{R}}]$  /*  $v_{\mathcal{R}}$  represents all 34 red indexes */
17         end
18         for  $\mathbf{u} \in \mathbb{F}_2^{10}$  do
19            $L \leftarrow []$ 
20           for  $(A_{\{10,0\}}^{(0)}, A_{\{20,0\}}^{(0)}, A_{\{42,0\}}^{(0)}, A_{\{52,0\}}^{(0)}) \in \mathbb{F}_2^4$  do
21             Compute forward to the 4-bit matching point  $v$ 
22              $L[v] \leftarrow (A_{\{10,0\}}^{(0)}, A_{\{20,0\}}^{(0)}, A_{\{42,0\}}^{(0)}, A_{\{52,0\}}^{(0)})$ 
23           end
24           for values in  $U[\mathbf{u}]$  do
25             Compute forward to the 4-bit matching point  $v'$ 
26             for values in  $L[v']$  do
27               Check if  $T$  is satisfied
28             end
29           end
30         end
31       end
32     end
33 end

```

---

1127 set the 2 ■ bits  $A_{\{11,0\}}^{(0)} = A_{\{50,0\}}^{(0)} = 1$ , and the remaining 22 ■ bits to 0. The  
 1128 simplified equations are given in Eq. (39).

1129 2. In our experiment, we traverse the values of the first 10-bit expressions  
 1130  $(e_1, e_2, \dots, e_{10})$  and fix  $e_{11} = e_{12} = \dots = e_{20} = 0$  in Eq. (39), *i.e.*,  $2^{10+14+4} =$   
 1131  $2^{28}$  states are tested with MitM approach and it is expected to find  $2^{28-24} =$   
 1132  $2^4$  preimages.

1133 Finally, there are  $17 = 2^{4.1}$  preimages are searched to satisfy the 24-bit all-  
 1134 zero target, which is close to the theoretical expectation. The results are listed  
 1135 in Table 7. The experiment can be run on a computer with an i9-13900KF  
 1136 CPU and 32 GB of memory in seconds. The source codes are available via  
 1137 <https://anonymous.4open.science/r/Triangulation-MitM-7373>.

Round	First row of preimage $(A_{\{*,0\}}^{(0)})$	24-bit target $S_{\{i,0\}}^{(3)}$ ( $i \in [16 - 19, 28 - 31, 48 - 63]$ )
$r = 4$	8a5a10a889023a8a	000000
	0e1812e80e48aa4e	000000
	0d5880e40762a0aa	000000
	2d1018282a48b08e	000000
	007810c42668ba62	000000
	2d5a90ec8c02284a	000000
	8e380aa80e603a8e	000000
	a538888c8c28a866	000000
	a73888a88c20a206	000000
	ab589240a42032aa	000000

Table 7: 24-bit Partial Target Preimage Examples of 4-round ASCON-XOF

$$\begin{aligned}
e_1 = A_{\{49,3\}}^{(2)} &= A_{\{0,0\}}^{(0)} \oplus A_{\{22,0\}}^{(0)} \oplus A_{\{39,0\}}^{(0)} \oplus A_{\{57,0\}}^{(0)} \\
e_2 = A_{\{17,3\}}^{(2)} &= A_{\{0,0\}}^{(0)} \oplus A_{\{25,0\}}^{(0)} \oplus A_{\{32,0\}}^{(0)} \\
e_3 = A_{\{44,4\}}^{(2)} &= A_{\{6,0\}}^{(0)} \left( A_{\{26,0\}}^{(0)} \oplus A_{\{48,0\}}^{(0)} \right) \oplus A_{\{5,0\}}^{(0)} A_{\{16,0\}}^{(0)} \oplus A_{\{5,0\}}^{(0)} A_{\{25,0\}}^{(0)} \oplus A_{\{26,0\}}^{(0)} A_{\{28,0\}}^{(0)} \oplus A_{\{28,0\}}^{(0)} A_{\{48,0\}}^{(0)} \oplus \\
&\quad A_{\{37,0\}}^{(0)} \left( A_{\{5,0\}}^{(0)} \oplus A_{\{9,0\}}^{(0)} \oplus A_{\{37,0\}}^{(0)} \right) \oplus A_{\{5,0\}}^{(0)} \oplus A_{\{34,0\}}^{(0)} \oplus A_{\{37,0\}}^{(0)} \oplus A_{\{44,0\}}^{(0)} \oplus A_{\{48,0\}}^{(0)} \oplus \\
&\quad A_{\{44,0\}}^{(0)} \left( A_{\{5,0\}}^{(0)} \oplus A_{\{16,0\}}^{(0)} \oplus A_{\{25,0\}}^{(0)} \oplus A_{\{37,0\}}^{(0)} \oplus A_{\{44,0\}}^{(0)} \right) \oplus 1 \\
e_4 = A_{\{12,4\}}^{(2)} &= A_{\{5,0\}}^{(0)} \left( A_{\{5,0\}}^{(0)} \oplus A_{\{12,0\}}^{(0)} \oplus A_{\{37,0\}}^{(0)} \oplus A_{\{41,0\}}^{(0)} \right) \oplus A_{\{12,0\}}^{(0)} \left( A_{\{12,0\}}^{(0)} \oplus A_{\{37,0\}}^{(0)} \oplus A_{\{48,0\}}^{(0)} \oplus A_{\{57,0\}}^{(0)} \right) \oplus \\
&\quad A_{\{16,0\}}^{(0)} A_{\{38,0\}}^{(0)} \oplus A_{\{37,0\}}^{(0)} A_{\{48,0\}}^{(0)} \oplus A_{\{37,0\}}^{(0)} A_{\{57,0\}}^{(0)} \oplus A_{\{38,0\}}^{(0)} A_{\{58,0\}}^{(0)} \oplus A_{\{16,0\}}^{(0)} A_{\{60,0\}}^{(0)} \oplus A_{\{58,0\}}^{(0)} A_{\{60,0\}}^{(0)} \oplus \\
&\quad A_{\{2,0\}}^{(0)} \oplus A_{\{5,0\}}^{(0)} \oplus A_{\{12,0\}}^{(0)} \oplus A_{\{16,0\}}^{(0)} \oplus A_{\{37,0\}}^{(0)} \oplus A_{\{41,0\}}^{(0)} \oplus 1 \\
e_5 = A_{\{51,1\}}^{(2)} &= A_{\{12,0\}}^{(0)} \left( A_{\{2,0\}}^{(0)} \oplus A_{\{12,0\}}^{(0)} \oplus A_{\{34,0\}}^{(0)} \oplus A_{\{37,0\}}^{(0)} \oplus A_{\{41,0\}}^{(0)} \right) \oplus A_{\{2,0\}}^{(0)} A_{\{37,0\}}^{(0)} \oplus A_{\{51,0\}}^{(0)} \left( A_{\{34,0\}}^{(0)} \oplus A_{\{41,0\}}^{(0)} \right) \oplus \\
&\quad A_{\{54,0\}}^{(0)} \left( A_{\{34,0\}}^{(0)} \oplus A_{\{37,0\}}^{(0)} \oplus A_{\{41,0\}}^{(0)} \oplus A_{\{44,0\}}^{(0)} \oplus A_{\{54,0\}}^{(0)} \right) \oplus A_{\{57,0\}}^{(0)} \left( A_{\{37,0\}}^{(0)} \oplus A_{\{44,0\}}^{(0)} \oplus A_{\{54,0\}}^{(0)} \right) \oplus \\
&\quad A_{\{2,0\}}^{(0)} \oplus A_{\{5,0\}}^{(0)} \oplus A_{\{12,0\}}^{(0)} \oplus A_{\{34,0\}}^{(0)} \oplus A_{\{37,0\}}^{(0)} \oplus A_{\{41,0\}}^{(0)} \oplus A_{\{48,0\}}^{(0)} \oplus A_{\{54,0\}}^{(0)} \oplus A_{\{57,0\}}^{(0)} \oplus 1 \\
e_6 = A_{\{19,1\}}^{(2)} &= A_{\{19,0\}}^{(0)} \left( A_{\{2,0\}}^{(0)} \oplus A_{\{9,0\}}^{(0)} \right) \oplus A_{\{22,0\}}^{(0)} \left( A_{\{2,0\}}^{(0)} \oplus A_{\{5,0\}}^{(0)} \oplus A_{\{9,0\}}^{(0)} \oplus A_{\{12,0\}}^{(0)} \oplus A_{\{22,0\}}^{(0)} \right) \oplus \\
&\quad A_{\{25,0\}}^{(0)} \left( A_{\{5,0\}}^{(0)} \oplus A_{\{12,0\}}^{(0)} \oplus A_{\{22,0\}}^{(0)} \right) \oplus A_{\{44,0\}}^{(0)} \left( A_{\{2,0\}}^{(0)} \oplus A_{\{5,0\}}^{(0)} \oplus A_{\{9,0\}}^{(0)} \oplus A_{\{34,0\}}^{(0)} \oplus A_{\{44,0\}}^{(0)} \right) \oplus \\
&\quad A_{\{5,0\}}^{(0)} A_{\{34,0\}}^{(0)} \oplus A_{\{2,0\}}^{(0)} \oplus A_{\{5,0\}}^{(0)} \oplus A_{\{9,0\}}^{(0)} \oplus A_{\{16,0\}}^{(0)} \oplus A_{\{22,0\}}^{(0)} \oplus A_{\{25,0\}}^{(0)} \oplus A_{\{34,0\}}^{(0)} \oplus A_{\{37,0\}}^{(0)} \oplus A_{\{44,0\}}^{(0)} \oplus 1 \\
e_7 = A_{\{60,1\}}^{(2)} &= A_{\{2,0\}}^{(0)} \oplus A_{\{14,0\}}^{(0)} \oplus A_{\{22,0\}}^{(0)} \oplus A_{\{41,0\}}^{(0)} \oplus A_{\{44,0\}}^{(0)} \oplus A_{\{56,0\}}^{(0)} \oplus A_{\{57,0\}}^{(0)} \\
e_8 = A_{\{28,1\}}^{(2)} &= A_{\{9,0\}}^{(0)} \oplus A_{\{12,0\}}^{(0)} \oplus A_{\{14,0\}}^{(0)} \oplus A_{\{24,0\}}^{(0)} \oplus A_{\{25,0\}}^{(0)} \oplus A_{\{34,0\}}^{(0)} \oplus A_{\{46,0\}}^{(0)} \oplus A_{\{54,0\}}^{(0)} \oplus A_{\{56,0\}}^{(0)} \oplus 1 \\
e_9 = A_{\{50,3\}}^{(2)} &= A_{\{36,0\}}^{(0)} \oplus A_{\{58,0\}}^{(0)} \oplus 1 \\
e_{10} = A_{\{18,3\}}^{(2)} &= A_{\{4,0\}}^{(0)} \oplus A_{\{26,0\}}^{(0)} \\
e_{11} = A_{\{60,3\}}^{(2)} &= A_{\{4,0\}}^{(0)} \oplus A_{\{36,0\}}^{(0)} \oplus A_{\{41,0\}}^{(0)} \oplus A_{\{46,0\}}^{(0)} \oplus 1 \\
e_{12} = A_{\{28,3\}}^{(2)} &= A_{\{9,0\}}^{(0)} \oplus A_{\{14,0\}}^{(0)} \oplus A_{\{36,0\}}^{(0)} \oplus 1 \\
e_{13} = A_{\{53,1\}}^{(2)} &= A_{\{7,0\}}^{(0)} \oplus A_{\{12,0\}}^{(0)} \oplus A_{\{25,0\}}^{(0)} \oplus A_{\{28,0\}}^{(0)} \oplus A_{\{34,0\}}^{(0)} \oplus A_{\{37,0\}}^{(0)} \oplus A_{\{46,0\}}^{(0)} \oplus A_{\{56,0\}}^{(0)} \\
e_{14} = A_{\{21,1\}}^{(2)} &= A_{\{2,0\}}^{(0)} \oplus A_{\{5,0\}}^{(0)} \oplus A_{\{14,0\}}^{(0)} \oplus A_{\{39,0\}}^{(0)} \oplus A_{\{44,0\}}^{(0)} \oplus A_{\{46,0\}}^{(0)} \oplus A_{\{57,0\}}^{(0)} \oplus A_{\{60,0\}}^{(0)} \\
e_{15} = A_{\{43,1\}}^{(2)} &= A_{\{5,0\}}^{(0)} \oplus A_{\{36,0\}}^{(0)} \oplus A_{\{39,0\}}^{(0)} \\
e_{16} = A_{\{11,1\}}^{(2)} &= A_{\{4,0\}}^{(0)} \oplus A_{\{7,0\}}^{(0)} \oplus A_{\{14,0\}}^{(0)} \oplus A_{\{36,0\}}^{(0)} \oplus A_{\{37,0\}}^{(0)} \oplus 1 \\
e_{17} = A_{\{53,3\}}^{(2)} &= A_{\{12,0\}}^{(0)} A_{\{25,0\}}^{(0)} \oplus A_{\{12,0\}}^{(0)} A_{\{34,0\}}^{(0)} \oplus A_{\{12,0\}}^{(0)} A_{\{25,0\}}^{(0)} A_{\{46,0\}}^{(0)} \oplus A_{\{34,0\}}^{(0)} A_{\{46,0\}}^{(0)} \oplus A_{\{4,0\}}^{(0)} \oplus \\
&\quad A_{\{14,0\}}^{(0)} \oplus A_{\{36,0\}}^{(0)} \oplus A_{\{39,0\}}^{(0)} \oplus A_{\{46,0\}}^{(0)} \oplus A_{\{56,0\}}^{(0)} \oplus A_{\{61,0\}}^{(0)} \\
e_{18} = A_{\{21,3\}}^{(2)} &= A_{\{2,0\}}^{(0)} A_{\{14,0\}}^{(0)} \oplus A_{\{2,0\}}^{(0)} A_{\{44,0\}}^{(0)} \oplus A_{\{14,0\}}^{(0)} A_{\{57,0\}}^{(0)} \oplus A_{\{44,0\}}^{(0)} A_{\{57,0\}}^{(0)} \oplus A_{\{2,0\}}^{(0)} \oplus A_{\{7,0\}}^{(0)} \\
&\quad \oplus A_{\{14,0\}}^{(0)} \oplus A_{\{24,0\}}^{(0)} \oplus A_{\{29,0\}}^{(0)} \oplus A_{\{36,0\}}^{(0)} \oplus A_{\{46,0\}}^{(0)} \oplus A_{\{57,0\}}^{(0)} \\
e_{19} = A_{\{50,1\}}^{(2)} &= A_{\{4,0\}}^{(0)} \oplus A_{\{12,0\}}^{(0)} \oplus A_{\{14,0\}}^{(0)} \oplus A_{\{25,0\}}^{(0)} \oplus A_{\{34,0\}}^{(0)} \oplus A_{\{46,0\}}^{(0)} \oplus A_{\{56,0\}}^{(0)} \oplus 1 \\
e_{20} = A_{\{18,1\}}^{(2)} &= A_{\{2,0\}}^{(0)} \oplus A_{\{4,0\}}^{(0)} \oplus A_{\{14,0\}}^{(0)} \oplus A_{\{36,0\}}^{(0)} \oplus A_{\{44,0\}}^{(0)} \oplus A_{\{46,0\}}^{(0)} \oplus A_{\{57,0\}}^{(0)}
\end{aligned} \tag{39}$$

## 1138 I MitM Preimage Attacks on Reduced KECCAK

### 1139 I.1 Memory Improved Preimage attack on 4-round KECCAK[1024]

1140 We reuse the same initialize structure of the attack on KECCAK[1024] in [46],  
1141 and get a new characteristic with lower attack memory, which is shown in Figure  
1142 27 (first part) and Figure 28 (second part). The starting state  $A^{(0)}$  contains 16  
1143 ■ bits and 216 ■ bits, and there are totally 464 conditions on ■ bits of  $\pi^{(0)}$ . Due  
1144 to the CP-kernel property, the initial degree of freedoms (DoFs) of ■ and ■ are  
1145  $\lambda^+ = 8$  and  $\lambda^- = 108$ . In the computation  $A^{(0)}$  to  $A^{(3)}$ , the consumed degrees of  
1146 freedom (DoFs) of ■ and ■ are  $l^+ = 0$  and  $l^- = 100$  bits, respectively. Therefore,  
1147  $\text{DoF}^+ = 8$ ,  $\text{DoF}^- = 8$ , and there are  $\text{DoM} = 8$  matching bits.

1148 We use two message blocks  $(M_1, M_2)$  to build the attack following the frame-  
 1149 work of Qin *et al.* [45] in Figure 22. Given an inner part, the 464 conditions can  
 1150 be seen as a linear system of  $1600 - 512 \times 2 - 116 = 460$  variables of  $M_2$  ( $512 \times 2$   
 1151 is the number of capacity bits, 116 are the DoFs of  $\blacksquare$  and  $\blacksquare$  bits in  $A^{(0)}$ ), which  
 1152 will act as global parameters. The rank of the coefficient matrix of the linear  
 1153 system is 250. In other words, through some linear transformations, there are  
 1154  $464 - 250 = 214$  equations determined only by the bits of the inner part. To find a  
 1155 right inner part, we have to randomly test  $2^{214} M_1$  and there are  $2^{460-250} = 2^{210}$   
 1156 solutions of  $M_2$ , which make all the conditions hold.

1157 Using TA, we can get 52 free variables and 56 dependent variables. We put  
 1158 the TA matrices in MATRIX/keccak[1024]\_4r\_eu23.txt at [https://anonymous.  
 1159 4open.science/r/Triangulation-MitM-7373](https://anonymous.4open.science/r/Triangulation-MitM-7373).

1160 The steps for the 4-round MitM attack are given in Algorithm 17. The total  
 1161 preimage attack on 4-round KECCAK[1024] is about  $2^{512-\min\{\text{DoF}^+, \text{DoF}^-, \text{DoM}\}} =$   
 1162  $2^{504}$  time and  $2^{52}$  memory.

## 1163 I.2 MitM Preimage Attack on 4-round KECCAK[1024]

1164 Using the same model in [46], we get a new characteristic as shown in Figure  
 1165 29. Due to the symmetry, in the full MitM path, the starting state  $A^{(0)}$  contains  
 1166 24  $\blacksquare$  bits and 424  $\blacksquare$  bits, and there are totally 338 conditions on  $\blacksquare$  bits of  $\pi^{(0)}$ .  
 1167 Due to the CP-kernel property, the initial degree of freedoms (DoFs) of  $\blacksquare$  and  
 1168  $\blacksquare$  are  $\lambda^+ = 12$  and  $\lambda^- = 212$ . In the computation  $A^{(0)}$  to  $A^{(3)}$ , the consumed  
 1169 degrees of freedom (DoFs) of  $\blacksquare$  and  $\blacksquare$  are  $l^+ = 0$  and  $l^- = 200$  bits, respectively.  
 1170 Therefore,  $\text{DoF}^+ = 12$ ,  $\text{DoF}^- = 12$ , and there is  $\text{DoM} = 12$  matching bits.

1171 We introduce 224 binary variables  $v = \{v_0, v_1, \dots, v_{223}\}$  and 224 binary  
 1172 variables  $c = \{c_0, c_1, \dots, c_{223}\}$ . Those variables  $v_i$ 's and  $c_i$ 's are placed at the  
 1173  $24 + 424 = 448$   $\blacksquare$  and  $\blacksquare$  bits in  $A^{(0)}$ . For example, set  $A_{\{0,0,0\}}^{(0)} = v_0$  and  $A_{\{0,1,0\}}^{(0)} =$   
 1174  $v_0 \oplus c_0$  due to the CP-kernel property.

1175 We use two message blocks  $(M_1, M_2)$  to build the attack. Given a value for  
 1176 the inner part of the 2nd block, the 338 conditions on  $A^{(0)}$  will be a linear system  
 1177 on 352 variables of  $M_2$ , including  $576 - 448 = 128$   $\blacksquare$  bits and 224 Binary variables  
 1178  $c = \{c_0, c_1, \dots, c_{223}\}$ . The rank of the coefficient matrix of the linear system is  
 1179 266. There are  $338 - 266 = 72$  conditions out of the total 338 only determined by  
 1180 the value of the inner part. Randomly test  $2^{72} M_1$  to expect one satisfying the  
 1181 72 conditions of the inner part. Then for the right  $M_1$ , there are  $2^{352-266} = 2^{86}$   
 1182 solutions of  $M_2$ , which make all the 338 equations hold.

1183 Using TA algorithm, we can get 118 free variables and 94 dependent variables.  
 1184 We put the TA matrices in MATRIX/keccak[1024]\_4r.txt at [https://anonymous.  
 1185 4open.science/r/Triangulation-MitM-7373](https://anonymous.4open.science/r/Triangulation-MitM-7373).

1186 The steps for the 4-round MitM attack are given in Algorithm 18. To find a  
 1187 512-bit target preimage, we need  $2^{\zeta_1 - 72 + \zeta_2 + \zeta_3 + 106 + 12 + 12} = 2^{512}$ . Set  $\zeta_1 = 274$ ,  
 1188  $\zeta_2 = 86$  and  $\zeta_3 = 94$ . The total preimage attack on 4-round KECCAK[1024] is  
 1189 about  $2^{512-\min\{\text{DoF}^+, \text{DoF}^-, \text{DoM}\}} = 2^{500}$  time and  $2^{118}$  memory.

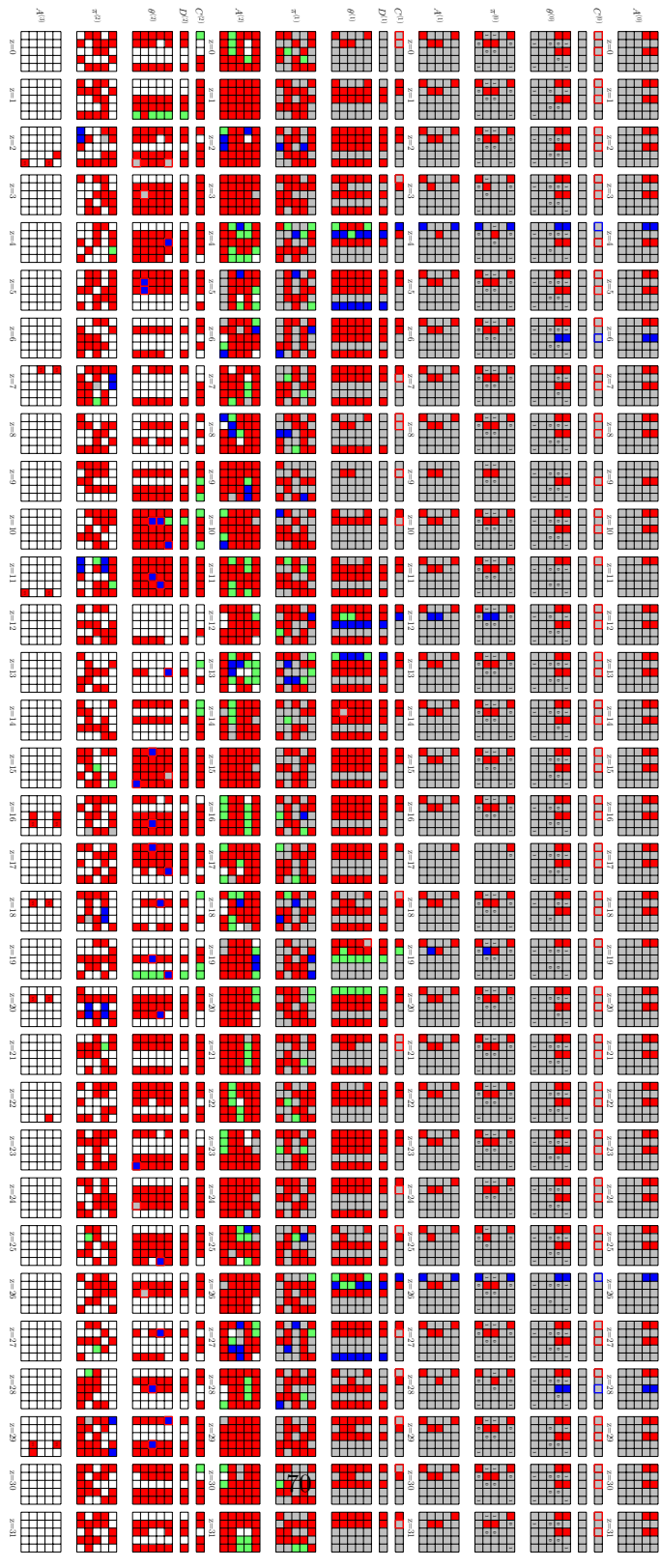


Fig. 27: Part-1: The 4-round MitM preimage attack on KECCAK[1024]

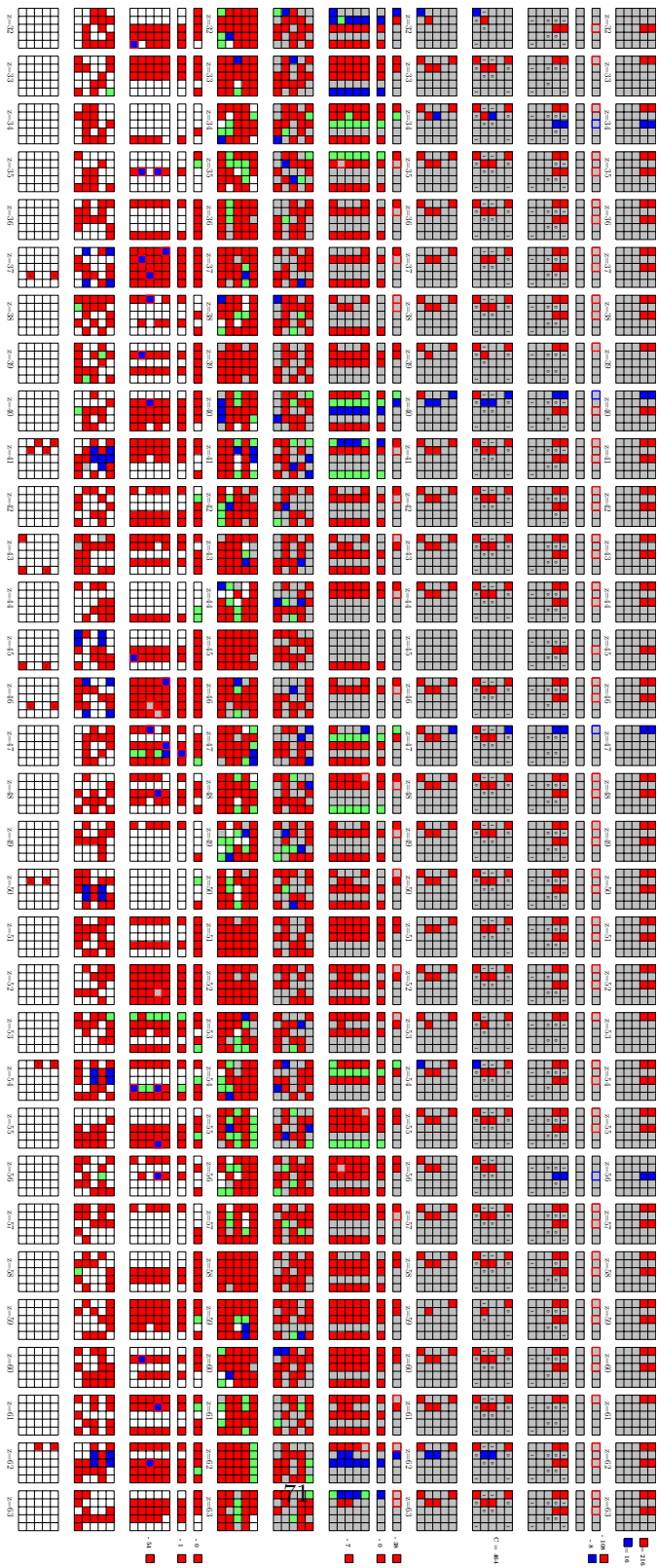


Fig. 28: Part-2: The 4-round MitM preimage attack on KECCAK[1024]

---

**Algorithm 17:** Memory Improved Preimage Attack on 4-round KEC-CAK[1024]

---

```

1  Precompute inversely from the target to  $A^{(3)}$ 
2  for  $2^{\zeta_1}$  values of  $M_1$     /*  $\zeta_1 = 400$  */
3  do
4      Compute the inner part of the 2nd block and solve the system of 464
        linear equations
5      if the equations have solutions /* with probability of  $2^{-214}$  */
6      then
7          for each of the  $2^{\zeta_2}$  solutions of  $M_2$     /*  $\zeta_2 = 210 \leq 210$  */
8          do
9              for  $2^{\zeta_3}$  values  $(e_1, e_2, \dots, e_{56}) \in \mathbb{F}_2^{56}$  do
10                  $U \leftarrow []$ 
11                 for 52 free variables  $\blacksquare$  in  $A^{(0)} \in 2^{52}$  do
12                     Assign  $(e_1, e_2, \dots, e_{56})$  to 56 expressions
13                     Deduce 56 dependent variables
14                     Compute forward to other 44-bit  $\blacksquare/\blacksquare$   $\mathbf{u} \in \mathbb{F}_2^{44}$ 
15                      $U[\mathbf{u}] \leftarrow A^{(0)}[v_{\mathcal{R}}]$  /*  $v_{\mathcal{R}}$  represents all 216 red indexes */
16                 end
17                 for  $\mathbf{u} \in \mathbb{F}_2^{44}$  do
18                      $L \leftarrow []$ 
19                     for  $A^{(0)}[v_{\mathcal{B}}] \in 2^8$  /*  $v_{\mathcal{B}}$  represents all 8 blue indexes */
20                     do
21                         Compute forward to the 8-bit matching point  $v$ 
22                          $L[v] \leftarrow A^{(0)}[v_{\mathcal{B}}]$ 
23                     end
24                     for values in  $U[\mathbf{u}]$  do
25                         Compute forward the 8-bit matching point  $v'$ 
26                         for values in  $L[v']$  do
27                             if it leads to the given hash value then
28                                 Output the preimage
29                             end
30                         end
31                     end
32                 end
33             end
34         end
35     end
36 end

```

---



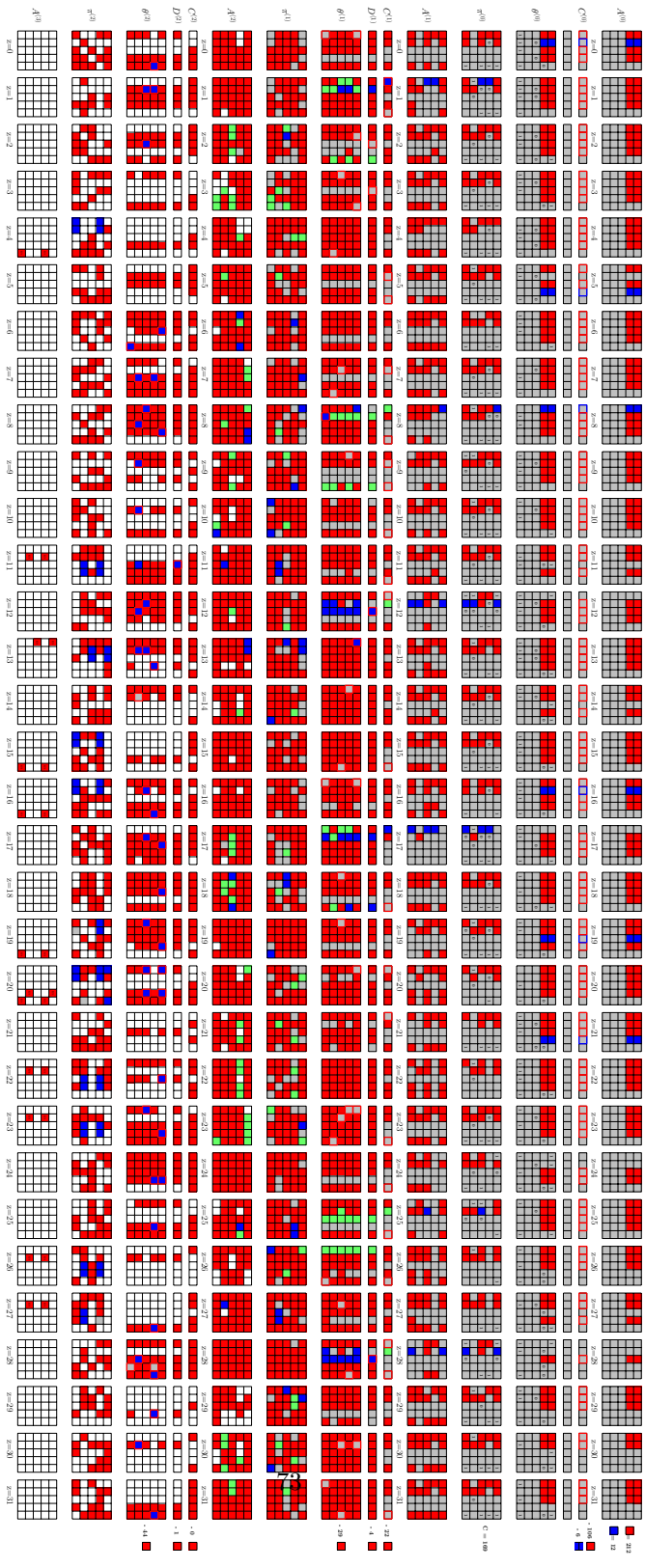


Fig. 29: The 4-round MitM preimage attack on KECCAK[1024]

---

**Algorithm 18:** The Preimage Attack on 4-round KECCAK[1024]

---

```

1 Precompute inversely from the target to  $A^{(3)}$ 
2 for  $2^{\zeta_1}$  values of  $M_1$  /*  $\zeta_1 = 274$  */
3 do
4   Compute the inner part of the 2nd block and solve the system of 338
   linear equations
5   if the equations have solutions /* with probability of  $2^{-72}$  */
6   then
7     for each of the  $2^{\zeta_2}$  solutions of  $M_2$  /*  $\zeta_2 = 86 \leq 86$  */
8     do
9       for  $2^{\zeta_3}$  values  $(e_1, e_2, \dots, e_{94}) \in \mathbb{F}_2^{94}$  do
10         $U \leftarrow []$ 
11        for 118 free variables  $\blacksquare$  in  $A^{(0)} \in 2^{118}$  do
12          Assign  $(e_1, e_2, \dots, e_{94})$  to 94 expressions
13          Deduce 94 dependent variables
14          Compute forward to other 106-bit  $\blacksquare/\blacksquare$   $\mathbf{u} \in \mathbb{F}_2^{106}$ 
15           $U[\mathbf{u}] \leftarrow A^{(0)}[v_{\mathcal{R}}]$  /*  $v_{\mathcal{R}}$  represents all 212 red indexes
          */
16        end
17        for  $\mathbf{u} \in \mathbb{F}_2^{106}$  do
18           $L \leftarrow []$ 
19          for  $A^{(0)}[v_{\mathcal{B}}] \in 2^{12}$  /*  $v_{\mathcal{B}}$  represents all 12 blue
          indexes */
20          do
21            Compute forward to the 12-bit matching point  $v$ 
22             $L[v] \leftarrow A^{(0)}[v_{\mathcal{B}}]$ 
23          end
24          for values in  $U[\mathbf{u}]$  do
25            Compute forward the 12-bit matching point  $v'$ 
26            for values in  $L[v']$  do
27              if it leads to the given hash value then
28                Output the preimage
29              end
30            end
31          end
32        end
33      end
34    end
35  end
36 end

```

---

### 1190 I.3 MitM Preimage Attacks on 4-round KECCAK[768]

1191 Using the same model in [46], we get a new characteristic as shown in Figure 30  
 1192 (first part) and Figure 31 (second part). In the full path, the starting state  $A^{(0)}$   
 1193 contains 28 ■ bits and 512 ■ bits, and there are totally 428 conditions on ■ bits  
 1194 of  $\pi^{(0)}$ . Due to the CP-kernel property, the initial degree of freedoms (DoFs) of ■  
 1195 and ■ are  $\lambda^+ = 17$  and  $\lambda^- = 316$ . In the computation  $A^{(0)}$  to  $A^{(3)}$ , the consumed  
 1196 degrees of freedom (DoFs) of ■ and ■ are  $l^+ = 0$  and  $l^- = 299$  bits, respectively.  
 1197 Therefore,  $\text{DoF}^+ = 17$ ,  $\text{DoF}^- = 17$ , and there are  $\text{DoM} = 17$  matching bits.

1198 We introduce 333 binary variables  $v = \{v_0, v_1, \dots, v_{332}\}$  and 207 binary  
 1199 variables  $c = \{c_0, c_1, \dots, c_{206}\}$ . Those variables  $v_i$ 's and  $c_i$ 's are placed at the  
 1200  $28 + 512 = 540$  ■ and ■ bits in  $A^{(0)}$ . For example, set  $A_{\{0,0,0\}}^{(0)} = v_0$ ,  $A_{\{0,1,0\}}^{(0)} = v_1$   
 1201 and  $A_{\{0,2,0\}}^{(0)} = v_0 \oplus v_1 \oplus c_0$  due to the CP-kernel property.

1202 We use two message blocks  $(M_1, M_2)$  to build the attack. Given an inner part,  
 1203 the 428 conditions can be seen as a linear system of  $1600 - 384 \times 2 - 333 = 499$   
 1204 variables of  $M_2$  ( $384 \times 2$  is the number of capacity bits, 333 are the DoFs of ■  
 1205 and ■ bits in  $A^{(0)}$ ), which will act as global parameters, including 292 ■ of  $M_2$   
 1206 and 207 binary variables  $c_{x,z}$ 's. The rank of the coefficient matrix of the linear  
 1207 system is 343. In other words, through some linear transformations, there are  
 1208  $428 - 343 = 85$  equations determined only by the bits of the inner part. We  
 1209 have to randomly test  $2^{85}$   $M_1$  to compute a right inner part satisfying the 85  
 1210 equations. Then for a right inner part, there are  $2^{499-343} = 2^{156}$  solutions of  $M_2$ ,  
 1211 which make all the conditions hold.

1212 Using TA, we can get 157 free variables and 159 dependent variables. We put  
 1213 the TA matrices in MATRIX/keccak[768]\_4r.txt at <https://anonymous.4open.science/r/Triangulation-MitM-7373>.  
 1214

1215 The steps for the 4-round MitM attack are given in Algorithm 19. To find a  
 1216 384-bit target preimage, we need  $2^{\zeta_1 - 85 + \zeta_2 + \zeta_3 + 140 + 17 + 17} = 2^{384}$ . Set  $\zeta_1 = 85$ ,  
 1217  $\zeta_2 = 51$  and  $\zeta_3 = 159$ . The total preimage attack on 4-round KECCAK[768] is  
 1218 about  $2^{384 - \min\{\text{DoF}^+, \text{DoF}^-, \text{DoM}\}} = 2^{367}$  time and  $2^{157}$  memory.

## 1219 J MitM Preimage Attacks on 10-round Gimli

1220 The 10-round MitM characteristic of Gimli-XOF-128 is shown in Figure 34. In  
 1221 the MitM path, the starting state  $A^{(0)}$  contains  $\lambda^+ = 6$  ■ bit and  $\lambda^- = 64$   
 1222 ■ bits. There are 63 conditions on  $A^{(0)}$  following Qin *et al.* MitM framework  
 1223 in Figure 22. In the computation from  $A^{(0)}$  to  $A^{(9)}$ , the consumed degrees of  
 1224 freedom (DoFs) of ■ and ■ are  $l^+ = 0$  and  $l^- = 61$  bits, respectively. Therefore,  
 1225  $\text{DoF}^+ = 6$ ,  $\text{DoF}^- = 3$ , and there is  $\text{DoM} = 3$  matching bits.

1226 The steps for the 10-round MitM attack are given in Algorithm 20. The total  
 1227 preimage attack on 10-round Gimli-XOF-128 is about  $2^{128 - \min\{\text{DoF}^+, \text{DoF}^-, \text{DoM}\}} =$   
 1228  $2^{125}$  time and  $2^{64}$  memory.

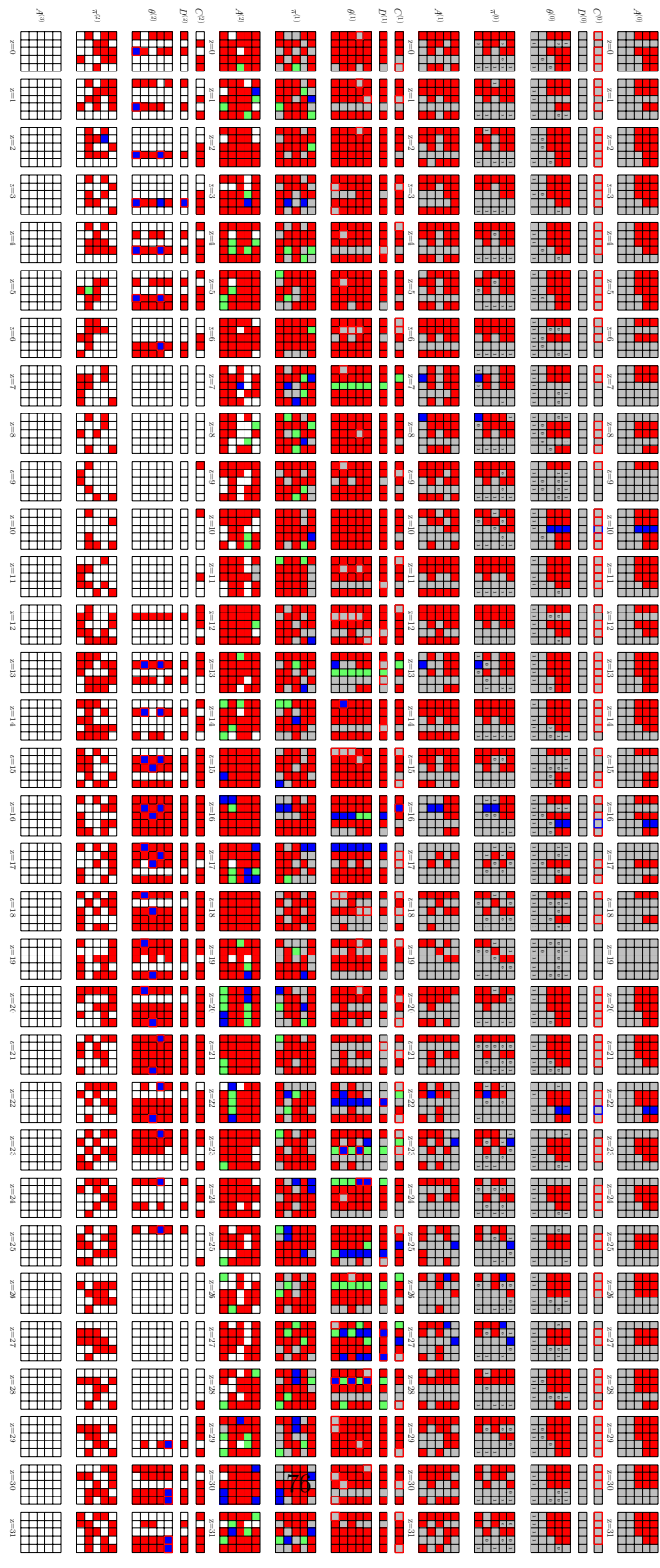


Fig. 30: Part-1: The 4-round Low Memory MITM preimage attack on KECCAK[768]

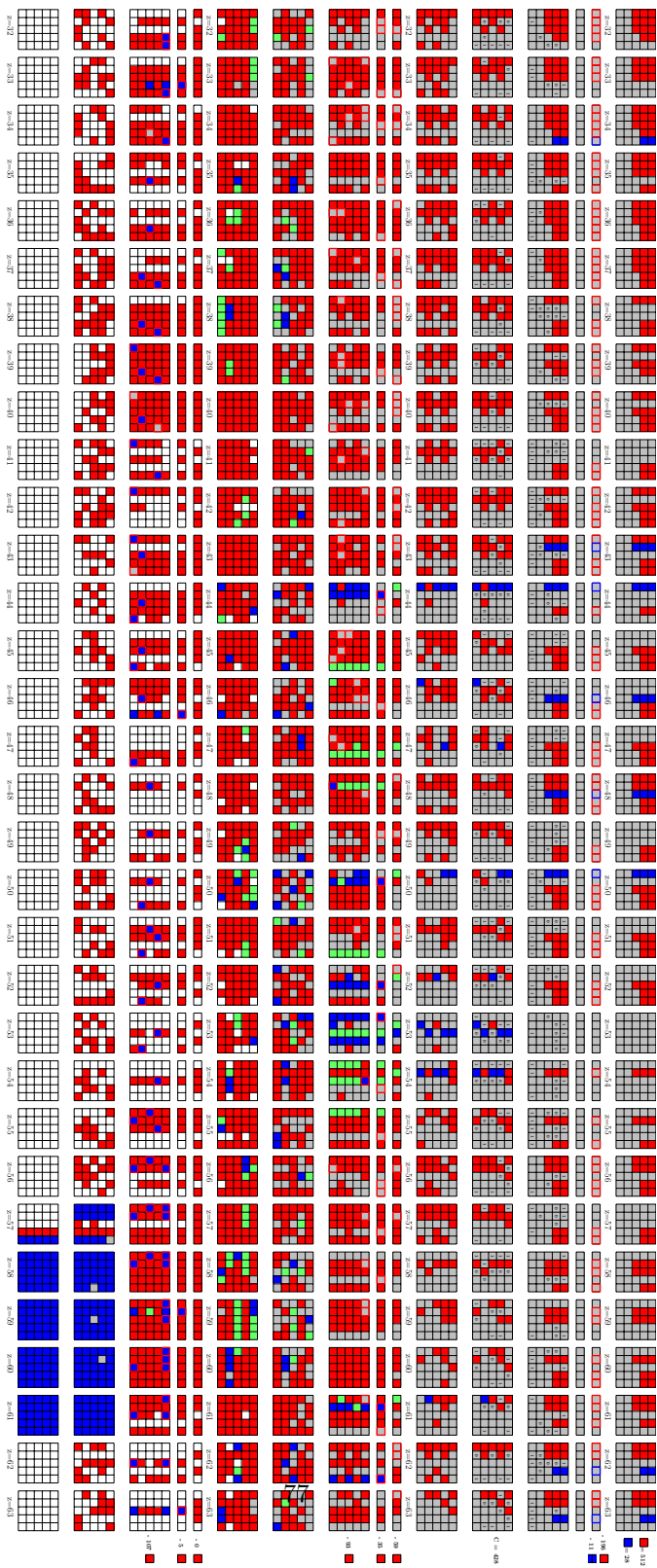


Fig. 31: Part-2: The 4-round Low Memory MITM preimage attack on KECCAK[768]

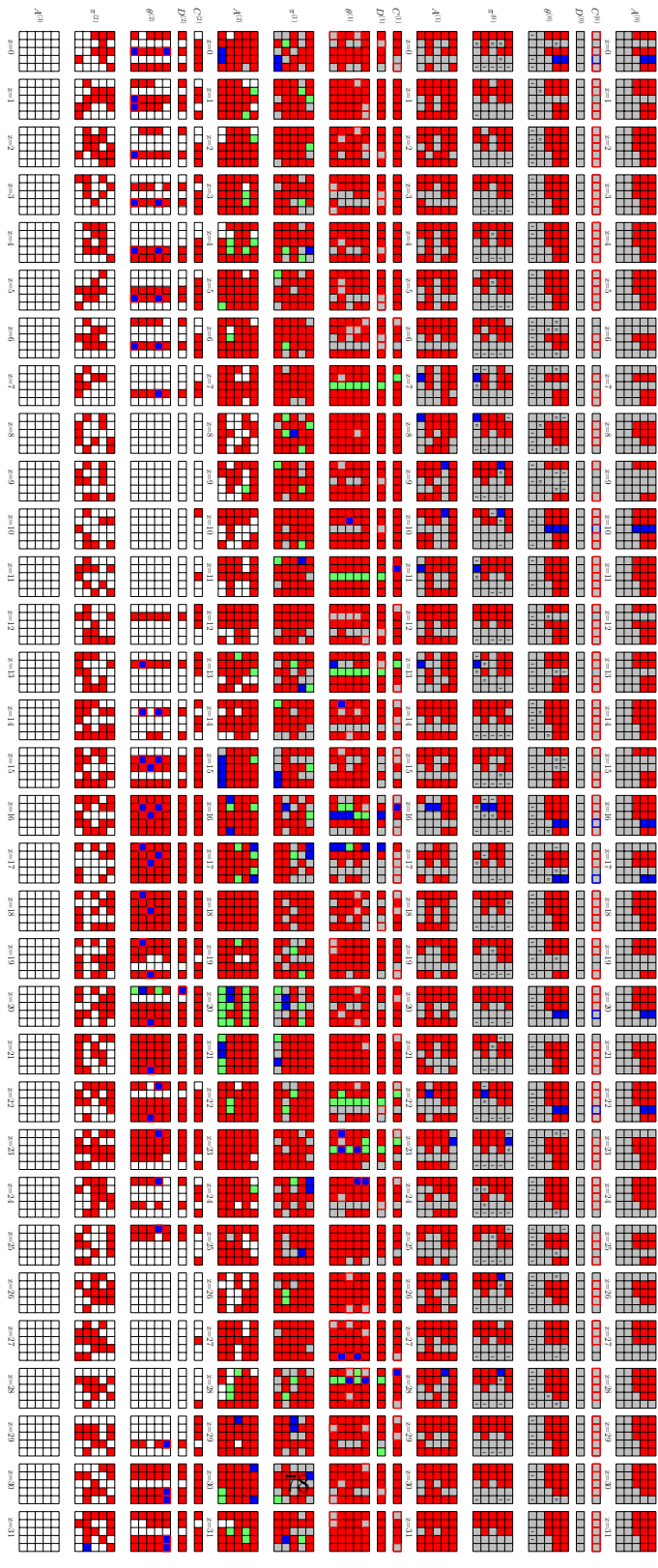


Fig. 32: Part-1: The 4-round MITM preimage attack on KECCAK[768]

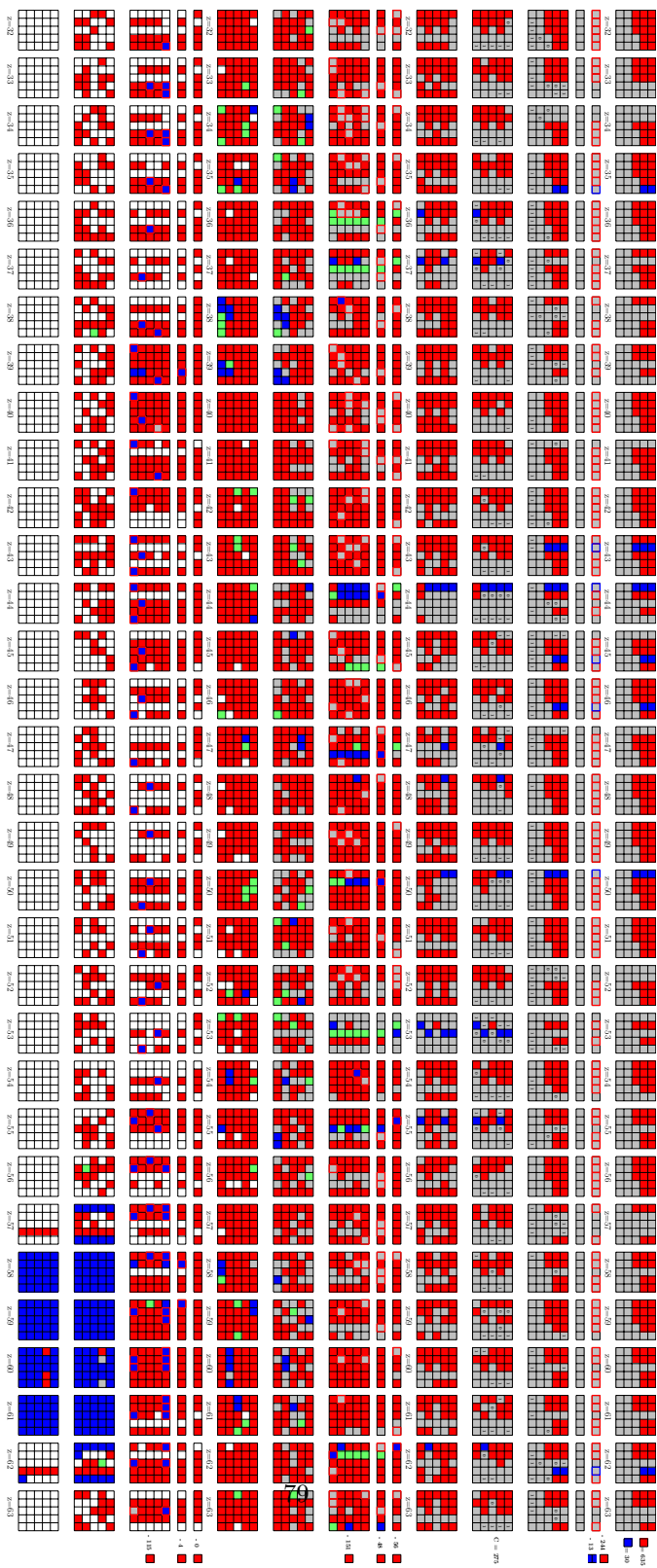


Fig. 33: Part-2: The 4-round MITM preimage attack on KECCAK[768]

---

**Algorithm 19:** The Low Memory Preimage Attack on 4-round KEC-CAK[768]

---

```

1  Precompute inversely from the target to  $\theta^{(3)}$ 
2  for  $2^{\zeta_1}$  values of  $M_1$     /*  $\zeta_1 = 85$  */
3  do
4      Compute the inner part of the 2nd block and solve the system of 428
        linear equations
5      if the equations have solutions /* with probability of  $2^{-85}$  */
6      then
7          for each of the  $2^{\zeta_2}$  solutions of  $M_2$     /*  $\zeta_2 = 51 \leq 156$  */
8          do
9              for  $2^{\zeta_3}$  values  $(e_1, e_2, \dots, e_{159}) \in \mathbb{F}_2^{159}$  do
10                  $U \leftarrow []$ 
11                 for 157 free variables  $\blacksquare$  in  $A^{(0)} \in 2^{157}$  do
12                     Assign  $(e_1, e_2, \dots, e_{159})$  to 159 expressions
13                     Deduce 159 dependent variables
14                     Compute forward to other 140-bit  $\blacksquare/\blacksquare$   $u \in \mathbb{F}_2^{140}$ 
15                      $U[u] \leftarrow A^{(0)}[v_{\mathcal{R}}]$  /*  $v_{\mathcal{R}}$  represents all 316 red indexes
                        */
16                 end
17                 for  $u \in \mathbb{F}_2^{140}$  do
18                      $L \leftarrow []$ 
19                     for  $A^{(0)}[v_{\mathcal{B}}] \in 2^{17}$  /*  $v_{\mathcal{B}}$  represents all 17 blue
                        indexes */
20                     do
21                         Compute forward to the 17-bit matching point  $v$ 
22                          $L[v] \leftarrow A^{(0)}[v_{\mathcal{B}}]$ 
23                     end
24                     for values in  $U[u]$  do
25                         Compute forward the 17-bit matching point  $v'$ 
26                         for values in  $L[v']$  do
27                             if it leads to the given hash value then
28                                 Output the preimage
29                             end
30                         end
31                     end
32                 end
33             end
34         end
35     end
36 end

```

---



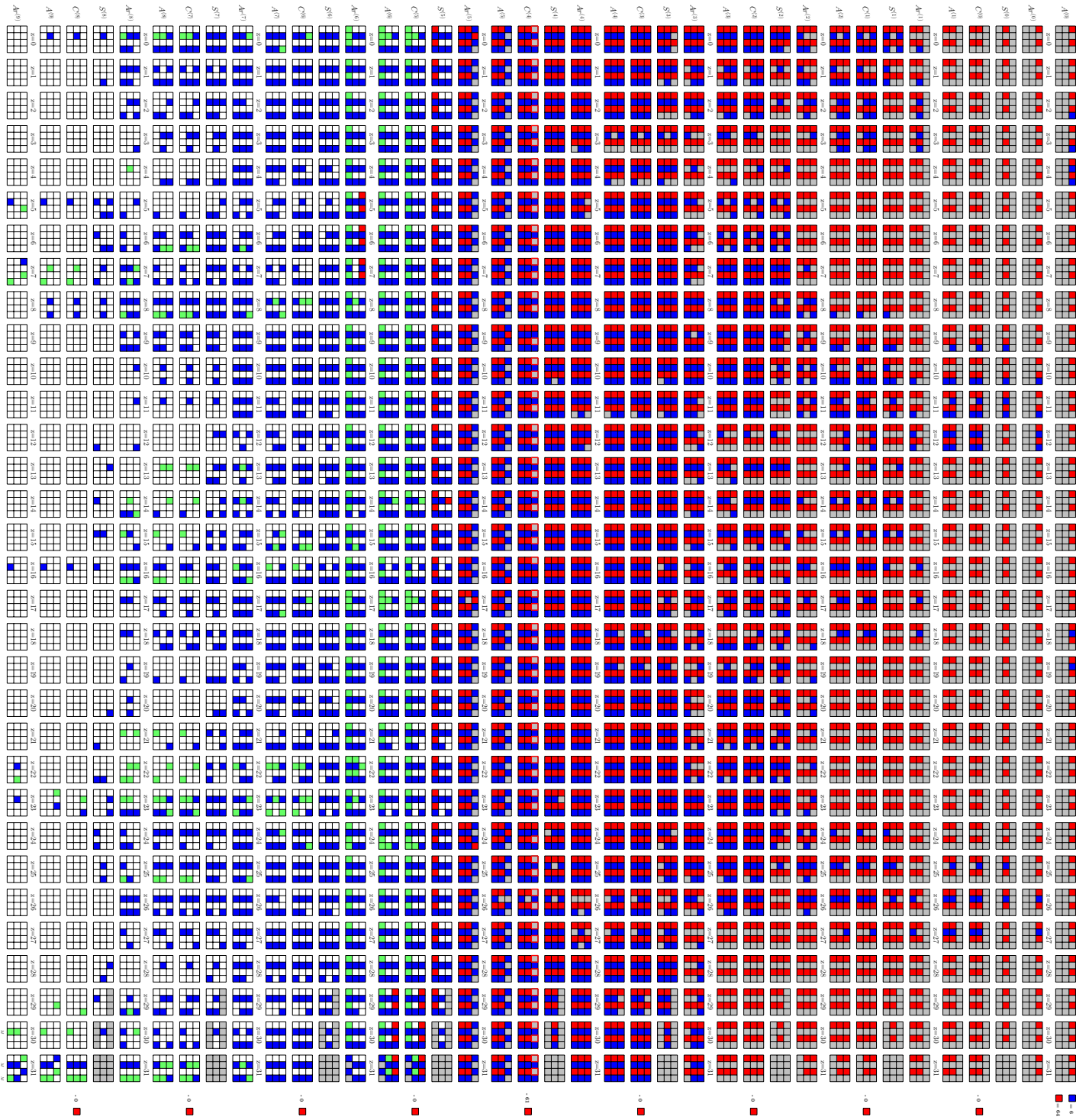


Fig. 34: The 10-round Preimage attack on Gimli-XOF-128

---

**Algorithm 20:** The Preimage Attack on 10-round Gimli-XOF-128

---

```

1 Precompute inversely from the target to  $A^{(9)}$ 
2 for  $2^{71}$  values of  $M_1$  /*  $\zeta_1 = 71$  */
3 do
4   Compute the inner part of the 2nd block and solve the system of 63 linear
   equations
5   if the equations have solutions /* with probability of  $2^{-63}$  */
6   then
7     for  $2^{50}$  values of the  $\blacksquare$  bits in  $M_2$  do
8        $U \leftarrow []$ 
9       for 64 free variables  $\blacksquare$  in  $A^{(0)} \in 2^{64}$  do
10        Compute forward to determine the 61-bit  $\blacksquare/\blacksquare \mathbf{u} \in \mathbb{F}_2^{61}$ 
11         $U[\mathbf{u}] \leftarrow A^{(0)}[v_{\mathcal{R}}]$  /*  $v_{\mathcal{R}}$  represents all 64 red indexes */
12      end
13      for  $\mathbf{u} \in \mathbb{F}_2^{61}$  do
14         $L \leftarrow []$ 
15        for  $A^{(0)}[v_{\mathcal{B}}] \in 2^6$  /*  $v_{\mathcal{B}}$  represents all 6 blue indexes */
16        do
17          Compute forward to the 3-bit matching point  $v$ 
18           $L[v] \leftarrow A^{(0)}[v_{\mathcal{B}}]$ 
19        end
20        for values in  $U[\mathbf{u}]$  do
21          Compute forward the 3-bit matching point  $v'$ 
22          for values in  $L[v']$  do
23            if it leads to the given hash value then
24              Output the preimage
25            end
26          end
27        end
28      end
29    end
30  end
31 end

```

---

## 1229 K MITM Preimage Attack on Subterranean 2.0

1230 **Subterranean 2.0**, designed by Daemen et al. [16], is a second round candidate  
 1231 of NIST LWC. For **Subterranean-XOF** with 256-bit digest ( $n = 256$ ,  $b = 257$ ,  
 1232  $r = 9$ ,  $r' = 32$ ,  $c = 248$ ), Lefevre and Mennink proved a tight bound of 224-  
 1233 bit preimage security [38] under ideal permutation model. The round function  
 1234 consists of four operations:  $\chi : s_i \leftarrow s_i + (s_{i+1} + 1)s_{i+2}$ ,  $\iota$  : constant addition,  
 1235  $\theta : s_i \leftarrow s_i + s_{i+3} + s_{i+8}$ , and  $\pi : s_i \leftarrow s_{12i}$ . The internal state of each round  
 1236 is updated as :  $A^{(r)} \xrightarrow{\chi \circ \iota} \chi^{(r)} \xrightarrow{\theta} \theta^{(r+1)} \xrightarrow{\pi} A^{(r+1)}$ . The output function is  $z_i =$   
 1237  $s_{12^{4i}} + s_{-12^{4i}}$ , ( $0 \leq i < 32$ ) as shown in Table 8, e.g., when  $i = 0$ ,  $z_0 = s_1 + s_{256}$ .  
 1238 After each 32-bit digest is squeezed out, 1-round function is executed to update  
 1239 the internal state.

1240 Since DoFs are only consumed through the XOR operation,  $\chi$  and  $\theta$  oper-  
 1241 ations can be represented by  $\chi^* : s_i^* \leftarrow (s_{i+1} + 1)s_{i+2}$  and  $\theta^* : s_i \leftarrow s_i + s_i^* +$   
 1242  $s_{i+3} + s_{i+3}^* + s_{i+8} + s_{i+8}^*$ . Thus, the DoFs consumption can be only restricted in  
 1243 the  $\theta^*$  operation. Here, we show a preimage attack against **Subterranean-XOF**  
 1244 as shown in Figure 35. The starting state starts at the internal state where the  
 1245 first 32-bit digest  $T_1$  is squeezed out, denoted as  $A^{(0)}$ . Since each bit of  $T_1$  is  
 1246 deduced by  $s_{12^{4i}} + s_{-12^{4i}}$ , the MitM attribute of  $(s_{12^{4i}}, s_{-12^{4i}})$  in  $A^{(0)}$  can be  
 1247 set as  $(\blacksquare, \blacksquare)$ ,  $(\blacksquare, \blacksquare)$  or  $(\blacksquare, \blacksquare)$  and is served as 1-bit degree of freedom. Therefore,  
 1248 there are  $\lambda^+ = 114$   $\blacksquare$  bits and  $\lambda^- = 92$   $\blacksquare$  bits in  $A^{(0)}$ . In the forward computa-  
 1249 tion path, the consumed degrees of freedom (DoFs) of  $\blacksquare$  and  $\blacksquare$  are  $l^+ = 42$  and  
 1250  $l^- = 20$  bits, such that  $\text{DoF}^+ = 72$ ,  $\text{DoF}^- = 72$ . In the matching phase, 1-bit  
 1251 matching point can be deduced if  $(s_{12^{4i}}, s_{-12^{4i}})$  in  $A^{(r)}$  has no unknown  $\square$  bit,  
 1252 for  $1 \leq r \leq 3$ . Hence, the final matching points are counted as  $\text{DoM} = 72$  bits  
 1253 and are marked with “m” in Figure 35.

1254 The detailed algorithm is given in Algorithm 21. In Line 25 to Line 36,  
 1255  $2^{72}$  solutions of  $A^{(0)}$  are left after the 72-bit matching. Hence, we need repeat  
 1256  $2^{\zeta+3+21+19+19} = 2^{224-72-72}$  times, i.e.,  $\zeta = 18$ .

- 1257 - In Line 2,  $A_{16}^{(1)}$  is a  $\blacksquare$  bit that is derived by imposing constraint on  $\blacksquare$  bits.  
 1258 However,  $\left(\overline{A_{15}^{(1)}} \wedge A_{16}^{(1)}\right)$  is involved in the constraint imposed on the  $A_{129}^{(2)}$  by  
 1259 consuming 1-bit  $\blacksquare$  DoF. Hence, it was considered at the outer loop. Similarly,  
 1260  $(A_{26}^{(1)}, A_{47}^{(1)})$  are two  $\blacksquare$  bits which are derived by imposing constraints on  $\blacksquare$   
 1261 bits, but  $\left(\overline{A_{25}^{(1)}} \wedge A_{26}^{(1)}\right)$  and  $\left(\overline{A_{46}^{(1)}} \wedge A_{47}^{(1)}\right)$  are involved in the constraints  
 1262 imposed on  $A_{66}^{(2)}$  and  $A_{132}^{(2)}$  by consuming 2-bit  $\blacksquare$  DoFs.
- 1263 - In Line 4 to Line 11, using the TA algorithm,  $A_{200}^{(0)}$  can be determined by  
 1264 free variables  $v_{\mathcal{R},1}$  and  $A_{16}^{(1)}$  as Eq. (40). Then, the remaining 86 free  $\blacksquare$   
 1265 bits are exhausted trivially. The time complexity of constructing table  $V$   
 1266 is  $2^{\zeta+3+5+86} = 2^{112}$ . The memory complexity is  $2^{5+86} = 2^{91}$ . Compared  
 1267 with the table-based method in [26], the memory cost is reduced by a factor

1268

of 2.

$$A_{16}^{(1)} = A_{192}^{(0)} \oplus (\overline{A_{193}^{(0,*)}} \wedge A_{194}^{(0)}) \oplus A_{195}^{(0)} \oplus (\overline{A_{196}^{(0)}} \wedge A_{197}^{(0,*)}) \oplus A_{200}^{(0)} \oplus (\overline{A_{201}^{(0)}} \wedge A_{202}^{(0)}) \quad (40)$$

1269

- In Line 12 to Line 21, using the TA algorithm, 23 bits in  $v_{\mathcal{B},1}^*$  can be determined by the 62 free bits in  $v_{\mathcal{B},1}$  and the 21 free bits in  $c_{\mathcal{B},1}$  as shown in Table 9. Then, the remaining 29 free bits in  $v_{\mathcal{B},2}$  are exhausted trivially. The time complexity of constructing table  $U$  is  $2^{\zeta+3+21+62+29} = 2^{133}$ . The memory complexity is  $2^{62+29} = 2^{91}$ . Compared with the table-based method in [26], the memory cost is reduced by a factor of  $2^{23}$ .

1270

1271

1272

1273

1274

1275

1276

1277

1278

Once finding such a proper  $A^{(0)}$ , an inner collision on 248-bit capacity between  $A^{(0)}$  and the initial value can be found by Floyd's cycle finding algorithm with  $2^{124}$  time and no memory. Therefore, the overall time complexity is about  $2^{152}$ . The memory cost is about  $2^{92}$  to store hash tables  $U$  and  $V$ .

$i$	state bits	$i$	state bits	$i$	state bits	$i$	state bits
0	(1, 256)	8	(64, 193)	16	(241, 16)	24	(4, 253)
1	(176, 81)	9	(213, 44)	17	(11, 246)	25	(190, 67)
2	(136, 121)	10	(223, 34)	18	(137, 120)	26	(30, 227)
3	(35, 222)	11	(184, 73)	19	(211, 46)	27	(140, 117)
4	(249, 8)	12	(2, 255)	20	(128, 129)	28	(225, 32)
5	(134, 123)	13	(95, 162)	21	(169, 88)	29	(22, 235)
6	(197, 60)	14	(15, 242)	22	(189, 68)	30	(17, 240)
7	(234, 23)	15	(70, 187)	23	(111, 146)	31	(165, 92)

Table 8: Mapping between state bits of matching phase in **Subterranean 2.0**

$c_{\mathcal{B},1}$	$\theta_{49}^{(0)}, \theta_{50}^{(0)}, \theta_{51}^{(0)}, \theta_{54}^{(0)}, \theta_{55}^{(0)}, \theta_{56}^{(0)}, \theta_{172}^{(0)}, \theta_{174}^{(0)}, \theta_{175}^{(0)}, \theta_{176}^{(0)}, \theta_{177}^{(0)}, \theta_{179}^{(0)}, \theta_{181}^{(0)}, \theta_{183}^{(0)}, \theta_{21}^{(1)}, \theta_{22}^{(1)},$ $\theta_{39}^{(1)}, \theta_{58}^{(1)}, \theta_{86}^{(1)}, \theta_{146}^{(1)}, \theta_{147}^{(1)}, \theta_{150}^{(1)}, \theta_{255}^{(1)}$
$c_{\mathcal{B},2}$	$\theta_3^{(1)}, \theta_6^{(1)}, \theta_{10}^{(1)}, \theta_{51}^{(1)}, \theta_{62}^{(1)}, \theta_{66}^{(1)}, \theta_{69}^{(1)}, \theta_{74}^{(1)}, \theta_{90}^{(1)}, \theta_{110}^{(1)}, \theta_{111}^{(1)}, \theta_{129}^{(1)}, \theta_{138}^{(1)}, \theta_{159}^{(1)}, \theta_{170}^{(1)}, \theta_{183}^{(1)},$ $\theta_{218}^{(1)}, \theta_{219}^{(1)}, \theta_{239}^{(1)}$
$v_{\mathcal{B},1}$	$A_{56}^{(0)}, A_{58}^{(0)}, A_{62}^{(0)}, A_{69}^{(0)}, A_{71}^{(0)}, A_{72}^{(0)}, A_{74}^{(0)}, A_{75}^{(0)}, A_{77}^{(0)}, A_{80}^{(0)}, A_{82}^{(0)}, A_{83}^{(0)}, A_{84}^{(0)}, A_{85}^{(0)}, A_{86}^{(0)},$ $A_{87}^{(0)}, A_{88}^{(0)}(A_{169}^{(0)}), A_{89}^{(0)}, A_{91}^{(0)}, A_{92}^{(0)}(A_{165}^{(0)}), A_{93}^{(0)}, A_{94}^{(0)}, A_{96}^{(0)}, A_{97}^{(0)}, A_{98}^{(0)}, A_{99}^{(0)}, A_{101}^{(0)}, A_{102}^{(0)},$ $A_{103}^{(0)}, A_{104}^{(0)}, A_{105}^{(0)}, A_{106}^{(0)}, A_{107}^{(0)}, A_{108}^{(0)}, A_{109}^{(0)}, A_{110}^{(0)}, A_{111}^{(0)}(A_{146}^{(0)}), A_{112}^{(0)}, A_{113}^{(0)}, A_{114}^{(0)}, A_{115}^{(0)},$ $A_{116}^{(0)}, A_{117}^{(0)}(A_{140}^{(0)}), A_{118}^{(0)}, A_{119}^{(0)}, A_{120}^{(0)}(A_{137}^{(0)}), A_{121}^{(0)}(A_{136}^{(0)}), A_{122}^{(0)}, A_{123}^{(0)}(A_{134}^{(0)}), A_{124}^{(0)}, A_{125}^{(0)},$ $A_{127}^{(0)}, A_{129}^{(0)}(A_{128}^{(0)}), A_{130}^{(0)}, A_{131}^{(0)}, A_{132}^{(0)}, A_{135}^{(0)}, A_{173}^{(0)}, A_{178}^{(0)}, A_{179}^{(0)}, A_{183}^{(0)}, A_{185}^{(0)}$
$v_{\mathcal{B},1}^*$	$A_{57}^{(0)}, A_{59}^{(0)}, A_{61}^{(0)}, A_{63}^{(0)}, A_{65}^{(0)}, A_{66}^{(0)}, A_{76}^{(0)}, A_{78}^{(0)}, A_{79}^{(0)}, A_{90}^{(0)}, A_{95}^{(0)}(A_{162}^{(0)}), A_{100}^{(0)}, A_{126}^{(0)}, A_{133}^{(0)},$ $A_{172}^{(0)}, A_{174}^{(0)}, A_{175}^{(0)}, A_{176}^{(0)}(A_{81}^{(0)}), A_{177}^{(0)}, A_{180}^{(0)}, A_{181}^{(0)}, A_{182}^{(0)}, A_{184}^{(0)}(A_{73}^{(0)})$
$v_{\mathcal{B},2}$	$A_{138}^{(0)}, A_{139}^{(0)}, A_{141}^{(0)}, A_{142}^{(0)}, A_{143}^{(0)}, A_{144}^{(0)}, A_{145}^{(0)}, A_{147}^{(0)}, A_{148}^{(0)}, A_{149}^{(0)}, A_{150}^{(0)}, A_{151}^{(0)}, A_{152}^{(0)}, A_{153}^{(0)},$ $A_{154}^{(0)}, A_{155}^{(0)}, A_{156}^{(0)}, A_{157}^{(0)}, A_{158}^{(0)}, A_{159}^{(0)}, A_{160}^{(0)}, A_{161}^{(0)}, A_{163}^{(0)}, A_{164}^{(0)}, A_{166}^{(0)}, A_{167}^{(0)}, A_{168}^{(0)}, A_{170}^{(0)},$ $A_{171}^{(0)},$

Table 9: The disjoint subsets of constraints and variables for triangulation

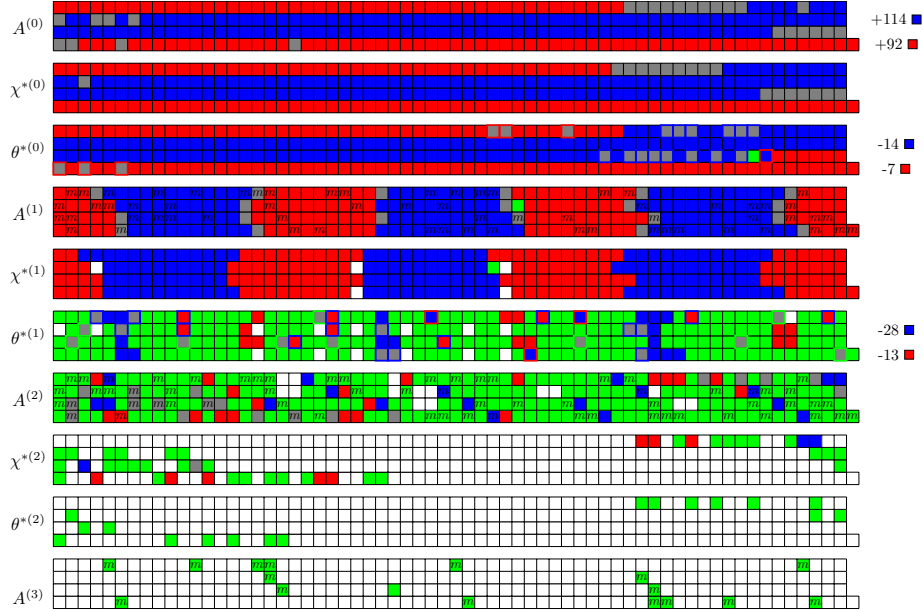


Fig. 35: The Full Round Preimage Attack on Subterranean-XOF

---

**Algorithm 21:** Preimage Attack on Full Round Subterranean
 

---

```

1  for  $2^\zeta$  possible values of the  $\blacksquare$  cells in  $A^{(0)}$ ,  $\zeta = 18$  do
2    for  $2^3$  possible values of  $A_{16}^{(1)} \| A_{26}^{(1)} \| A_{47}^{(1)}$  do
3       $U \leftarrow [], V \leftarrow []$ 
4      for 5-bit values of  $v_{\mathcal{R},1} = (A_{194}^{(0)}, A_{195}^{(0)}, A_{196}^{(0)}, A_{201}^{(0)}, A_{202}^{(0)})$  do
5        Deduce 1-bit value of  $A_{200}^{(0)}$  according to  $A_{16}^{(1)}$ 
6        for  $v_{\mathcal{R},2} \in \mathbb{F}_2^{86}$  of the remaining  $\blacksquare$  cells in  $A^{(0)}$  do
7          Compute forward to the 19-bit  $\mathbf{u}$  with  $A_{26}^{(1)}$  and  $A_{47}^{(1)}$ 
8           $V[\mathbf{u}] \leftarrow v_{\mathcal{R},1} \| v_{\mathcal{R},2} \| A_{200}^{(0)}$ 
9          /* There are  $2^{5+86-19} = 2^{72}$  elements under each index
              */
10         end
11       end
12     for  $g_{\mathcal{B}} \in \mathbb{F}_2^{21}$  of  $c_{\mathcal{B},1}$  /* except for  $\theta_{50}^{(0)} = A_{47}^{(1)}$  and  $\theta_{55}^{(0)} = A_{26}^{(1)}$  */
13     do
14       for 62-bit values of  $v_{\mathcal{B},1}$  do
15         Deduce 23-bit values of  $v_{\mathcal{B},1}^*$ 
16         for  $v_{\mathcal{B},2} \in \mathbb{F}_2^{29}$  of the remaining  $\blacksquare$  cells in  $A^{(0)}$  do
17           Compute forward to the 19-bit  $c_{\mathcal{B},2}$  with  $A_{16}^{(1)}$ 
18            $U[c_{\mathcal{B},2}] \leftarrow v_{\mathcal{B},1} \| v_{\mathcal{B},1}^* \| v_{\mathcal{B},2}$ 
19           /* There are  $2^{62+29-19} = 2^{72}$  elements under each
              index
              */
20         end
21       end
22     for  $\mathbf{u} \in \mathbb{F}_2^{19}$  do
23       for  $c_{\mathcal{B},2} \in \mathbb{F}_2^{19}$  do
24          $L \leftarrow []$ 
25         for  $v_{\mathcal{R}} \in V[\mathbf{u}]$  do
26           Compute forward to the 72-bit matching points  $End_{\mathcal{R}}$ 
              and store  $v_{\mathcal{R}}$  in  $L$  with  $End_{\mathcal{R}}$  as index
27         end
28         for  $v_{\mathcal{B}} \in V[c_{\mathcal{B},2}]$  do
29           Compute forward to the 72-bit matching points  $End_{\mathcal{B}}$ 
30           for  $v_{\mathcal{R}} \in L[End_{\mathcal{B}}]$  do
31             Reconstruct the input state with  $v_{\mathcal{R}}$  and  $v_{\mathcal{B}}$ 
32             if it leads to the given 224-bit hash value
               $(T_2, T_3, \dots, T_8)$  then
33               Output the preimage
34             end
35           end
36         end
37       end
38     end
39   end
40 end
41 end

```

---